

Dynamics of RC Trees with Distributed Constant-Power Loads

by

Ben Wing Lup Leong

Submitted to the Department of Electrical Engineering and Computer Science

in partial fulfillment of the requirements for the degrees of
Bachelor of Science in Electrical Science and Engineering

and

Master of Engineering in Electrical Engineering and Computer Science

at the

MASSACHUSETTS INSTITUTE OF TECHNOLOGY

May 1997

© Ben Wing Lup Leong, MCMXCVII. All rights reserved.


The author hereby grants to MIT permission to reproduce and distribute publicly paper and electronic copies of this thesis document in whole or in part, and to grant others the right to do so.

Elect Eng. OCT 29 1997

Author..........

Department of Electrical Engineering and Computer Science

May 17, 1997

Certified by.....

George C. Verghese

Professor of Electrical Engineering

Thesis Supervisor

Accepted by..........

Arthur C. Smith

Chairman, Department Committee on Graduate Theses



Dynamics of RC Trees with Distributed Constant-Power Loads

by

Ben Wing Lup Leong

Submitted to the Department of Electrical Engineering and Computer Science
on May 17, 1997, in partial fulfillment of the
requirements for the degrees of
Bachelor of Science in Electrical Science and Engineering

and

Master of Engineering in Electrical Engineering and Computer Science

Abstract

Broadband (fiber optic or coaxial cable) systems are becoming more common as the consumer's demand for more bandwidth to the home increases. This thesis presents the results of a study into the dynamic and static stability properties of the networks used to power such systems. An RC tree is used to model the network itself, and a constant-power (P) model is used to represent the loads at each node of the network.

Given an RCP-tree network that satisfies a set of layout constraints, we show that it can be modeled as a gradient system. From this fact, we conclude that the system must end up at one of the possible equilibria of the system. Simple sufficient conditions for the system to end up at a desirable equilibrium are derived from the study of these equilibria. Finally, the application of these results to network and load design is demonstrated, and a proposed approximation model for estimating total current consumption and power dissipation is evaluated.

We show in this thesis that the sufficient stability conditions derived are good guidelines for network design, and that the proposed approximation model is effective in obtaining good estimates.

Thesis Supervisor: George C. Verghese
Title: Professor of Electrical Engineering

Acknowledgments

First and foremost, I want to express my heartfelt gratitude towards Professor George C. Verghese, my thesis supervisor. Without his encouragement and guidance, this thesis could never have become reality. George has also been my academic advisor here at MIT since my sophomore year. He strikes me as a patient teacher and a hardworking man who is always in need of sleep. Yet, he makes the effort to find time in his busy schedule to be available to his students. It is impossible for me to thank him enough with a finite number of words. At the same time, I want to thank Vivian Mizuno, George's secretary, for all her help with the administrative trivia that I have had to deal with over the years.

With regard to the technical assistance that I received while working on this thesis, I would like to thank Dr. Joseph Thottuvelil from Lucent Technologies for providing me with valuable information and data on practical broadband power networks, as well as the benchmark model that was eventually used to evaluate the results derived in this thesis. Also, I would like to thank Professor John Wyatt for his pointers and suggestions which were extremely helpful during the initial stages of the work for this thesis.

Among all the people that have made my last four years at MIT memorable, I would first like to acknowledge Tracey Ho, my girlfriend, for her undying love and dedication. I would also like to thank her for encouraging me on during the times when I got depressed over this thesis, and for assisting in the writing and proof-reading of this document.

Pistol has been an integral part of my life over the last four years. I would like to thank Pat Melaragno, my former pistol coach, for teaching me the art of pistol shooting and for

being a wonderful friend and mentor. The road trips that we made together will forever remain my fondest memories of life in MIT.

Without friends, life at MIT would be pretty bleak. I would like to thank all my friends here at MIT — Alice Wang, Chiangkai Er, Danny Yu, Evelyn Huang, Huan Yao, Michael Sy, Myong-Sin Yi, Steve Lee, Tammy Yap, Tommy Ng, Tseh-Hwan Yong, Weiyang Cheong, and lots of other wonderful people, for making MIT a most memorable experience.

Finally, I want to thank my parents and family members for being supportive all these years that I have been away from home. I also would like to acknowledge the support that I received from the Public Service Commission of Singapore, which made it possible for me to finance my four years of education here at MIT.

Contents

1	Introduction	17
1.1	Background	17
1.2	Interesting Problems	19
1.3	Constant-Power Load	21
1.4	Circuit Models	22
1.5	First-Order System	23
1.5.1	Basic System	24
1.5.2	Non-Ideal Constant-Power Load with Voltage Cutoff	25
1.6	Summary of Contributions of this Thesis	26
2	System Modeling and Dynamics: Second-Order System	29
2.1	Preliminary Analysis	30
2.2	Gradient System Representation	32
2.2.1	Gradient System	33
2.2.2	Energy Function for Ideal Loads	35
2.2.3	Energy Function for Non-Ideal Loads	36
2.2.4	Application	38
2.3	Boundary Behavior	40
2.4	Steady-State Analysis	44
2.5	Summary of Results for Second-Order System	47
3	System Modeling and Dynamics: Higher-Order Systems	49

3.1	Gradient System Representation	49
3.2	Characterizing Equilibria	51
3.2.1	Types of Equilibria	51
3.2.2	Boundary Conditions	52
3.3	Static Equilibria	53
3.3.1	Constraint on Cutoff Voltages	53
3.3.2	Characterization of the Hessian	54
3.3.3	Guaranteeing Stability for Regular Ladder Network	56
3.4	Dynamic Equilibria	60
3.4.1	Boundary Behavior of Modified Gradient System	60
3.4.2	Application of Steady-State Analysis to Regular Ladder Network	63
3.5	Summary of Results for Higher-Order Systems	69
4	Computing Equilibria for a Network	71
4.1	Static Equilibria	71
4.1.1	Direct Numerical Solution	71
4.1.2	Small-Resistance Approximation	73
4.1.3	Approximation Using Aggregated Models	80
4.1.4	Iteration and Circuit Simulation	84
4.2	Dynamic Equilibria	85
5	Network Design	87
5.1	Background	87
5.2	Benchmark Model for a Practical Broadband Power Network	89
5.3	Stability Conditions	90
5.3.1	Static Equilibria	90
5.3.2	Dynamic Equilibria	90
5.4	Application of Results	91
5.4.1	Guaranteeing Stability	91

5.4.2	Estimating Operational Current Load and Power Dissipation	94
5.5	Varying the Cutoff Voltage	96
5.6	Summary	97
6	Conclusion	99
6.1	Future Work	101
A	Detailed Boundary Analysis for Second-Order System	103
A.1	Boundary: $v_1 = V_c$	104
A.2	Boundary: $v_2 = V_c$	105
B	Determinant Calculations	109
B.1	Second-Order System	110
B.2	Third-Order System	111
B.3	Higher-Order Generalization	112
B.4	Computing the Inequality Coefficient	114
B.5	Approximation for Sufficient Condition Coefficient	114
C	Numerical Solutions with Maple V	117
C.1	Second-Order System	117
C.2	Third-Order Ladder	120
D	Small-Resistance Approximation	125
D.1	Third-Order System	125
D.2	Generalization	127
E	Evaluation of Aggregated Models	133
E.1	The Models	133
E.1.1	Series Model	133
E.1.2	Parallel Model	134
E.2	Evaluation of the Series Model	134

E.2.1	Approximation in Second-order System	134
E.2.2	Approximation in Third-order System	135
E.3	Evaluation of the Parallel Model	138
E.3.1	Approximation in Second-order System	139
E.3.2	Approximation in Third-order System	140

List of Figures

1-1	Diagram showing an example HFC powering network.	18
1-2	Diagram showing an example FTTC powering network.	19
1-3	Current versus voltage characteristic for ideal constant-power load.	21
1-4	Typical input current versus voltage characteristic for constant-power load with voltage cutoff V_c	22
1-5	Modeling of system dynamics.	23
1-6	Equivalent second-order model.	23
1-7	Circuit diagram for first-order system.	24
1-8	Dynamic behavior for first-order system.	25
1-9	Dynamic behavior for first-order system with cutoff V_c	26
1-10	Dynamic behavior for situation with no real roots.	26
2-1	Circuit diagram for second-order system.	30
2-2	Plot of $\dot{v}_1 = 0$ and $\dot{v}_2 = 0$ loci for second-order system.	32
2-3	Vector fields for second-order system.	33
2-4	Example plot of $E(v_1, v_2)$	37
2-5	Example plot of $E(v_1, v_2)$ (different angle).	38
2-6	Phase-plane portrait for second-order system with cutoff.	42
2-7	Regular second-order system.	44
3-1	An n th-order tree network with branching.	50
3-2	An example of current flow.	54
3-3	Field lines moving in the same general direction.	61

3-4	Converging field lines at the non-differentiable boundary.	61
3-5	Sliding effect along non-differentiable boundary.	62
3-6	Third-order system.	64
3-7	Example n th-order system.	66
4-1	Second-order system.	73
4-2	Third-order system.	76
4-3	Error convergence.	80
4-4	Second-order series configuration.	83
4-5	Second-order parallel configuration.	83
4-6	Aggregated model.	84
5-1	Schematic for practical series broadband network layout.	89
5-2	Practical model for broadband network.	89
5-3	First-order aggregated-model approximation.	95
A-1	Diagram of boundary $v_1 = V_c$	105
A-2	Diagram of boundary $v_2 = V_c$	107
B-1	Plot of $f(n)$ against n	116
B-2	Error for approximation of $f(n)$	116
C-1	Graphical method for obtaining solutions to a second-order system.	120
C-2	Example field plot for second-order system (ideal loads).	121
C-3	Example field plot for second-order system (non-ideal loads).	122
D-1	Third-order system.	125
D-2	Circuit diagram for first-order system.	128
D-3	A third-order example with branching.	129
D-4	Example loop with equivalent circuit.	129
D-5	Example loop II with equivalent circuit.	130

E-1	Second-order series configuration with aggregated model.	134
E-2	Plot of current vs time for second-order series configuration.	136
E-3	Plot of current vs time for series aggregated model (second-order).	137
E-4	Example third-order series configuration.	137
E-5	Aggregated models for third-order series configuration.	138
E-6	Plot of v_1 vs t for third-order series configuration.	139
E-7	Plot of v'_1 vs t for series approximation (third-order).	140
E-8	Second-order parallel configuration with aggregated model	141
E-9	Example third-order parallel configuration.	141
E-10	Aggregated model for third-order parallel configuration.	141
E-11	Plot of v_1 vs t for third-order parallel configuration.	142
E-12	Plot of v'_1 vs t for parallel approximation (third-order).	143

List of Tables

3.1	Cutoff Voltage Coefficients for Regular Ladder Networks (Static Equilibria)	59
3.2	Cutoff Voltage Coefficients for Regular Ladder Networks (Dynamic Equilibria)	68
4.1	Table of Approximation Results for a Second-Order System	78
4.2	Demonstration of Convergence	79
5.1	Cutoff Voltage Coefficients for Broadband Power Network Model (Static Equilibria)	91
5.2	Cutoff Voltage Coefficients for Broadband Power Network Model (Dynamic Equilibria)	92
5.3	Steady-State Voltages and Currents for 9th-order System	93
5.4	Steady-State Voltages and Currents for 10th-order System	94
5.5	Steady-State Currents and Aggregated-Model Estimates	95
5.6	Minimization of Coefficient $g_\alpha(n)$	97
B.1	Errors for Approximation of $f(n)$	115
E.1	Table of Results for Series Configuration (Second-Order)	135
E.2	Table of Results for Series Configuration (Third-Order)	138
E.3	Table of Results for Parallel Configuration (Second-Order)	139
E.4	Table of Results for Parallel Configuration (Third-Order)	142

Chapter 1

Introduction

1.1 Background

Broadband (fiber optic or coaxial cable) systems are becoming more common as the consumer's demand for more bandwidth to the home increases. The analysis of broadband networks to obtain accurate cost and performance predictions becomes correspondingly important. This thesis focuses on issues of "broadband power," namely those associated with delivering power to broadband networks, and is concerned mainly with the dynamic and static stability properties of such networks. Very little analytical work has been done so far on this in the literature. In this thesis, an RC-tree is used to model the network itself, and a constant-power (P) model is used to represent the load at each node of the network once the load voltage exceeds a certain critical level.

There are two broadband architectures that are currently being implemented [1]: the Hybrid Fiber Coax (HFC) architecture and the Fiber-To-The-Curb (FTTC) architecture. For the HFC architecture, fiber serves a group of many homes and coaxial cable is used to provide both power and RF to the homes via amplifiers and Network Interface Units (NIUs) at each home. For the FTTC architecture, Optical Network Units (ONUs) are powered by a network that is independent of the data network. Topologically, HFC networks are

either bus-like or tree-like networks, while FTTC networks are either bus-like or point-to-point networks. Since a bus-type network requires a shorter total length of fiber than a corresponding point-to-point network, the former is generally a more attractive approach for a FTTC network.

Examples of HFC and FTTC networks discussed in [1] are reproduced in Figures 1-1 and 1-2. In these examples, the cables have the following resistances per unit length: Type 860 – 0.724 mΩ/foot, Type 715 – 0.997 mΩ/foot, Type 750 – 0.75 mΩ/foot and Type 540 – 1.61 mΩ/foot. The power ratings for typical NIUs and ONUs are 7 W and 100 W respectively; typical capacitances associated with these loads are about 10 to 20 μF/watt, i.e. a 100 W load might have a capacitance of 1000 μF to 2000 μF. Current safety regulations prohibit the power source voltage from exceeding 150 V and the typical power source is rated at 90 V, though this value can fall to about 75 V at the end of the battery life for these sources.

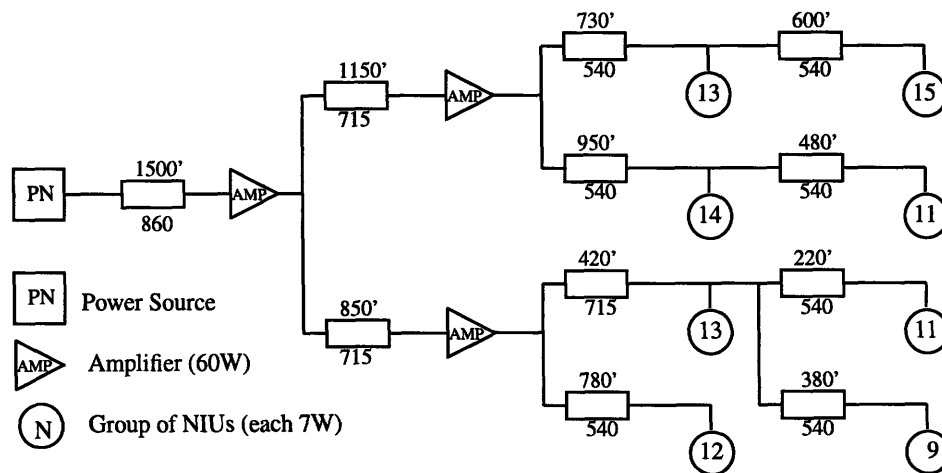


Figure 1-1: Diagram showing an example HFC powering network.

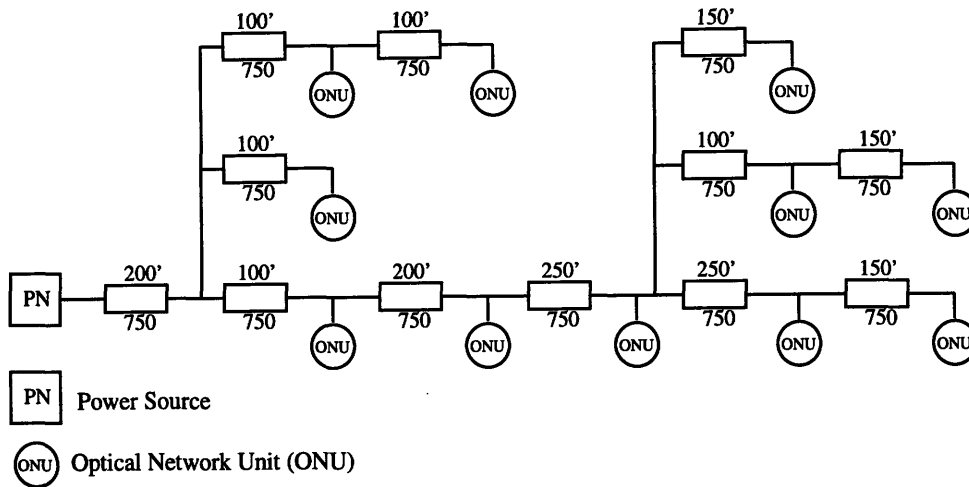


Figure 1-2: Diagram showing an example FTTC powering network.

1.2 Interesting Problems

Since there is presently very little analytical knowledge of the properties of broadband networks, there is a whole spectrum of questions that are of interest to a network designer. This section outlines a variety of relevant problems of interest.

At a very basic level, it is straightforward to obtain an analytical solution for a first-order system, but with higher-order systems there is too much nonlinearity to obtain analytical solutions. As a result, the equilibria for higher-order networks are only obtained numerically. The questions of interest include: how many equilibria are there for arbitrary higher-order network topologies? How many of these are stable operating points? We will show later in Section 3.2.2 that for any arbitrary RCP-tree network at least one stable equilibrium is guaranteed to exist.

Also of interest is the dynamic behavior of a network. Basically, given the initial condition of a network, it would be useful if the dynamical evolution of the system can be modeled accurately. This would allow for the prediction of the eventual steady state of the system, if such a state exists. It is known that the operating point of a network depends critically on the cutoff voltage of the constant-power load. Empirical observations from

low-order network topologies suggest that for a reasonable network with real equilibria, there exists at least one stable and desirable equilibrium and one undesirable equilibrium. It is clear that if the cutoff voltage is chosen carefully, all the undesirable equilibria can be eliminated and the network can be guaranteed to reach a desired stable equilibrium, but it is unclear if there is a systematic way to arrive at a good choice, or even what constitutes a good choice. Do we want the system to settle at the desired operating point in the shortest amount of time from any initial state? Do we just want a guarantee that a desired operating point is reached at steady state? For the purposes of this thesis, we focus on guaranteeing that the system will end up at a desired operating point, starting from any initial conditions. In this thesis, a network will be termed *stable* if it will end up at a desired steady-state equilibrium starting from any initial conditions.

For a first-order system, it is obvious from some elementary analysis (see Section 1.5) that $\frac{V}{2}$ is the optimal cutoff to guarantee stability, where V is the voltage of the power source. With this cutoff voltage, the system is guaranteed to reach the desirable operating point from any initial state. The appropriate choice of cutoff for higher-order systems is not obvious. In fact, it is unclear whether there always exists a cutoff that guarantees stability for an arbitrary network topology. At present, the recommended cutoff for constant-power nodes in existing broadband power networks is $\frac{V}{2}$, but no one can say anything more than “it seems to work.” The analytical justification that this is a good choice under certain conditions is a major result for this thesis.

As mentioned in Section 1.1 above, bus-like networks are common in both HFC and FTTC architectures. Regular ladder networks, where all resistances, all capacitances and all loads are identical, are of particular interest in network design, because many practical networks are well modeled this way, and also because the results for this case form a benchmark and guide to the behavior of more general networks. This thesis devotes particular attention to regular ladder networks.

1.3 Constant-Power Load

The loads in a broadband power network typically comprise high-efficiency regulated switching power supplies that maintain essentially constant voltage across the components that they feed. Such loads are therefore well-modeled as constant-power loads. A constant-power (P) load is a component that dissipates a constant amount of power independent of the voltage across it. Ideally, the voltage-current characteristic would look like the curve shown in Figure 1-3.

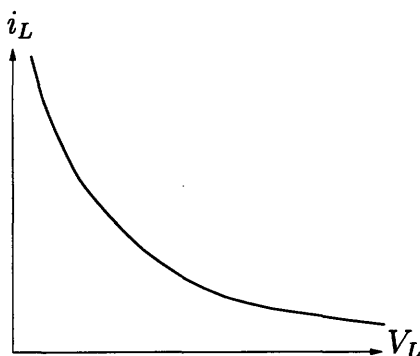


Figure 1-3: Current versus voltage characteristic for ideal constant-power load.

In practice, however, it is impossible and impractical to have an ideal constant-power load because there is an upper limit on the current that can be supplied. Limits on voltage are naturally imposed by the fact that the source voltage is fixed at V . A more realistic model of a practical constant-power load would be one with a low-voltage cutoff, V_c , such that the load turns off and draws close to zero current once the voltage across it drops below the cutoff voltage, i.e.

$$i_L = \begin{cases} \frac{P}{v_L}, & 0 < v_L \leq V_c^* \\ 0, & v_L < V_c^* \end{cases}$$

A typical input current versus voltage characteristic for such a load is shown in Figure 1-4. Henceforth, a load with the characteristic in Figure 1-3 will be referred to as a “ideal constant-power load” while the load in Figure 1-4 will be referred to as a “non-ideal constant-power load” or simply as a “constant-power load.”

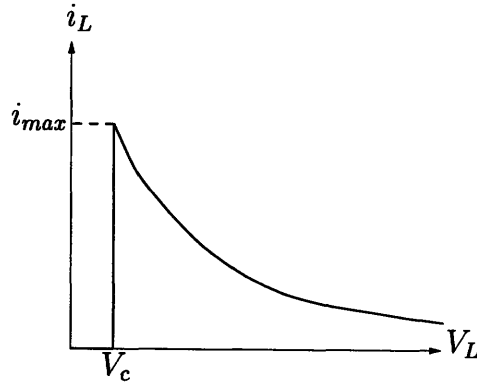


Figure 1-4: Typical input current versus voltage characteristic for constant-power load with voltage cutoff V_c .

In practice, some hysteresis is designed into a constant-power load, i.e. the voltage at which the load turns “on” and draws current is set a little higher than the voltage at which it shuts off once turned “on.” In this thesis, we will assume that loads behave ideally, and that the cutoff voltage is the same when the system moves in either direction. Also, we assume that when $v_L = V_c$ it is possible for the load to operate at any current between 0 and i_{max} (e.g. by switching between the “on” and “off” states with the appropriate duty cycle). We will refer to this region of operation when the current-voltage characteristic is vertical with $v_L = V_c$ as the *metastable* region. Similarly, we will refer to the region when the load is “off” as the *cutoff* region. When the load is operating past the metastable region, we will refer to the load as being *on*.

1.4 Circuit Models

In the network topologies to be analyzed, the constant-power load elements are modeled as described in Section 1.3, with current-voltage characteristics as shown in Figure 1-4. In addition, the dynamics of the systems are modeled by introducing a suitable capacitor across each constant-power load. Figure 1-5 shows a typical second-order example. The main network topologies studied in this thesis are RCP trees, with particular emphasis on

ladder networks since they effectively model bus-like networks common in both HFC and FTTC architectures.

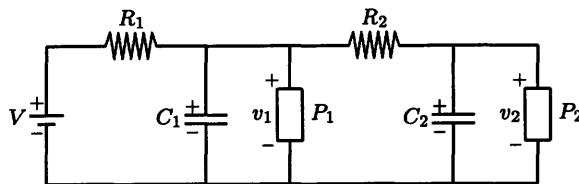


Figure 1-5: Modeling of system dynamics.

In [1], networks are modeled with another resistor along the return path instead of having all the constant-power loads attached to a common ground. An example of a second-order system modeled in this way is shown in Figure 1-6. A closer look, however, reveals that the two circuit models in Figures 1-5 and 1-6 are in fact entirely equivalent in terms of dynamic behavior and steady-state current flow and power dissipation when $R_1 = R_{1,a} + R_{1,b}$ and $R_2 = R_{2,a} + R_{2,b}$. The model in Figure 1-5 is simpler, however, since there are fewer resistors, so it is the model of choice for this thesis.

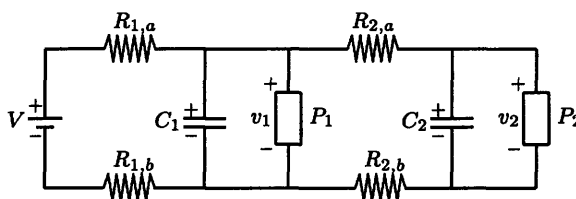


Figure 1-6: Equivalent second-order model.

1.5 First-Order System

Before diving into the detailed analysis of general RCP networks, we present the analysis of the simplest possible RCP configuration — a first-order RCP system. This analysis will provide some preliminary insight into the dynamics of RCP networks. We begin with the simpler ideal constant-power model and then later extend the results to the non-ideal model.

1.5.1 Basic System

We analyze the dynamics of a simple network with one constant-power load by modeling the load as a capacitor in parallel with an ideal constant-power load of the sort described in Section 1.3; it draws a constant amount of power regardless of the voltage across it. Figure 1-7 shows this first-order model.

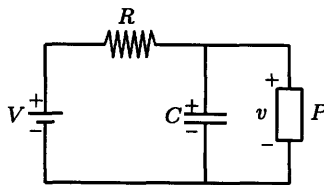


Figure 1-7: Circuit diagram for first-order system.

By Kirchhoff's Current Law,

$$C \frac{dv}{dt} = \frac{V - v}{R} - \frac{P}{v} \quad (1.1)$$

$$= -\frac{1}{Rv}(v^2 - Vv + PR) \quad (1.2)$$

Solving for the roots of the quadratic expression, we obtain

$$v = \frac{V}{2} \pm \frac{\sqrt{V^2 - 4PR}}{2} \quad (1.3)$$

Assuming $V^2 > 4PR$, there are two real roots. Defining $v_+ = \frac{V}{2} + \frac{\sqrt{V^2 - 4PR}}{2}$ and $v_- = \frac{V}{2} - \frac{\sqrt{V^2 - 4PR}}{2}$, (1.2) can be written as

$$\frac{dv}{dt} = -\frac{(v - v_+)(v - v_-)}{CRv} \quad (1.4)$$

From (1.4), we deduce that the sign of the derivative is negative when $0 < v < v_-$, positive when $v_- < v < v_+$, and finally negative when $v_+ < v < V$. Figure 1-8 is a graphical representation of this result. The interpretation of this result is straightforward: v_- is an

unstable equilibrium point, while v_+ is a stable equilibrium point. If the system starts at an initial condition such that $v_- < v < V$, the system will come to rest at v_+ , while an initial condition where $0 < v < v_-$ will result in v falling to 0.

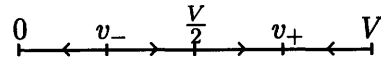


Figure 1-8: Dynamic behavior for first-order system.

1.5.2 Non-Ideal Constant-Power Load with Voltage Cutoff

From the analysis of the system dynamics in the previous subsection, it is that apparent that there is no obvious way for the system to make a transition from a zero initial condition to the desired stable operating equilibrium. If the system were to start off at the origin, it would stay stuck at the origin. We can get around this problem by replacing the ideal load with a non-ideal load that has a voltage cutoff, V_c , chosen higher than v_- .

With this new load, the circuit is equivalent when $v < V_c$ to a simple DC voltage source charging a capacitive load. The behavior of the system when $v > V_c$ is the same as that described in the previous subsection. With this, we effectively remove the lower equilibrium and the system ends up with a single stable static equilibrium at the desired level. Figure 1-9 is a graphical representation of this result. We know that $v_- \leq \frac{V}{2}$, so choosing $V_c = \frac{V}{2}$ guarantees that the system has a unique stable equilibrium. Of course, there is also our assumption of $V^2 > 4PR$ to ensure that the roots in (1.3) are real. If $V^2 < 4PR$, then the right-hand side of (1.2) is always negative. As a result, $\frac{dv}{dt} < 0 \forall v$ and so the voltage across the load will be decreasing for all values of v . The introduction of a cutoff will simply create a stable equilibrium at the cutoff voltage. Since this equilibrium actually corresponds to the load operating in the metastable region, we refer to it as a dynamic equilibrium. The graphical representation of this situation is shown in Figure 1-10.

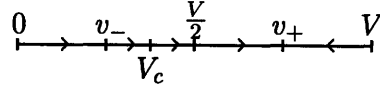


Figure 1-9: Dynamic behavior for first-order system with cutoff V_c .

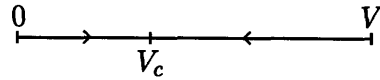


Figure 1-10: Dynamic behavior for situation with no real roots.

1.6 Summary of Contributions of this Thesis

Chapter 2 is arguably the most important chapter of this thesis; it lays the analytical foundation for the thesis with the detailed analysis of a simple second-order network. The modeling of an RCP-tree network as a gradient system is introduced. The properties of gradient systems are then used to derive dynamic properties, as well as some sufficient conditions for a desired operating point to be a stable static equilibrium of the system. The chapter also presents a worked example of how the analysis of possible steady states may be used to derive simple sufficient conditions to guarantee that a system will end up at a desired operating point in the steady state.

Chapter 3 builds on the results of Chapter 2 and derives corresponding results for higher-order systems. It presents a method for constructing the energy function of the gradient system for any arbitrary network topology, as well as a detailed analysis of the energy function thus derived. The identification and characterization of both static and dynamic equilibria are discussed in detail. Finally, the chapter wraps up with a general way of deriving simple sufficient conditions for system stability from the characterization of the equilibria. In particular, the specific results are applied to regular ladder networks.

From the fact that all RCP-tree networks can be modeled as gradient systems, we know that the state of an RCP-tree network will eventually settle down at a static or dynamic equilibrium point within the region \mathcal{W} , where $0 < v_i < V$ for $i = 1, \dots, n$. Thus, the

computation of equilibria for a system is a very important issue. In Chapter 4, we present a survey of the methods that can be employed to obtain both the static and dynamic equilibria of an RCP-tree network. An aggregated-model approximation that allows us to quite accurately approximate the steady-state behavior of a high-order network with a first-order network is also introduced.

In Chapter 5, the theoretical results from Chapters 2 to 4 are applied to the actual process of designing a network. Some important issues in network design are discussed and our theoretical results are evaluated in the context of a broadband power network. In particular, a proposed benchmark model is examined in detail and our conditions for guaranteeing stability are evaluated. The effectiveness of the aggregated-model approximation as a means for estimating total operational current and power dissipation is also discussed. Finally, the chapter concludes with an evaluation of the merit of choosing $\frac{V}{2}$ as the cutoff voltage.

Chapter 6 concludes this thesis with a summary of the major results presented and proposes some interesting questions that can be the basis for future work on RCP-tree networks and broadband power network design.

Chapter 2

System Modeling and Dynamics: Second-Order System

This chapter lays the analytical foundation for the thesis with a preliminary analysis of a simple second-order RCP network. We first analyze a system with ideal constant-power loads. Next, we obtain gradient system representations for both a system with ideal loads and one with non-ideal loads. We then present an analysis of the dynamics of the system with non-ideal loads and derive conditions sufficient to ensure convergence to a desired stable equilibrium. As mentioned in Section 1.2, the network will be simply termed *stable* if it will end up at a desired steady-state equilibrium starting from any initial conditions. Finally, we analyze the steady state in detail to obtain simple sufficient conditions for stability. Overall, this chapter illustrates the major results of this thesis in the context of a simple second-order system. Generalizations of the results described here for higher-order systems are given in Chapter 3.

2.1 Preliminary Analysis

We repeat the analysis in Section 1.5.1 on a second-order RCP system with ideal constant-power loads. As before, the idealized assumption simplifies the analysis by allowing us to avoid dealing with discontinuities. A second-order system is obtained by cascading two first-order systems, as shown in Figure 2-1. The parallel configuration is not considered here because it can essentially be decoupled into two independent first-order systems.

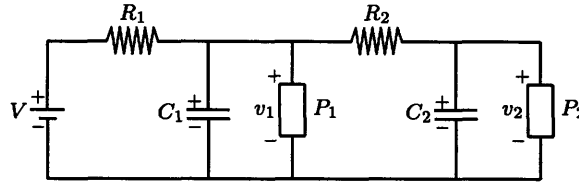


Figure 2-1: Circuit diagram for second-order system.

To analyze this circuit, we apply Kirchoff's Current Law to the two intermediate nodes to obtain

$$\frac{V - v_1}{R_1} = C_1 \frac{dv_1}{dt} + \frac{P_1}{v_1} + \frac{v_1 - v_2}{R_2} \quad (2.1)$$

$$\frac{v_1 - v_2}{R_2} = C_2 \frac{dv_2}{dt} + \frac{P_2}{v_2} \quad (2.2)$$

Equations (2.1) and (2.2) are evidently nonlinear, and an explicit solution is not to be expected. Instead, we rewrite (2.1) and (2.2) into the following state-space form:

$$\frac{dv_1}{dt} = \frac{1}{C_1} \left(\frac{V - v_1}{R_1} - \frac{P_1}{v_1} - \frac{v_1 - v_2}{R_2} \right) \quad (2.3)$$

$$= -\frac{R_1 + R_2}{C_1 R_1 R_2 v_1} \left(v_1^2 - \frac{V R_2 + v_2 R_1}{R_1 + R_2} v_1 + \frac{P_1 R_1 R_2}{R_1 + R_2} \right) \quad (2.4)$$

$$= -\frac{1}{C_1 R_{\parallel} v_1} \left(v_1^2 - R_{\parallel} \left(\frac{V}{R_1} + \frac{v_2}{R_2} \right) v_1 + P_1 R_{\parallel} \right) \quad (2.5)$$

$$\frac{dv_2}{dt} = \frac{1}{C_2} \left(\frac{v_1 - v_2}{R_2} - \frac{P_2}{v_2} \right) \quad (2.6)$$

$$= -\frac{1}{C_2 R_2 v_2} \left(v_2^2 - v_1 v_2 + P_2 R_2 \right) \quad (2.7)$$

where $R_{||} = \frac{R_1 R_2}{R_1 + R_2}$. Next, we solve for $\frac{dv_1}{dt} = 0$ (assuming $v_1 \neq 0$) and $\frac{dv_2}{dt} = 0$ (assuming $v_2 \neq 0$) to obtain the following equilibrium points:

$$v_1 = \frac{R_{||}}{2} \left(\frac{V}{R_1} + \frac{v_2}{R_2} \right) \pm \sqrt{\frac{R_{||}^2}{4} \left(\frac{V}{R_1} + \frac{v_2}{R_2} \right)^2 - P_1 R_{||}} \quad (2.8)$$

$$v_2 = \frac{v_1}{2} \pm \sqrt{\frac{v_1^2}{4} - P_2 R_2} \quad (2.9)$$

The equations (2.8) and (2.9) define two curves in the v_1 - v_2 plane. Figure 2-2 is a plot of these curves. The turning points of the two curves respectively are

$$(\alpha, \gamma) = \left(\sqrt{P_1 R_{||}}, 2 \frac{R_2}{R_{||}} \sqrt{P_1 R_{||}} - \frac{R_2}{R_1} V \right) \text{ and} \quad (2.10)$$

$$(\beta, \delta) = \left(2\sqrt{P_2 R_2}, \sqrt{P_2 R_2} \right) \quad (2.11)$$

It is observed that there are two points of static equilibrium for the system; one point is near (V, V) , while the other is closer to the origin. Graphically, the dynamics of the system can be represented as a vector field. Figure 2-3 shows the directions of the field along the curve where $\frac{dv_1}{dt} = 0$ and similarly along the curve where $\frac{dv_2}{dt} = 0$. For the given example, it can be deduced from the direction of the field lines that the equilibrium nearer to (V, V) is stable while the one near the origin is not.

There can also exist configurations of parameters for which the two curves do not intersect and there is no real solution to (2.8) and (2.9). Physically, this represents a situation where the current drawn by the loads is so large that the current supplied by the source cannot ever charge up the capacitors, and hence the equilibrium state will be one where all nodal voltages are stuck at zero. In practice, this is not a particularly interesting or desirable situation. For the remainder of this chapter, we will assume that the system is such that (2.8) and (2.9) have a pair of real solutions.

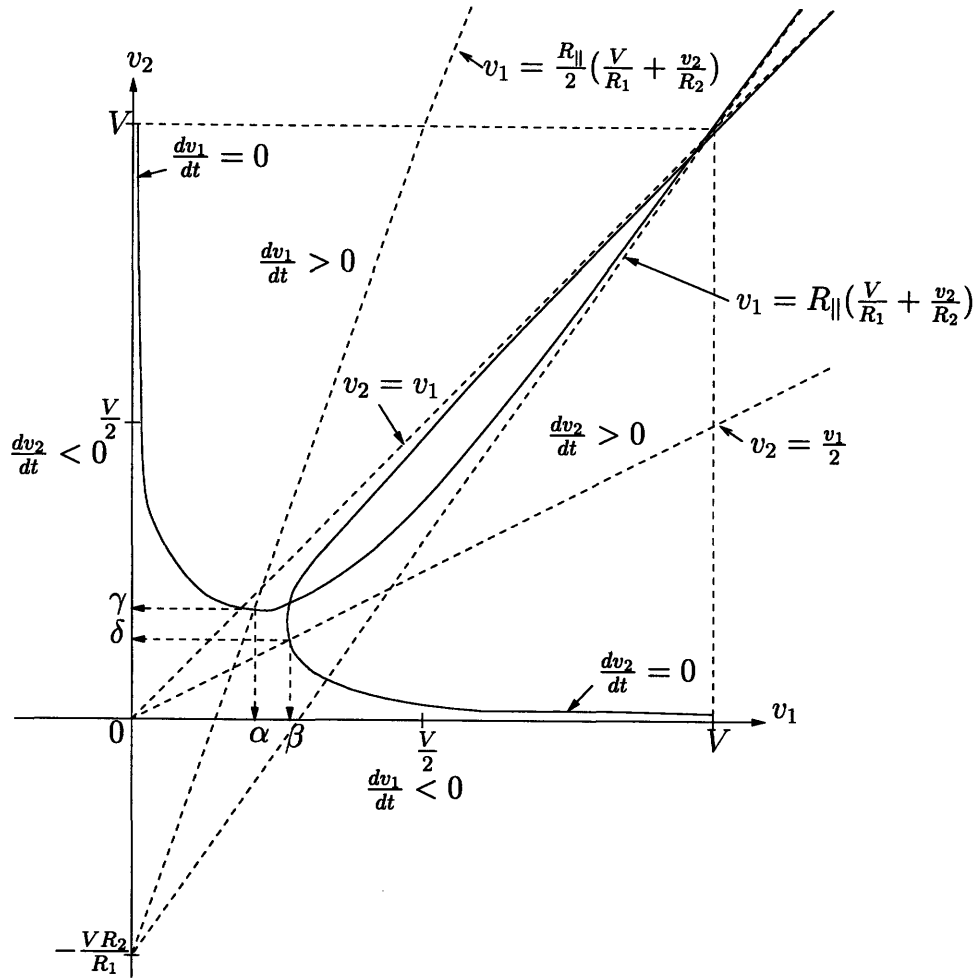


Figure 2-2: Plot of $\dot{v}_1 = 0$ and $\dot{v}_2 = 0$ loci for second-order system.

2.2 Gradient System Representation

In this section, we demonstrate that it is possible to express a RCP second-order system as a gradient system [2, 3]. Such a system has many well-understood properties which are useful in characterizing the dynamics and stability properties of the system.

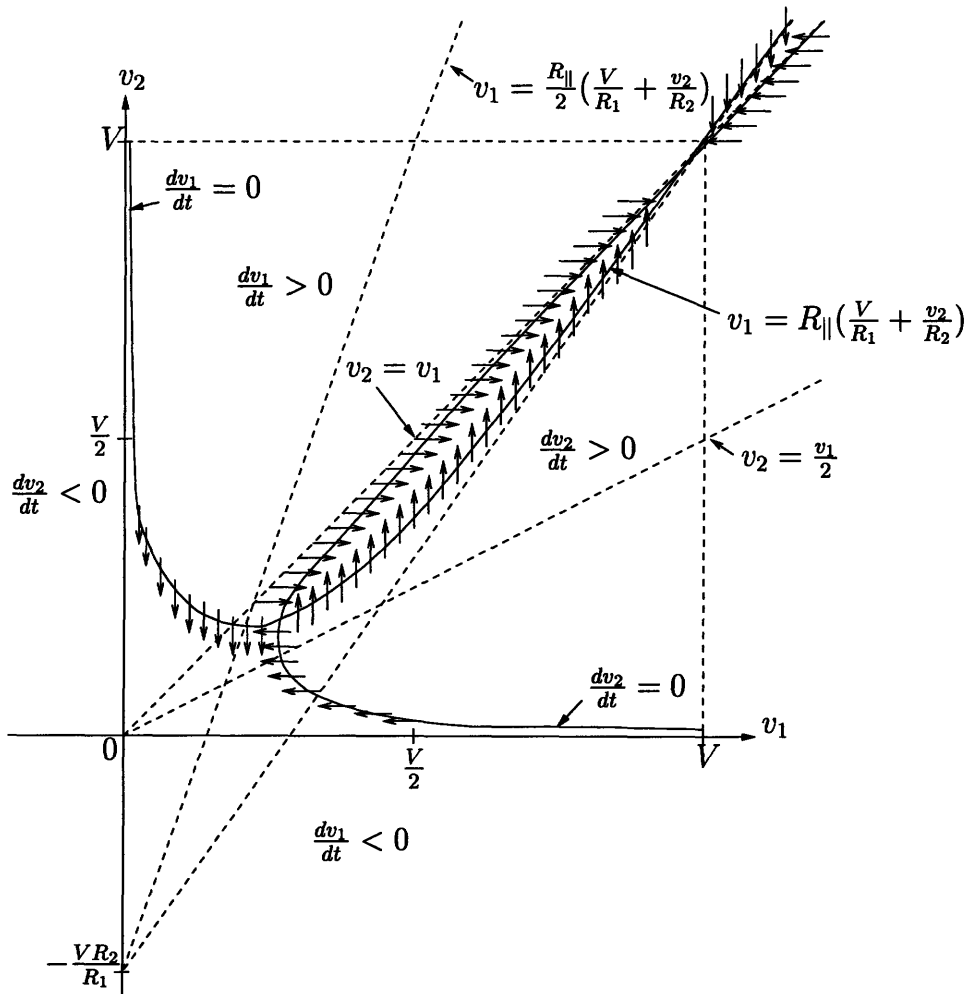


Figure 2-3: Vector fields for second-order system.

2.2.1 Gradient System

Definition

We begin with the definition of a gradient system. A gradient system is a vector field defined by

$$\frac{d\mathbf{v}}{dt} = -\text{grad } E(\mathbf{v}) \quad (2.12)$$

where $E(\mathbf{v})$ is a scalar function referred to as the *energy function* and $\text{grad } E(\mathbf{v})$ is defined by the following fundamental equality:

$$dE = \langle \text{grad } E(\mathbf{v}), d\mathbf{v} \rangle$$

with $\langle \mathbf{x}, \mathbf{y} \rangle$ denoting an inner product for the vectors \mathbf{x} and \mathbf{y} . The rate of change of $E(\mathbf{v})$ along the field is given by

$$\dot{E}(\mathbf{v}) = \langle \text{grad } E(\mathbf{v}), \frac{d\mathbf{v}}{dt} \rangle \quad (2.13)$$

$$= -|\text{grad } E(\mathbf{v})|^2 \quad (2.14)$$

so, $\dot{E}(\mathbf{v}) \leq 0, \forall \mathbf{v}$, and $\dot{E}(\mathbf{v}) = 0$ iff $\mathbf{v} = \bar{\mathbf{v}}$ is an equilibrium point, i.e. a point where $\text{grad } E(\mathbf{v}) = 0$ and correspondingly $\frac{d\mathbf{v}}{dt} = 0$.

Weighted Euclidean Inner Product

For the models in of this thesis, we need to use the following weighted Euclidean inner product for the definition of the gradient:

$$\langle \mathbf{x}, \mathbf{y} \rangle = \sum_{i=1}^n C_i x_i y_i, \quad C_i > 0 \text{ for all } i \quad (2.15)$$

We can verify that this constitutes a valid inner product since the following properties are satisfied:

$$\langle \alpha \mathbf{x} + \beta \mathbf{y}, \mathbf{z} \rangle = \alpha \langle \mathbf{x}, \mathbf{z} \rangle + \beta \langle \mathbf{y}, \mathbf{z} \rangle$$

$$\langle \mathbf{x}, \mathbf{y} \rangle = \langle \mathbf{y}, \mathbf{x} \rangle$$

$$\langle \mathbf{x}, \mathbf{x} \rangle > 0 \Leftrightarrow \mathbf{x} \neq 0$$

With this definition,

$$\text{grad } E(\mathbf{v}) = \mathbf{C}^{-1} \frac{dE}{d\mathbf{v}}(\mathbf{v}) \quad (2.16)$$

where

$$\mathbf{C} = \begin{bmatrix} C_1 & 0 & \cdots & 0 \\ 0 & C_2 & \cdots & 0 \\ \vdots & \vdots & \ddots & \vdots \\ 0 & 0 & \cdots & C_n \end{bmatrix}, \mathbf{v} = \begin{bmatrix} v_1 \\ v_2 \\ \vdots \\ v_n \end{bmatrix}$$

If \mathbf{C} is the identity matrix, the inner product reduces to the usual Euclidean inner product, and the definition of the gradient becomes the conventional one.

2.2.2 Energy Function for Ideal Loads

Consider the second-order system with ideal loads as described in Section 2.1. First, we rewrite (2.5) and (2.7) as

$$C_1 \frac{dv_1}{dt} = -\frac{1}{R_{||}} v_1 + \left(\frac{V}{R_1} + \frac{v_2}{R_2} \right) - \frac{P_1}{v_1} \quad (2.17)$$

$$C_2 \frac{dv_2}{dt} = -\frac{1}{R_2} v_2 + \frac{v_1}{R_2} - \frac{P_2}{v_2} \quad (2.18)$$

Our goal is to express (2.17) and (2.18) in the following form, for an appropriate $E(v_1, v_2)$:

$$C_1 \frac{dv_1}{dt} = -\frac{\partial E}{\partial v_1} \quad (2.19)$$

$$C_2 \frac{dv_2}{dt} = -\frac{\partial E}{\partial v_2} \quad (2.20)$$

Integrating the right hand sides of (2.17) and (2.18) yields

$$E(v_1, v_2) = -\int C_1 \frac{dv_1}{dt} dv_1 = \frac{1}{2R_{||}} v_1^2 - \left(\frac{V}{R_1} - \frac{v_2}{R_2} \right) v_1 - P_1 \ln(v_1) + f(v_2) \quad (2.21)$$

$$E(v_1, v_2) = -\int C_2 \frac{dv_2}{dt} dv_2 = \frac{1}{2R_2} v_2^2 - \frac{v_1 v_2}{R_2} + P_2 \ln(v_2) + g(v_1) \quad (2.22)$$

Matching $f(v_2)$ and $g(v_1)$ yields

$$E(v_1, v_2) = \frac{1}{2R_{||}} v_1^2 + \frac{1}{2R_2} v_2^2 - \frac{V}{R_1} v_1 - \frac{v_1 v_2}{R_2} + P_1 \ln(v_1) + P_2 \ln(v_2) \quad (2.23)$$

Hence, we can write the system of equations as

$$\mathbf{C} \frac{d\mathbf{v}}{dt} = -\frac{dE}{d\mathbf{v}}(\mathbf{v}) \quad (2.24)$$

where

$$\mathbf{C} = \begin{bmatrix} C_1 & 0 \\ 0 & C_2 \end{bmatrix}, \quad \mathbf{v} = \begin{bmatrix} v_1 \\ v_2 \end{bmatrix}$$

Comparing (2.16) and (2.24), we conclude that

$$\frac{d\mathbf{v}}{dt} = -\text{grad } E(\mathbf{v}) \quad (2.25)$$

which shows that that this second-order system is in fact a gradient system with respect to a weighted Euclidean inner product. If the capacitances C_1 and C_2 are equal, the system reduces to an ordinary Euclidean system where flow lines are normal to the level surfaces; if the capacitances C_1 and C_2 are not equal, the flow lines are normal to the level surfaces in the generalized sense defined by (2.15).

2.2.3 Energy Function for Non-Ideal Loads

The derivation of the results in the previous section assumed that the constant-power loads in the system were ideal, but a small modification yields the energy function for a system with non-ideal loads. We define

$$K_1(v_1) = \begin{cases} P_1, & v_1 \geq V_1^* > 0 \\ 0, & v_1 < V_1^* \end{cases} \quad (2.26)$$

$$K_2(v_2) = \begin{cases} P_2, & v_2 \geq V_2^* > 0 \\ 0, & v_2 < V_2^* \end{cases} \quad (2.27)$$

where V_1^* and V_2^* are the cutoff voltages for the first and second loads respectively. Then notice that $\frac{K_1(v_1)}{v_1}$ and $\frac{K_2(v_2)}{v_2}$ are exactly the currents flowing through the two loads for all values of v_1 and v_2 . Replacing $\frac{P_1}{v_1}$ and $\frac{P_2}{v_2}$ in (2.17) and (2.18) respectively by $\frac{K_1(v_1)}{v_1}$ and

$\frac{K_2(v_2)}{v_2}$, we can repeat our earlier derivation to conclude that now

$$E(v_1, v_2) = \frac{1}{2R_{||}}v_1^2 + \frac{1}{2R_2}v_2^2 - \frac{V}{R_1}v_1 - \frac{v_1v_2}{R_2} + K_1(v_1) \ln\left(\frac{v_1}{V_1^*}\right) + K_2(v_2) \ln\left(\frac{v_2}{V_2^*}\right) \quad (2.28)$$

It is easily verified that the energy function remains continuous at the cutoff boundaries, although its gradient is discontinuous at the boundaries.

With this modification to $E(\mathbf{v})$, the equation

$$\frac{dE(\mathbf{v})}{dt} = -\text{grad } E(\mathbf{v}) \quad (2.29)$$

holds even for a system with non-ideal loads, except that a more detailed analysis is required at the cutoff boundaries. Figures 2-4 and 2-5 show a 3-dimensional plot of an example of a typical energy function from two different angles.

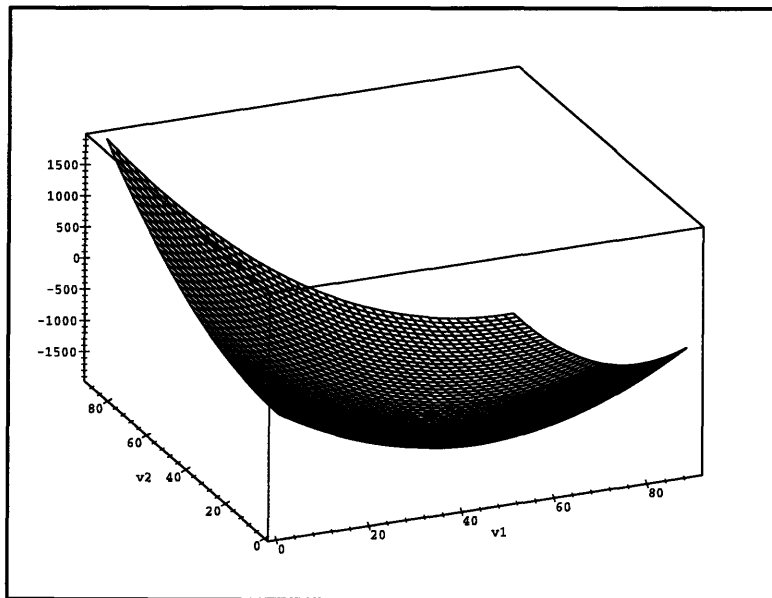


Figure 2-4: Example plot of $E(v_1, v_2)$.

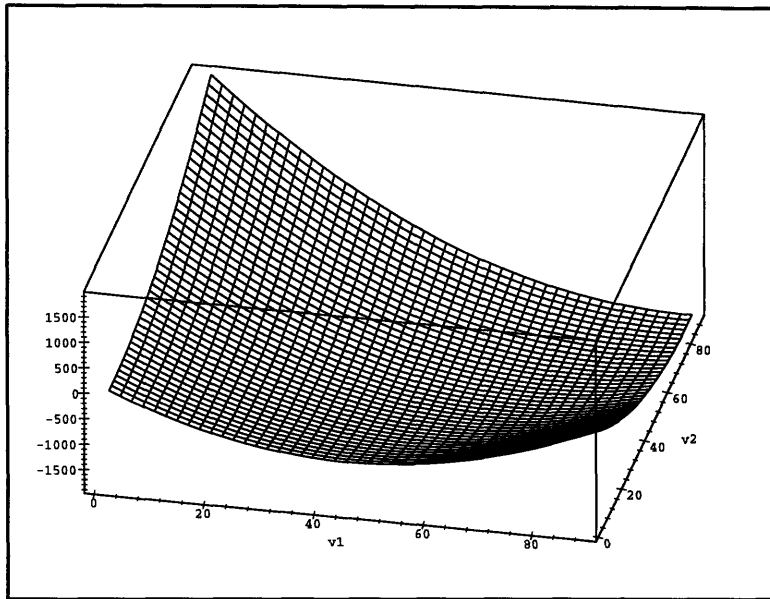


Figure 2-5: Example plot of $E(v_1, v_2)$ (different angle).

2.2.4 Application

The fact that the system is a gradient system allows us to draw several conclusions about the system [2, 3]. For example, in any region in which the energy function has continuous second-order partial derivatives, any (strict) local minimum of $E(\mathbf{v})$ is an asymptotically stable equilibrium point of the system.

It is also possible to characterize the equilibria of the system by examining the Hessian (i.e. the matrix of second partial derivatives) of the energy function, as long as the equilibria are not on the boundary lines defined by the cutoff voltages. Although our energy function is non-differentiable at these boundary lines, it is continuously twice-differentiable everywhere else in the region $0 < v_1 < V$, $0 < v_2 < V$.

Consider a regular second-order system with identical components, i.e. $R_1 = R_2 = R$, $P_1 = P_2 = P$ and $C_1 = C_2 = C$, and identical cutoff voltages of V_c for both loads. From (2.28), we find that the Hessian of the energy function at any point (v_1, v_2) in the quadrant

$V_c < v_1 < V$, $V_c < v_2 < V$ is given by

$$\frac{d^2 E}{d\mathbf{v}^2}(\mathbf{v}) = \begin{bmatrix} \frac{d^2 E}{dv_1^2} & \frac{d^2 E}{dv_1 dv_2} \\ \frac{d^2 E}{dv_2 dv_1} & \frac{d^2 E}{dv_2^2} \end{bmatrix} = \begin{bmatrix} -\frac{P}{v_1^2} + \frac{2}{R} & -\frac{1}{R} \\ -\frac{1}{R} & -\frac{P}{v_2^2} + \frac{1}{R} \end{bmatrix} \quad (2.30)$$

Note that for $v_1 > V_c$, $v_2 > V_c$ we have

$$\frac{d^2 E}{d\mathbf{v}^2}(v_1, v_2) - \frac{d^2 E}{d\mathbf{v}^2}(V_c, V_c) > 0 \quad (2.31)$$

where ' > 0 ' here denotes positive definiteness, and the notation $\frac{d^2 E}{d\mathbf{v}^2}(V_c, V_c)$ is used to denote the rightmost matrix in (2.30) evaluated at $v_1 = V_c$, $v_2 = V_c$, but not to imply that this is actually the Hessian of $E(\mathbf{v})$ at $v_1 = v_2 = V_c$. Hence if

$$\frac{d^2 E}{d\mathbf{v}^2}(V_c, V_c) > 0, \quad (2.32)$$

then any equilibria in the region $v_1 > V_c$, $v_2 > V_c$ must be asymptotically stable, because the matrix $-\frac{d^2 E}{d\mathbf{v}^2}(\mathbf{v})$ evaluated at any such equilibrium governs the small-signal dynamics at this equilibrium, and (2.31) and (2.32) together imply that $-\frac{d^2 E}{d\mathbf{v}^2}(\mathbf{v})$ is negative definite, i.e. has all its eigenvalues real and negative. It is easy to show that any convex region where the Hessian is positive definite can have at most one equilibrium (which must be stable). The condition (2.32) is equivalent to requiring

$$\begin{aligned} -\frac{P}{V_c^2} + \frac{1}{R} &> 0, \\ \left(-\frac{P}{V_c^2} + \frac{2}{R}\right)\left(-\frac{P}{V_c^2} + \frac{1}{R}\right) - \frac{1}{R^2} &> 0 \end{aligned} \quad (2.33)$$

From inequality (2.34), we obtain

$$R < \frac{3 - \sqrt{5} V_c^2}{2} \frac{V_c^2}{P} < \frac{V_c^2}{P} \quad (2.34)$$

The following condition therefore guarantees that for a regular second-order system with cutoff voltages set at V_c , any equilibrium in the box bounded by $(V_c + \epsilon, V_c + \epsilon)$ and (V, V)

will be stable and unique:

$$V_c^2 > \frac{2}{3 - \sqrt{5}} PR \quad (2.35)$$

There is also a possibility that equilibria may occur at the cutoff boundaries. These equilibria cannot be characterized by considering the Hessian of the energy function because the function is non-differentiable at these points. In order to understand the dynamic behavior of the system at these points, more detailed analysis is required. The following section follows up on this analysis.

2.3 Boundary Behavior

In this section, we examine a second-order system much like the one discussed in the Section 2.1, but with the ideal constant-power loads replaced by non-ideal loads. To make the analysis more tractable, we assume that both loads have the same cutoff voltage, V_c . Figure 2-1 is still the relevant circuit diagram for this discussion. For this analysis, we divide the v_1 - v_2 plane into 4 regions: $\{v_1 < V_c, v_2 < V_c\}$, $\{v_1 > V_c, v_2 < V_c\}$, $\{v_1 < V_c, v_2 > V_c\}$ and $\{v_1 > V_c, v_2 > V_c\}$, and consider each of these cases separately.

Region I: $v_1 < V_c, v_2 < V_c$

In this region, both constant-power loads are in cutoff. The equivalent circuit is one with a voltage source V charging up the two capacitors, C_1 and C_2 , through resistors R_1 and R_2 . The corresponding state equations are

$$\frac{dv_1}{dt} = \frac{1}{C_1 R_1} \left(V - \left(1 + \frac{R_1}{R_2}\right) v_1 + \frac{R_1}{R_2} v_2 \right) \quad (2.36)$$

$$\frac{dv_2}{dt} = \frac{1}{C_2 R_2} (v_1 - v_2) \quad (2.37)$$

Region II: $v_1 > V_c, v_2 < V_c$

In this region, P_1 is on, but P_2 is still in cutoff. The corresponding state equations are

$$\frac{dv_1}{dt} = -\frac{1}{C_1 R_{||} v_1} (v_1^2 - R_{||} (\frac{V}{R_1} + \frac{v_2}{R_2}) v_1 + P_1 R_{||}) \quad (2.38)$$

$$\frac{dv_2}{dt} = \frac{1}{C_2 R_2} (v_1 - v_2) \quad (2.39)$$

Region III: $v_1 < V_c, v_2 > V_c$

In this region, P_2 is on, but P_1 is still in cutoff. The corresponding state equations are

$$\frac{dv_1}{dt} = \frac{1}{C_1 R_1} \left(V - (1 + \frac{R_1}{R_2}) v_1 + \frac{R_1}{R_2} v_2 \right) \quad (2.40)$$

$$\frac{dv_2}{dt} = -\frac{1}{C_2 R_2 v_2} (v_2^2 - v_1 v_2 + P_2 R_2) \quad (2.41)$$

Region IV: $v_1 > V_c, v_2 > V_c$

In this region, both constant-power loads are functioning normally and the overall behavior of the system is identical to that of the system analyzed in Section 2.1. The corresponding state equations are (2.5) and (2.7).

Piecing together the dynamics in these four regions for an example of a second-order system, we obtain the phase-plane portrait shown in Figure 2-6. In this particular example, having a cutoff at V_c has effectively eliminated the unstable equilibrium point near the origin that was presented in Figure 2-3, creating a steady transition from zero initial state to the final stable equilibrium point. In order to more fully appreciate the effect of the cutoff voltage on the dynamics, it is essential to examine the boundary of the above regions of operation in more detail.

It is found that the steady state operating point for a second-order system is intrinsically tied to the behavior of the system at the cutoff boundaries $v_1 = V_c$ and $v_2 = V_c$. We analyze

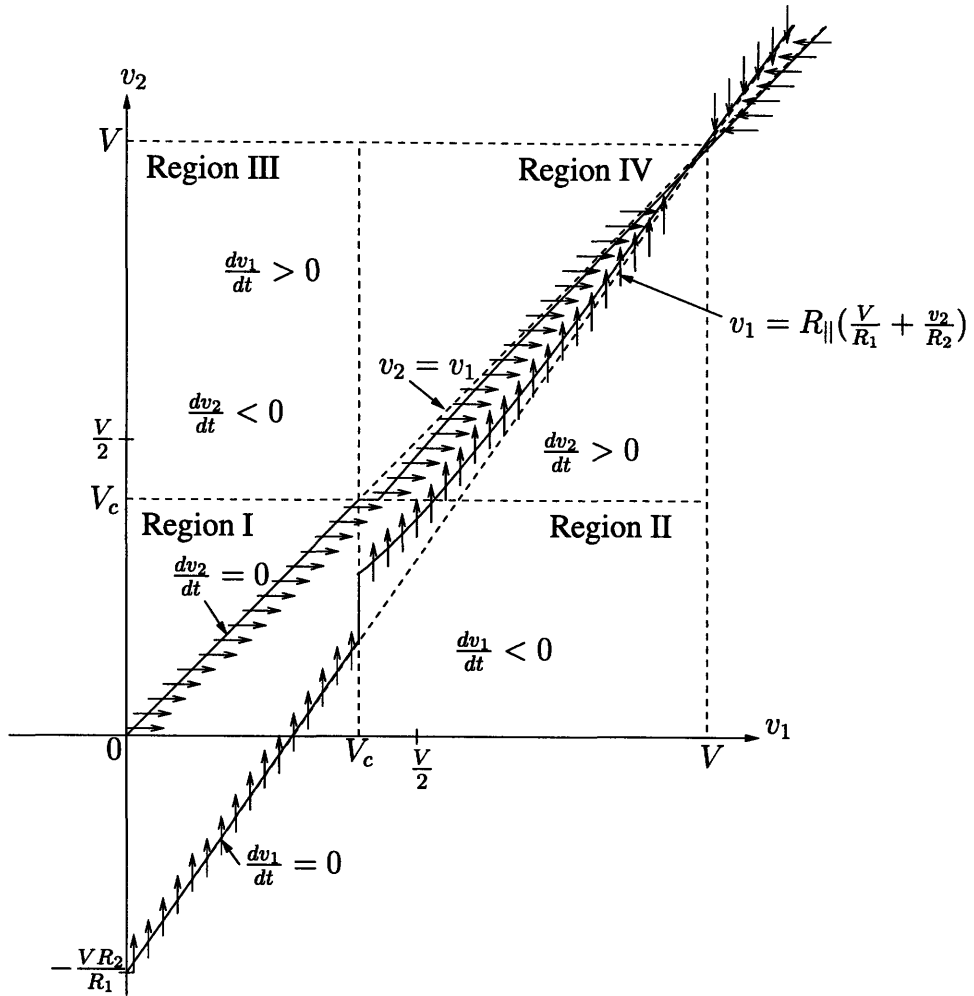


Figure 2-6: Phase-plane portrait for second-order system with cutoff.

the system in detail and find that the behavior of the system at a cutoff boundary is the limit of the behavior of the system on both sides of the boundary. More specifically, when the cutoff voltages of both loads are equal to V_c , it is possible for a dynamic equilibrium to occur on the boundary $v_1 = V_c$ iff

$$\frac{P_1 R_2}{V_c} + (1 + \frac{R_2}{R_1})V_c > V_c \quad (2.42)$$

Hence, to ensure that this does not happen, we require

$$V > \frac{P_1 R_1}{V_c} + V_c \quad (2.43)$$

Similarly, it is possible for a dynamic equilibrium to occur on the boundary $v_2 = V_c$ iff

$$\frac{\frac{V}{R_1} + \frac{V_c}{R_2} + \sqrt{\left(\frac{V}{R_1} + \frac{V_c}{R_2}\right)^2 - 4\left(\frac{1}{R_1} + \frac{1}{R_2}\right)P_1}}{2\left(\frac{1}{R_1} + \frac{1}{R_2}\right)} < \frac{P_2 R_2}{V_c} + V_c \quad (2.44)$$

but we can prevent this if

$$V > V_c + \frac{P_2 R_1 R_2}{V_c R_{||}} + \frac{P_1 R_1}{\frac{P_2 R_2}{V_c} + V_c} \quad (2.45)$$

where $R_{||} = \frac{R_1 R_2}{R_1 + R_2}$. For the case where $V_c = \frac{V}{2}$, $R_1 = R_2 = R$ and $P_1 = P_2 = P$, this condition simplifies to

$$V^2 > 4(1 + \sqrt{3})PR \quad (2.46)$$

The details for these derivations are found in Appendix A.

The exact details of the derivations of the above conditions are not important. The essential point is that, through a detailed algebraic analysis of the dynamic behavior at the cutoff boundaries, we can derive sufficient conditions that guarantee that dynamic equilibria cannot exist for the system. However, this technique is not practical for higher-order systems. Later in Section 3.4.1, we will demonstrate that although the system is only a conventional gradient system in a piecewise sense, the system is well-behaved at the cutoff boundaries. In particular, the system satisfies the property that the energy function is monotonically decreasing with time even on the cutoff boundaries, if the system is not in equilibrium. This observation together with the fact that the energy function is lower bounded within \mathcal{W} , the region of \mathfrak{R}^2 such that $0 \leq v_k < V$ for $k = 1, 2$, allow us to conclude that limit cycles cannot occur and the system must eventually settle at an equilibrium. Hence, sufficient conditions to ensure that the system ends up at a desired equilibrium can be obtained simply from studying the steady-state behavior. We will demonstrate this

concept for the second-order case with identical cutoff voltages in the following section.

2.4 Steady-State Analysis

In Section 2.3 we derived general conditions that ensure a second-order system will not get stuck at the cutoff voltages of the loads by examining the dynamics of the system at the boundaries defined by the cutoff voltages. Here, for a regular second-order system where all the resistances, all the capacitances and all the loads are identical, we present an alternative approach that involves examining possible steady states. The circuit diagram for the system to be analyzed is given in Figure 2-7.

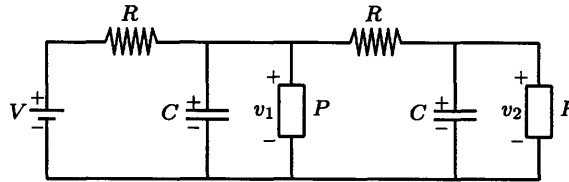


Figure 2-7: Regular second-order system.

We will define an *operational equilibrium* as an equilibrium where all the constant-power loads are on. We begin with the assumption that the component values have been chosen such that there exists an operational equilibrium where $v_1 > v_2 > \frac{V}{2}$. The associated equations are

$$2v_1^2 - (V + v_2)v_1 + PR = 0 \quad (2.47)$$

$$v_2^2 - v_1v_2 + PR = 0 \quad (2.48)$$

which we can solve to obtain

$$v_1 = \frac{V + v_2}{4} + \sqrt{\frac{1}{16}(V + v_2)^2 - \frac{PR}{2}} \quad (2.49)$$

$$v_2 = \frac{v_1}{2} + \sqrt{\frac{v_1^2}{4} - PR} \quad (2.50)$$

Since we know that the roots are real, the expressions under the square root signs must be positive. Hence,

$$v_1^2 > 4PR, \quad (2.51)$$

which implies $V^2 > 4PR$, since $V > v_1$.

We assume that both loads have cutoff voltage V_c . We now attempt to find conditions on V_c , P , R and V , which will guarantee that the system cannot get stuck at the cutoff boundaries. If the system is in dynamic equilibrium, there are only two possible situations: either both v_1 is pinned at V_c or v_1 is operating above V_c while v_2 is pinned. In the former case, since both cutoff voltages are equal and voltages are non-increasing with distance from the source, v_2 is also pinned at V_c .

Case I: $v_1 = v_2 = V_c$ Under these circumstances, $i_1 = \frac{V-V_c}{R}$ while $i_2 = 0$. We next observe that if that $i_1 > \frac{P}{v_1} = \frac{P}{V_c}$, then this situation cannot occur. Hence, we impose the condition

$$\frac{V - V_c}{R} > \frac{P}{V_c} \quad (2.52)$$

$$V_c^2 - VV_c + PR < 0 \quad (2.53)$$

$$\frac{V}{2} - \frac{\sqrt{V^2 - 4PR}}{2} < V_c < \frac{V}{2} + \frac{\sqrt{V^2 - 4PR}}{2} \quad (2.54)$$

Since $V^2 > 4PR$, if $V_c = \frac{V}{2}$, this situation cannot arise. Hence, we choose $V_c = \frac{V}{2}$.

Case II: $v_1 > v_2 = \frac{V}{2}$ Considering the current at the first node,

$$\frac{V - v_1}{R} = \frac{P}{v_1} + \frac{v_1 - \frac{V}{2}}{R} \quad (2.55)$$

$$2v_1^2 - \frac{3V}{2}v_1 + PR = 0 \quad (2.56)$$

$$v_1 = \frac{3V}{8} + \sqrt{\left(\frac{3V}{8}\right)^2 - \frac{PR}{2}} \text{ since } v_1 > \frac{V}{2} \quad (2.57)$$

(2.58)

A condition which prevents this case from occurring is

$$\frac{v_1 - \frac{V}{2}}{R} > \frac{2P}{V} \quad (2.59)$$

$$v_1 - \frac{V}{2} > \frac{2PR}{V} \quad (2.60)$$

$$\frac{3V}{8} + \sqrt{\left(\frac{3V}{8}\right)^2 - \frac{PR}{2}} > \frac{2PR}{V} + \frac{V}{2} \quad (2.61)$$

$$\sqrt{\left(\frac{3V}{8}\right)^2 - \frac{PR}{2}} > \frac{2PR}{V} + \frac{V}{8} \quad (2.62)$$

$$\frac{9V^2}{64} - \frac{PR}{2} > 4\left(\frac{PR}{V}\right)^2 + \frac{PR}{2} + \frac{V^2}{64} \quad (2.63)$$

$$\frac{V^2}{8} > 4\left(\frac{PR}{V}\right)^2 + PR \quad (2.64)$$

$$V^2 > 32\left(\frac{PR}{V}\right)^2 + 8PR \quad (2.65)$$

$$V^2 > 4(1 + \sqrt{3})PR \quad (2.66)$$

Hence, if (2.66) holds and if the cutoff voltages are set at $\frac{V}{2}$, we can guarantee that the system cannot get stuck at the cutoff boundaries.

In summary, we have shown that under the following conditions:

- The resistances, capacitances and loads are identical,
- There exists an operational equilibrium such that $v_1 > v_2 > \frac{V}{2}$,
- The cutoff voltages for both loads are set at $\frac{V}{2}$, and
- $V^2 > 4(1 + \sqrt{3})PR$,

a regular second-order ladder system is guaranteed to have all its equilibria constrained within \mathcal{P} , the region of \mathfrak{R}^2 such that $\frac{V}{2} \leq v_k < V$ for $k = 1, 2$, not including its boundaries. If we compare this result with the sufficient condition for stability obtained in Section 2.3 (see equation (2.46)), we find that the results are identical. This is important because the

detailed analysis of the system dynamics at the boundaries is extremely involved and hence becomes impractical for higher-order systems. On the other hand, the results for this section can be generalized quite easily for higher-order systems.

In Section 3.2.2, we will prove that there must be at least one stable equilibrium in \mathcal{W} , the region of \mathfrak{R}^2 such that $0 \leq v_k < V$ for $k = 1, 2$, and that all static equilibria must occur in \mathcal{P} when the cutoff voltages for all loads are equal. We have shown that dynamic equilibrium cannot occur in \mathcal{W} , and that there must be at least one stable equilibrium in \mathcal{P} . So since the condition

$$V^2 > \frac{8}{3 - \sqrt{5}} PR \quad (2.67)$$

as derived from (2.34) in Section 2.2.4 is satisfied, the operational equilibrium found is guaranteed to be globally stable and unique and the system is guaranteed to end up at this equilibrium starting from any initial conditions.

2.5 Summary of Results for Second-Order System

In summary, we have presented in this chapter the detailed analysis of a second-order RCP network. In general, a second-order system is found to have at most 2 equilibria, at least one of which is stable. We have also shown that it is possible to express a second-order system as a gradient system. From this fact, we know the the system is guaranteed to end up at an equilibrium in steady-state since there cannot be limit cycles. This is easy to see in the second-order case because the cutoff boundaries are straight lines which partition the phase-plane into 4 rectangular quadrants. We will show that this is true even for higher-order systems in Section 3.4.1.

Using the analytical properties of the gradient system, we can derive conditions for stability for a given equilibrium. In particular, for the second-order system shown in Figure 2-7, where cutoffs voltages set at V_c , all equilibria in the box bounded by $(V_c + \epsilon, V_c + \epsilon)$

and (V, V) are guaranteed to be stable if

$$V_c^2 > \frac{2}{3 - \sqrt{5}} PR \quad (2.68)$$

is satisfied.

Although the energy function fully characterizes the dynamic behavior of the system, the non-differentiability of the function at the cutoff voltages made the analysis of the behavior of the system at these points particularly tricky. After much detailed analysis of the system at these boundary points, it was found that in order to guarantee that a second-order system does not get stuck at these boundaries, the following stability condition must be satisfied:

$$V > V_c + \frac{P_2 R_1 R_2}{V_c R_{||}} + \frac{P_1 R_1}{\frac{P_2 R_2}{V_c} + V_c} \quad (2.69)$$

where $R_{||} = \frac{R_1 R_2}{R_1 + R_2}$. In particular, for a regular second-order system with cutoff voltages set at $\frac{V}{2}$, this condition simplifies to:

$$V^2 > 4(1 + \sqrt{3})PR \quad (2.70)$$

Finally, a steady-state analysis was performed and it was found that we can relatively easily derive conditions that guarantee a second-order system does not get stuck at cutoff boundaries. The conditions obtained for a regular second-order system with cutoff voltages set at $\frac{V}{2}$ were found to be identical to those obtained with detailed boundary analysis. We conclude that steady-state analysis is a more practical way of obtaining simple sufficient conditions for stability, even though the results obtained by boundary analysis may possibly be more general.

Chapter 3

System Modeling and Dynamics: Higher-Order Systems

In this chapter, we will generalize the results presented in Chapter 2 for higher-order systems. We will demonstrate that any higher-order system can be expressed as a gradient system by presenting a method for constructing the energy function for a general RCP network. We showed in the previous chapter that both static and dynamic equilibria can exist. Here, we will discuss the identification and characterization of each of these types of equilibria in detail. Since the steady-state operating point of a network is completely determined by these equilibria, we present a general way of deriving simple sufficient conditions for system stability from the characterization of the equilibria. In particular, we derive specific results for regular RCP-ladder networks.

3.1 Gradient System Representation

In the previous chapter, we showed that we can express a second-order system as a gradient system. In fact, there is a systematic way to construct the energy function for any arbitrary network topology, as long as it satisfies some layout constraints. More specifically, each

node in the network is connected to only one capacitor and one constant-power load, and all loads share a common ground connection. There is no constraint on the number of resistors attached to each node. Figure 3-1 is an example of an n th-order tree with branching that satisfies the above constraints.

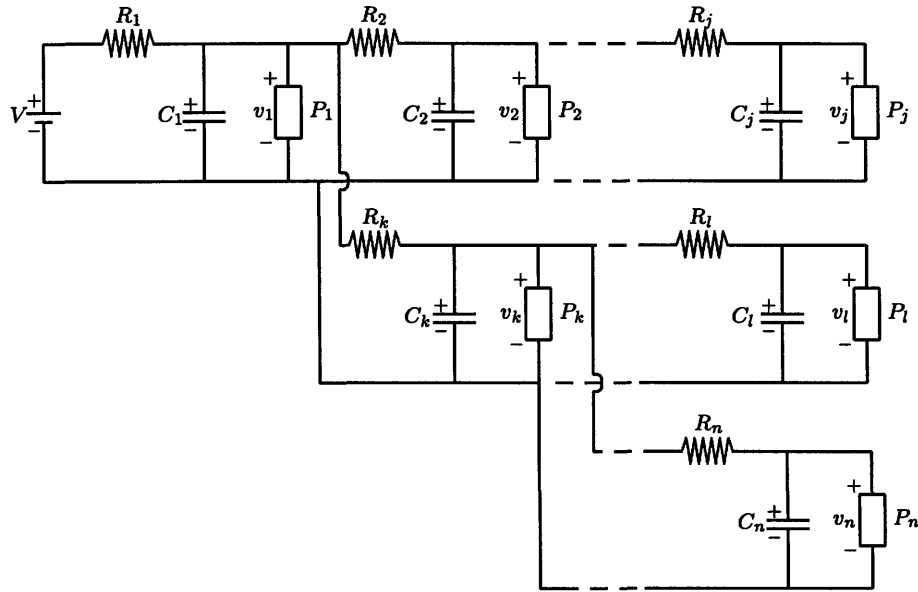


Figure 3-1: An n th-order tree network with branching.

We can apply Kirchoff's Current Law to find the current flowing through the capacitors. The system of equations obtained is of the following form:

$$C_k \frac{dv_k}{dt} = -\frac{K_k(v_k)}{v_k} + \sum_{R_j \in \mathcal{R}_k} \frac{v_{j,k} - v_k}{R_j}, \text{ for } k = 1, \dots, n \quad (3.1)$$

where \mathcal{R}_k is the set of all resistors connected to node k and $v_k - v_{j,k}$ is the potential difference across resistor R_j . Notice that if we define the partial sums

$$E_{n,k}(\mathbf{v}) = 2K_k(v_k) \ln\left(\frac{v_k}{V_k^*}\right) + \left(\sum_{R_j \in \mathcal{R}_k} \frac{1}{R_j} \right) v_k^2 - \sum_{R_j \in \mathcal{R}_k} \frac{1}{R_j} v_k v_{j,k} \quad (3.2)$$

then the energy function is simply given by

$$E_n(\mathbf{v}) = \frac{1}{2} \sum_{k=1}^n E_{n,k}(\mathbf{v}) \quad (3.3)$$

Thus, the energy function of any arbitrary network takes the following form:

$$E_n(\mathbf{v}) = \sum_{k=1}^n K_k(v_k) \ln\left(\frac{v_k}{V_k^*}\right) + \frac{1}{2} \sum_{k=1}^n \left(\sum_{R_j \in \mathcal{R}_k} \frac{1}{R_j} \right) v_k^2 - \sum_{k=1}^n \left(\sum_{R_j \in \mathcal{R}_k} \frac{1}{R_j} v_k v_{j,k} \right) \quad (3.4)$$

where \mathcal{R}_k is the set of all resistors connected to node k and $v_k - v_{j,k}$ is the potential difference across resistor R_j . This is proved simply by partial differentiation of (3.4) which yields the negative of expressions of the form given on the right side of (3.1).

3.2 Characterizing Equilibria

In this section, we study the equilibria of a general higher-order system in detail. Let us first define \mathcal{W} as the region of \mathfrak{R}^n such that $0 \leq v_i \leq V$ for $i = 1, \dots, n$. It is easy to show that \mathcal{W} is the positive-invariant bounding box for the state of any higher-order system. The rationale here is that voltages cannot be negative and they also cannot exceed the source voltage. We show in this section that there is at least one stable equilibrium in \mathcal{W} , and that all equilibria must be contained within \mathcal{W} and cannot occur on the upper or lower boundaries, i.e. where $v_k = 0$ or $v_k = V$ for some node k .

3.2.1 Types of Equilibria

At this point, it is important to note that there are two classes of equilibria for RCP-tree networks: static (asymptotically stable and unstable) equilibria and dynamic (stable) equilibria. In both cases, the voltages at the nodes of a system in equilibrium are constant in the absence of perturbation; the difference between these two classes of equilibria lies in the operating point of the constant-power loads.

When a system is in static equilibrium, all the loads are either on or in cutoff and their voltages are constant over time. In contrast, when a system is in dynamic equilibrium, at least one of the loads is operating in the metastable region with its voltage at cutoff. In the context of the energy functions, static equilibria occur over continuously twice-differentiable regions, while dynamic equilibria occur in the hyperplanes defined by the cutoff voltages on which the gradient is not continuous. As a result, static equilibria are substantially easier to identify and characterize from the energy function.

3.2.2 Boundary Conditions

We show that an equilibrium cannot occur at the boundary of the bounding box except at the origin, by showing that $E_n(\mathbf{v})$ is decreasing in the direction of \mathcal{W} at the boundaries.

We consider

$$\frac{dE_n(\mathbf{v})}{dv_k} = \frac{K_k(v_k)}{v_k} + \left(\sum_{R_j \in \mathcal{R}_k} \frac{1}{R_j} \right) v_k - \sum_{R_j \in \mathcal{R}_k} \frac{1}{R_j} v_{j,k} \quad (3.5)$$

At the lower boundaries,

$$\frac{dE_n(\mathbf{v})}{dv_k} \Big|_{v_k=0} = - \sum_{R_j \in \mathcal{R}_k} \frac{1}{R_j} v_{j,k} \leq 0 \quad (3.6)$$

since $V_k^* > 0$. This shows that $E_n(\mathbf{v})$ is non-increasing in the direction of \mathcal{W} along the boundary. Consider the case when equality holds. This means that $v_{j,k} = 0 \forall R_j \in \mathcal{R}_k$. So instead we repeat the above argument with each $v_{j,k}$ in \mathcal{R}_k . Eventually, we end up with a situation where $\frac{dE_n(\mathbf{v})}{dv_j}$ can be shown to be negative for some $j \in \{1, \dots, n\}$, or else the entire network is at zero voltage. In the latter case, we know that $E_n(\mathbf{v})$ is strictly decreasing in the direction of \mathcal{W} since the network simply looks like a static source charging up a network of capacitors and resistors.

At the upper boundaries,

$$\frac{dE_n(\mathbf{v})}{dv_k} \Big|_{v_k=V} = \frac{P_k}{V} + \left(\sum_{R_j \in \mathcal{R}_k} \frac{1}{R_j} \right) V - \sum_{R_j \in \mathcal{R}_k} \frac{1}{R_j} v_{j,k} > 0 \quad (3.7)$$

The inequality is apparent because $\frac{P_k}{V} > 0$ and $v_{j,k} \leq V$. This inequality shows that $E_n(\mathbf{v})$ is strictly decreasing in the direction of \mathcal{W} along the boundary.

These results, together with the observation that $E_n(\mathbf{v})$ is finite at the boundary of \mathcal{W} and that $E_n(\mathbf{v})$ is lower bounded within \mathcal{W} , allow us to conclude that there exists at least one stable equilibrium within \mathcal{W} and that the stable equilibrium cannot lie on the boundary of \mathcal{W} . We will show in Section 3.4.1 that we can rule out limit cycles and other kinds of oscillatory behavior because the system behaves like a gradient system even at the non-differentiable cutoff boundaries.

3.3 Static Equilibria

3.3.1 Constraint on Cutoff Voltages

We define \mathcal{P} as the region of \mathfrak{R}^n such that $V_k^* \leq v_k < V$ for $k = 1, \dots, n$. Within \mathcal{P} , all loads are on. We now show that $\frac{dE_n(\mathbf{v})}{dv_k} < 0$ for some $v_k < V_k^*$ under the cutoff voltage constraint where the cutoff voltages of the loads all equal, i.e. $V_1^* = V_2^* = \dots = V_n^*$, as long as the system is not on a cutoff boundary. In other words, we want to show that when all the cutoff voltages are equal, static equilibria can only occur within \mathcal{P} .

From the topology, we know that any equilibrium must satisfy the condition that nodal voltages are monotonically decreasing with distance from the source, since the only source of current in the system is the voltage source. As current flows away from the voltage source, it induces voltage drops across the resistors, so nodal voltages must be monotonically non-increasing. If the system is in a state which does not satisfy the above condition, some of the capacitors in the system will be discharged, and eventually the system will satisfy this voltage constraint.

If the system is not in \mathcal{P} , there will be a node k with a load in cutoff, since $v_k < V_k^*$.

So,

$$\frac{dE_n(\mathbf{v})}{dv_k} = \left(\sum_{R_j \in \mathcal{R}_k} \frac{1}{R_j} \right) v_k - \sum_{R_j \in \mathcal{R}_k} \frac{1}{R_j} v_{j,k} \quad (3.8)$$

Next, we observe that $\frac{dE_n(\mathbf{v})}{dv_k}$ is identically equal to the total current entering node k , which can only get stored on the capacitor since the load at that node is in cutoff. Assuming that the condition $V \geq v_1 \geq v_2 \geq \dots \geq v_n$ is not violated, we do in fact know the direction of flow for the current. Since the network has a tree structure, current flows into node v_k through only one neighboring node, say v_{k-1} , as shown in Figure 3-2.

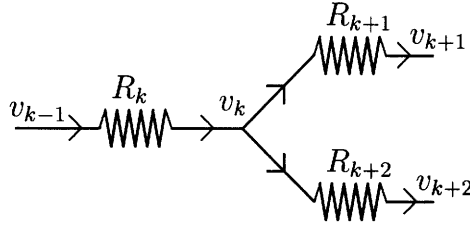


Figure 3-2: An example of current flow.

As long as $v_{k-1} > v_k$, current flows into v_k , but $v_k < V_k^*$ implies that the nodes downstream of node k will all have their loads in cutoff, and so the current flowing in will charge the some capacitor in the subtree and hence $\frac{dE_n(\mathbf{v})}{dv_k} < 0$. This will only stop if $v_{k-1} = v_k$. If this is true, we move down the chain and consider v_{k-1} . Eventually, since all cutoff voltages are equal and the system is not at a cutoff boundary, we find that there has to be some node which is charging up. With this, we conclude that even though $v_{k-1} = v_k$, the system is not in equilibrium.

In summary, we conclude that under the condition that all cutoff voltages are equal, all static equilibria must occur in \mathcal{P} .

3.3.2 Characterization of the Hessian

We have established that there is least one stable equilibrium point in \mathcal{W} , and also that static equilibria must occur within \mathcal{P} if all cutoff voltages are equal. We can characterize

the stability of equilibria within \mathcal{P} using a fundamental result from system theory: given a static equilibrium point $\bar{\mathbf{v}} \in \mathcal{P}$ such that $\frac{dE_n}{d\mathbf{v}}(\bar{\mathbf{v}}) = 0$, a fundamental condition for stability is

$$\frac{d^2 E_n}{d\mathbf{v}^2}(\bar{\mathbf{v}}) > 0 \quad (3.9)$$

In other words, the Hessian of the energy function $E_n(\mathbf{v})$ evaluated at the equilibrium point must be positive definite for the equilibrium to be stable. As mentioned previously, dynamic equilibria that occur in the hyperplanes corresponding the cutoff voltages of the constant-power loads cannot be characterized in this way since the energy function is non-differentiable within these hyperplanes.

In principle, given the static equilibria of a system, we can compute the Hessian for each equilibrium point and then test for positive definiteness. There are two common methods to check if a symmetric square matrix is positive definite. One way is to check that all the eigenvalues of the matrix are positive; the other is to invoke *Sylvester's Test*:

Theorem 3.1 (Sylvester's Test) *Let \mathbf{A} be a symmetric square matrix, i.e.*

$$\mathbf{A} = \begin{bmatrix} a_{11} & a_{12} & \cdots & a_{1n} \\ a_{12} & a_{22} & \cdots & a_{2n} \\ \vdots & \vdots & \ddots & \vdots \\ a_{1n} & a_{2n} & \cdots & a_{nn} \end{bmatrix}$$

then $\mathbf{A} > 0$ iff the determinant of every leading principal submatrix of \mathbf{A} is positive, i.e.,

$$\begin{aligned} & a_{11} > 0 \\ & \begin{vmatrix} a_{11} & a_{12} \\ a_{12} & a_{22} \end{vmatrix} > 0 \\ & \begin{vmatrix} a_{11} & a_{12} & a_{13} \\ a_{12} & a_{22} & a_{23} \\ a_{13} & a_{23} & a_{33} \end{vmatrix} > 0 \\ & \text{etc.} \end{aligned}$$

In the event where the exact location of an equilibrium is known, the testing of the Hessian for positive definiteness is straightforward. However, this test is useful even in the event where the exact location of the equilibrium is not known exactly, but we know that the equilibrium lies in a box, \mathcal{Q} , bounded by the points $\tilde{\mathbf{v}}$ and (V, V, \dots, V) , where $\tilde{\mathbf{v}} = (\tilde{v}_1, \tilde{v}_1, \dots, \tilde{v}_n)$, $\tilde{v}_k < V \forall k = 1, \dots, n$. The reason for this is that we can decompose the Hessian at any point within \mathcal{Q} in the following way:

$$\frac{d^2 E_n}{d\mathbf{v}^2}(\mathbf{v}) = \frac{d^2 E_n}{d\mathbf{v}^2}(\tilde{\mathbf{v}}) + \begin{bmatrix} \frac{P}{v_1^2} - \frac{P}{\tilde{v}_1^2} & 0 & \cdots & 0 \\ 0 & \frac{P}{v_2^2} - \frac{P}{\tilde{v}_2^2} & \cdots & 0 \\ \vdots & \vdots & \ddots & \vdots \\ 0 & 0 & \cdots & \frac{P}{v_n^2} - \frac{P}{\tilde{v}_n^2} \end{bmatrix} \quad (3.10)$$

where $\tilde{v}_k \leq v_k \forall k = 1, \dots, n$. Clearly $\frac{P}{v_k^2} - \frac{P}{\tilde{v}_k^2} \geq 0 \forall k = 1, \dots, n$. Hence, if we can show that $\frac{d^2 E_n}{d\mathbf{v}^2}(\tilde{\mathbf{v}})$ is positive definite, we can conclude that $\frac{d^2 E_n}{d\mathbf{v}^2}(\mathbf{v})$ must also be positive definite, since it is the sum of a positive definite matrix and a positive semidefinite matrix. We will use this result in the next section to derive conditions sufficient for stability in a regular ladder network.

3.3.3 Guaranteeing Stability for Regular Ladder Network

General Ladder Network

The energy function of a generalized ladder network takes the following form

$$E_n(\mathbf{v}) = \sum_{k=1}^{n-1} \left(\frac{1}{2R_k} + \frac{1}{2R_{k+1}} \right) v_k^2 + \frac{1}{2R_n} v_n^2 - \frac{V}{R_1} v_1 - \sum_{k=1}^{n-1} \frac{v_k v_{k+1}}{R_{k+1}} + \sum_{k=1}^n K_k(v_k) \ln\left(\frac{v_k}{V_k^*}\right) \quad (3.11)$$

where

$$K_k(v_k) = \begin{cases} P_k, & v_k \geq V_k^* > 0 \\ 0, & v_k < V_k^* \end{cases}$$

and V_k^* is the cutoff voltage for the k th load. From this equation, we obtain

$$\frac{d^2 E_n}{d\mathbf{v}^2}(\mathbf{v}) = \begin{bmatrix} -\frac{K(v_1)}{v_1^2} + \frac{1}{R_1} + \frac{1}{R_2} & -\frac{1}{R_2} & 0 & \cdots & 0 \\ -\frac{1}{R_2} & -\frac{K(v_2)}{v_2^2} + \frac{1}{R_2} + \frac{1}{R_3} & -\frac{1}{R_3} & \cdots & 0 \\ \vdots & \vdots & \ddots & \ddots & \vdots \\ 0 & 0 & \cdots & -\frac{1}{R_n} & -\frac{K(v_n)}{v_n^2} + \frac{1}{R_n} \end{bmatrix} \quad (3.12)$$

Assume for now that we do not know the exact location of the equilibrium, but we do know that it lies in \mathcal{P} . So, we apply *Sylvester's Test* to evaluate positive definiteness of the Hessian at the lower corner. This involves the computation of the determinant for the Hessian at that point. We define

$$A_n = \begin{vmatrix} -\frac{P_1}{V_1^{*2}} + \frac{1}{R_1} + \frac{1}{R_2} & -\frac{1}{R_2} & 0 & \cdots & 0 \\ -\frac{1}{R_2} & -\frac{P_2}{V_2^{*2}} + \frac{1}{R_2} + \frac{1}{R_3} & -\frac{1}{R_3} & \cdots & 0 \\ \vdots & \vdots & \ddots & \ddots & \vdots \\ 0 & 0 & \cdots & -\frac{1}{R_n} & -\frac{P_n}{V_n^{*2}} + \frac{1}{R_n} \end{vmatrix} \quad (3.13)$$

and

$$B_{n+1} = \begin{vmatrix} -\frac{P_1}{V_1^{*2}} + \frac{1}{R_1} + \frac{1}{R_2} & -\frac{1}{R_2} & 0 & \cdots & 0 \\ -\frac{1}{R_2} & -\frac{P_2}{V_2^{*2}} + \frac{1}{R_2} + \frac{1}{R_3} & -\frac{1}{R_3} & \cdots & 0 \\ \vdots & \vdots & \ddots & \ddots & \vdots \\ 0 & 0 & \cdots & -\frac{1}{R_n} & -\frac{P_n}{V_n^{*2}} + \frac{1}{R_n} + \frac{1}{R_{n+1}} \end{vmatrix} \quad (3.14)$$

By expanding the determinant along the n th column, we obtain

$$A_0 = B_1 = 1, \quad (3.15)$$

$$A_1 = -\frac{P_1}{V_1^{*2}} + \frac{1}{R_1}, \quad (3.16)$$

$$B_2 = -\frac{P_1}{V_1^{*2}} + \frac{1}{R_1} + \frac{1}{R_2}, \quad (3.17)$$

$$A_n = \left(-\frac{P_n}{V_n^{*2}} + \frac{1}{R_n}\right)B_n - \frac{1}{R_n^2}B_{n-1}, \quad n \geq 2, \quad (3.18)$$

$$B_{n+1} = \left(-\frac{P_n}{V_n^{*2}} + \frac{1}{R_n} + \frac{1}{R_{n+1}}\right)B_n - \frac{1}{R_n^2}B_{n-1}, \quad n \geq 2 \quad (3.19)$$

By *Sylvester's Test*, the condition for stability is

$$\frac{d^2 E_n}{d\mathbf{v}^2}(\mathbf{v}) > 0 \text{ iff } A_i > 0 \forall i = 1, \dots, n \quad (3.20)$$

Regular Networks

Let us consider a regular ladder network where all the resistors, all the capacitors and all the loads are identical. Let R be the resistance of the resistors, C be the capacitance of the capacitors, V be the supply voltage, V^* be the common cutoff voltage and P be the power rating of the loads.

From the results of Section 3.3.1, we know that all static equilibria must occur within \mathcal{P} . In order to ensure positive definiteness, we must have $A_k > 0 \forall k = 1, \dots, n$, where A_k is evaluated at the point (V^*, V^*, \dots, V^*) . We apply the recurrence relation defined by equations (3.15) to (3.19) to derive conditions on V^* sufficient to guarantee that $\frac{d^2 E_n}{d\mathbf{v}^2}(\mathbf{v})$ is positive definite at any static equilibrium point within \mathcal{P} . These conditions were found to take the following form, where $f(n)$ is a function that is monotonically increasing with n :

$$V^{*2} > f(n)PR \quad (3.21)$$

The values of $f(n)$ for $n = 1, \dots, 15$ are listed in Table 3.1.

Empirically, it is found that for $n \geq 3$, $f(n)$ can be approximated by a quadratic function $f'(n)$, where

$$f'(n) = 0.4n^2 + 0.5n - 0.3 \quad (3.22)$$

Hence, we propose the following as sufficient conditions:

$$n = 1 \quad : \quad V^{*2} > PR \quad (3.23)$$

Table 3.1: Cutoff Voltage Coefficients for Regular Ladder Networks (Static Equilibria)

Order, n	$f(n)$
1	1.0000000
2	2.6180339
3	5.0489077
4	8.2908599
5	12.3435379
6	17.2068587
7	22.8807819
8	29.3652984
9	36.6603989
10	44.7660837
11	53.6823401
12	63.4091685
13	73.9465573
14	85.3179715
15	97.4530641

$$n = 2 : V^{*2} > 2.62PR \quad (3.24)$$

$$n \geq 3 : V^{*2} > f'(n)PR \quad (3.25)$$

To summarize, a regular ladder network which satisfies inequality (3.21) is guaranteed to have at most one stable static equilibrium in \mathcal{P} . As mentioned in Section 2.2.4, it is easy to show that any convex region where the Hessian is positive definite can have at most one equilibrium (which must be stable). So, if it is known that an equilibrium does indeed exist in \mathcal{P} , then it is both stable and unique within \mathcal{P} . The details for the computation and approximation of $f(n)$ are given in Appendix B.

3.4 Dynamic Equilibria

3.4.1 Boundary Behavior of Modified Gradient System

As noted in Section 2.2.3, equation (2.29) holds at all points except for those on the cutoff boundaries, and hence we do not have a gradient system in the global twice-differentiable sense. Here, we will show that like a conventional gradient system with no discontinuities, our modified gradient system is well-behaved even at the cutoff boundaries.

For a general n th-order system, we know that the dynamic behavior of the system at all points not on the cutoff boundaries is determined by the set of n state equations

$$\mathbf{C} \frac{d\mathbf{v}}{dt} = -\frac{dE}{d\mathbf{v}}(\mathbf{v}) \quad (3.26)$$

We define V_k^* , $k = 1, \dots, n$ to be the cutoff voltage of the k th load. In order to understand the behavior of the system at the boundary $v_k = V_k^*$, we consider the dynamic behavior of the system at $v_k = V_k^* + \epsilon$ and $v_k = V_k^* - \epsilon$ to obtain

$$\left. \frac{dE_n(\mathbf{v})}{dv_k} \right|_{v_k=V_k^*+\epsilon} = \frac{P_k}{V^*} + \left(\sum_{R_j \in \mathcal{R}_k} \frac{1}{R_j} \right) V^* - \sum_{R_j \in \mathcal{R}_k} \frac{1}{R_j} v_{j,k}, \quad (3.27)$$

$$\left. \frac{dE_n(\mathbf{v})}{dv_k} \right|_{v_k=V_k^*-\epsilon} = \left(\sum_{R_j \in \mathcal{R}_k} \frac{1}{R_j} \right) V^* - \sum_{R_j \in \mathcal{R}_k} \frac{1}{R_j} v_{j,k} \quad (3.28)$$

where \mathcal{R}_k is the set of all resistors connected to node k and $v_k - v_{j,k}$ is the potential difference across resistor R_j .

There are two possible scenarios: $\left. \frac{dE_n(\mathbf{v})}{dv_k} \right|_{v_k=V_k^*+\epsilon}$ and $\left. \frac{dE_n(\mathbf{v})}{dv_k} \right|_{v_k=V_k^*-\epsilon}$ are either of the same polarity, or they are of opposite polarity. In the former case, the field lines that hit the non-differentiable boundary leave the boundary in the same general direction at the opposite side. A graphical representation is shown in Figure 3-3.

If instead, we have a condition where $\left. \frac{dE_n(\mathbf{v})}{dv_k} \right|_{v_k=V_k^*-\epsilon} < 0$, but $\left. \frac{dE_n(\mathbf{v})}{dv_k} \right|_{v_k=V_k^*+\epsilon} > 0$, or vice versa, field lines are instead converging at the discontinuous boundary from two

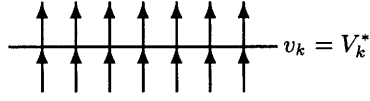


Figure 3-3: Field lines moving in the same general direction.

opposite directions. This effectively causes the system to be pinned on the boundary. The dynamic behavior of the system is then governed by the remaining $n - 1$ equations from (3.26) for v_i , $i = 1, \dots, n$, $i \neq k$. We recognize this new set of $n - 1$ state equations as a gradient system of order $n - 1$, and that $E_n(\mathbf{v})|_{v_k=V_k^*}$ is the appropriate energy function. This reduced-order gradient system is a conventional gradient system where all components of the energy function are twice-differentiable and hence satisfies (2.14), i.e.

$$\dot{E}_n(\mathbf{v})|_{v_k=V_k^*} = -|\text{grad } E_n(\mathbf{v})|_{v_k=V_k^*}|^2 \leq 0 \quad (3.29)$$

where $\text{grad } E_n(\mathbf{v})|_{v_k=V_k^*}$ is evaluated in the the set of $n - 1$ vector components which excludes v_k . We conclude that the energy function $E_n(\mathbf{v})$ is strictly decreasing on the boundary $v_k = V_k^*$ unless $\text{grad } E_n(\mathbf{v})|_{v_k=V_k^*} = 0$ for some \mathbf{v} , which occurs only at a dynamic equilibrium point.

In general, the net effect is a sliding motion along the cutoff $v_k = V_k^*$, where the direction of flow depends on the voltages of the adjacent nodes. This situation may produce a stable but undesirable dynamic equilibrium when $\text{grad } E_n(\mathbf{v})|_{v_k=V_k^*} = 0$, as illustrated in Figure 3-4.

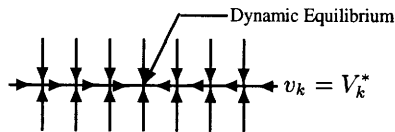


Figure 3-4: Converging field lines at the non-differentiable boundary.

At the same time, there is also a possibility that the state of the system will simply slide along the non-differentiable boundary to a point where $\frac{dE_n(\mathbf{v})}{dv_k}|_{v_k=V_k^*+\epsilon}$ changes sign.

At this point, the state of the system will leave the discontinuous boundary, as illustrated in Figure 3-5. Since the abovementioned cases are exhaustive, it is clear that all dynamic equilibria arising from the cutoffs are stable and undesirable.

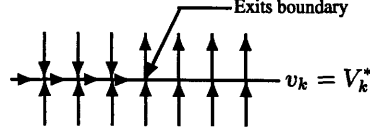


Figure 3-5: Sliding effect along non-differentiable boundary.

There is also the possibility that the system ends up at the intersection of two or more cutoff boundaries. In this case, the situation is analogous to the single boundary case described above. If the system is pinned to the region of intersection, the dynamic behavior is determined by the other non-constrained components and there is again a corresponding reduced-order conventional gradient system for this region. If the system is not pinned to this region, the dynamic behavior would be determined by the state equations for the new region that the system moves into.

The situation where all nodal voltages are at cutoff is a special case, i.e. $v_1 = V_1^*$, $v_2 = V_2^*$, \dots , $v_n = V_n^*$. In this case, the behavior of the system depends on the cutoff voltages and the system parameters. If the cutoff voltages are not monotonically non-decreasing from the source, the system will not stay at this point since there will be a capacitor charging up at some intermediate node. If the cutoff voltages are indeed monotonically non-decreasing from the source, the system can exhibit one of two possible behaviors. If $V^2 < 4P_1R_1$, the system will be stuck at $v_1 = V_1^*$, $v_2 = V_2^*$, \dots , $v_n = V_n^*$, since the source cannot produce enough current to cause even the first load to turn on fully. On the other hand, if $V^2 > 4P_1R_1$, we can easily show that the system is not at steady-state and that the first load will eventually be turned on.

What this discussion leaves us is that if we consider one boundary at a time,

$$\frac{P_k}{V^*} + \left(\sum_{R_j \in \mathcal{R}_k} \frac{1}{R_j} \right) V^* - \sum_{R_j \in \mathcal{R}_k} \frac{1}{R_j} v_{j,k} = 0 \quad (3.30)$$

defines the locus of the set of points in the hyperplane $v_k = V^*$ where $\frac{dE_n(\mathbf{v})}{dv_k}|_{v_k=V^*+\epsilon}$ changes sign. By checking the partial derivatives in the other components, it is conceptually possible to determine all the dynamic equilibria arising from the non-differentiable boundary much as it was done in Section 2.3. In practical terms however, this is a non-trivial analytical feat for higher-order systems. With this note, we conclude that the obvious way to ensure that a system does not get stuck at these dynamic equilibria is to derive the conditions necessary for dynamic equilibria to exist and then adjust system parameters to ensure that these conditions are not met. Since we have shown that any RCP system will eventually settle at an equilibrium, a more practical way to obtain sufficient conditions is to simply consider all the possible steady states.

3.4.2 Application of Steady-State Analysis to Regular Ladder Network

The analysis of all the possible steady states is in general a computationally expensive task. For an n th-order system there are 2^n possible combinations of on/off states for the loads. If we were to have to examine all these possibilities, the task would be take an exponential amount of computation.

Fortunately, under the condition where cutoff voltages are non-decreasing with distance from the load, i.e $V_1^* \leq V_2^* \leq \dots \leq V_n^*$, the number of possibilities is reduced to a linear function. The reason is this: given that a load at node k is in cutoff, all loads further down the tree are guaranteed to be at a voltage no higher than v_k ; this means that they would all have to be in cutoff too. Hence, under this assumption, the systematic approach to this problem would be to start from the load nearest the source and then work down branches of the tree. This concept will be used in the following section to derive conditions to guarantee that a regular ladder network with cutoff voltages set at $\frac{V}{2}$ does not get stuck at any dynamic equilibria. This idea has already been demonstrated for the second-order case in Section 2.4.

Regular Third-Order System

Now, we repeat the derivation of a sufficient condition to avoid dynamic equilibria for a regular third-order RCP-ladder system, as shown in Figure 3-6, because the results from Section 2.4 do not generalize directly. We assume that all loads have a cutoff voltage of $\frac{V}{2}$.

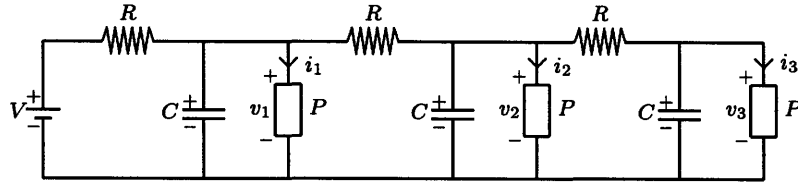


Figure 3-6: Third-order system.

First, the following is the system of associated equations

$$2v_1^2 - (V + v_2)v_1 + PR = 0 \quad (3.31)$$

$$2v_2^2 - (v_1 + v_3)v_2 + PR = 0 \quad (3.32)$$

$$v_3^2 - v_2v_3 + PR = 0 \quad (3.33)$$

This equations yield

$$v_1 = \frac{V + v_2}{4} \pm \sqrt{\frac{1}{16}(V + v_2)^2 - \frac{PR}{2}} \quad (3.34)$$

$$v_2 = \frac{v_1 + v_3}{4} \pm \sqrt{\frac{1}{16}(v_1 + v_3)^2 - \frac{PR}{2}} \quad (3.35)$$

$$v_3 = \frac{v_2}{2} \pm \sqrt{\frac{v_2^2}{4} - PR} \quad (3.36)$$

We assume that the system satisfies the following conditions:

- All the resistances, all the capacitances and all the loads are identical,
- There exists an operational equilibrium such that $v_1 > v_2 > v_3 > \frac{V}{2}$,

- The cutoff voltages for the loads are set at $\frac{V}{2}$,
- $V^2 > 4(1 + \sqrt{3})PR$.

As such, there are only three possible states of dynamic equilibrium for the system:

1. $v_1 = v_2 = v_3 = \frac{V}{2}$
2. $v_1 > v_2 = v_3 = \frac{V}{2}$
3. $v_1 > v_2 > v_3 = \frac{V}{2}$

The analysis of the first two of these cases is identical to that performed in Section 2.4. The net result is $V^2 > 4(1 + \sqrt{3})PR$. Hence, we examine the last case, where $v_1 > v_2 > v_3 = \frac{V}{2}$. Considering the second node, we obtain from (3.35),

$$v_2 = \frac{V}{8} + \frac{v_1}{4} + \sqrt{\left(\frac{V}{8} + \frac{v_1}{4}\right)^2 - \frac{PR}{2}} \quad (3.37)$$

since $v_3 = \frac{V}{2}$ and $v_2 > \frac{V}{2}$. We impose the condition that the current entering the third node exceeds the current drawn by the third load, which is

$$\frac{v_2 - \frac{V}{2}}{R} > \frac{2P}{V} \quad (3.38)$$

This yields

$$v_1\left(\frac{2PR}{V} + \frac{V}{2}\right) > 8\left(\frac{PR}{V}\right)^2 + \frac{V^2}{4} + 4PR \quad (3.39)$$

after some algebraic manipulation. Since $v_1 > v_2 > \frac{V}{2}$ and so each load can draw at most a current of $\frac{2PR}{V}$, we observe that $v_1 > V - \frac{6PR}{V}$ under equilibrium conditions. Hence, a sufficient condition is

$$\left(V - \frac{6PR}{V}\right)\left(\frac{2PR}{V} + \frac{V}{2}\right) > 8\left(\frac{PR}{V}\right)^2 + \frac{V^2}{4} + 4PR \quad (3.40)$$

which yields

$$V^2 > 21.41640787PR > 4(1 + \sqrt{3})PR \quad (3.41)$$

after some algebraic manipulation. We notice here that this is more stringent than the condition:

$$V^2 > 20.196PR \quad (3.42)$$

as derived from (3.21). So, if (3.42) is satisfied, the operational equilibrium found is guaranteed to be stable and unique. and the overall system is guaranteed to be stable, i.e. it is guaranteed to end up at this equilibrium starting from any initial conditions.

Generalization for Regular Ladder Networks

We can repeat the above exercise with an n th-order ladder like the one shown in Figure 3-7. We only have to consider the situation when $v_1 > v_2 > \dots > v_{n-1} > v_n = \frac{V}{2}$ since the first $n - 1$ situations are exactly the same as that for the $n - 1$ shorter ladder networks.

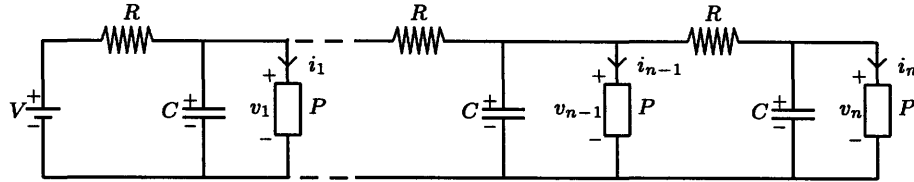


Figure 3-7: Example n th-order system.

As before, the voltage at node $n - 1$ is

$$v_{n-1} = \frac{V}{8} + \frac{v_{n-2}}{4} + \sqrt{\left(\frac{V}{8} + \frac{v_{n-2}}{4}\right)^2 - \frac{PR}{2}} \quad (3.43)$$

Next, we impose the condition that the current entering the last node exceeds the current drawn by it:

$$\frac{v_{n-1} - \frac{V}{2}}{R} > \frac{2P}{V} \quad (3.44)$$

which yields

$$v_{n-2} \left(\frac{2PR}{V} + \frac{V}{2} \right) > 8 \left(\frac{PR}{V} \right)^2 + \frac{V^2}{4} + 4PR \quad (3.45)$$

after some algebraic manipulation. Again, we observe that the maximum current draw by

any load in the system is bounded by $\frac{2P}{V}$ and thus conclude that $v_{n-2} > V - h(n)\frac{PR}{V}$ where $h(n) = n^2 + n - 6$. To obtain the bound for the n th-order network, we solve

$$(V - h(n)\frac{PR}{V})(\frac{2PR}{V} + \frac{V}{2}) > 8(\frac{PR}{V})^2 + \frac{V^2}{4} + 4PR, \text{ for } n \geq 3 \quad (3.46)$$

The bound obtained is

$$V^2 > g(n)PR \quad (3.47)$$

where $g(n)$ is given by the larger root of

$$g(n)^2 - (2h(n) + 8)g(n) - (8h(n) + 32) = 0, \text{ for } n \geq 3 \quad (3.48)$$

A little algebra yields

$$g(n) = h(n) + 4 + \sqrt{h(n)^2 + 16h(n) + 48}, \text{ for } n \geq 3 \quad (3.49)$$

Results for $n = 1, \dots, 15$ are given in Table 3.2. We observe, by comparing these results to that of Table 3.1, that the bound to ensure that the given static equilibrium is stable is less stringent than the corresponding sufficient condition to guarantee that dynamic equilibria do not occur. Hence, in general, if a given regular ladder network with an operational equilibrium satisfies this bound given in inequality (3.47), the equilibrium is guaranteed to be globally stable and unique.

It is found that $g(n)$ can be approximated very well with a quadratic function for $n \geq 3$. In particular, $g(n) \simeq 2h(n) + 10$. Hence,

$$n = 1 : V^2 > 4PR \quad (3.50)$$

$$n = 2 : V^2 > 10.928PR \quad (3.51)$$

$$n \geq 3 : V^2 > g'(n)PR \quad (3.52)$$

Table 3.2: Cutoff Voltage Coefficients for Regular Ladder Networks (Dynamic Equilibria)

Order, n	$g(n)$	$g'(n)$	$4f(n)$
1	4.0000000	4	4.0
2	10.9282032	12	10.5
3	23.4164079	24	20.2
4	39.6333077	40	33.2
5	59.7490157	60	49.4
6	83.8178046	84	68.8
7	111.8619046	112	91.5
8	143.8918128	144	117.5
9	179.9130023	180	146.6
10	219.9285486	220	179.1
11	263.9402852	264	214.7
12	311.9493590	312	253.6
13	363.9565166	364	295.8
14	419.9622508	420	341.3
15	479.9669399	480	389.8

where

$$g'(n) = 2n^2 + 2n \quad (3.53)$$

It should be noted at this point that the above method for deriving these sufficient conditions is applicable to any network that satisfies the condition that cutoff voltages are monotonically non-decreasing from the source. The only reason why the above analysis was restricted to regular networks is that it simplifies the algebra involved without losing the essence of the whole exercise. All cutoff voltages were assumed to be equal so that we can use the result that all static equilibria must occur in \mathcal{P} . The entire exercise can easily be repeated with a different choice of cutoff voltage. In fact, the equation corresponding to (3.46) for a cutoff of αV is

$$(V - h(n)\frac{PR}{2\alpha V})(\frac{2PR}{V} + \frac{V}{2}) > 8(\frac{PR}{V})^2 + \alpha^2 V^2 + (6\alpha + 1)PR \quad (3.54)$$

3.5 Summary of Results for Higher-Order Systems

We have shown in this chapter how the results for second-order systems in Chapter 2 may be generalized for higher-order systems. We presented a method for constructing the energy function for any arbitrary network topology that satisfies a common layout constraint. Since the stability of a system is intrinsically related to the static and dynamic equilibria, we examined these two classes of equilibria in detail.

It was shown that for any given network there exists at least one stable equilibrium within \mathcal{W} , and that no equilibrium can lie on the boundary of \mathcal{W} . In fact, when the cutoff voltage of the loads in the system are equal, we are able to constrain the location of static equilibria to an even smaller region. In particular, under the cutoff voltage constraint $V_1^* = V_2^* = \dots = V_n^*$, all static equilibria must occur in \mathcal{P} , the region of \mathfrak{R}^n such that $V_k^* \leq v_k < V$ for $k = 1, \dots, n$.

The stability of static equilibria was characterized through the Hessian of the energy function. We observed that if $\frac{d^2 E_n}{dv^2}(\tilde{\mathbf{v}})$ is positive definite, where $\tilde{\mathbf{v}} = (\tilde{v}_1, \tilde{v}_1, \dots, \tilde{v}_n)$, $\tilde{v}_k < V$, $k = 1, \dots, n$, the Hessian evaluated at all points in \mathcal{Q} , the box bounded by $\tilde{\mathbf{v}}$ and (V, V, \dots, V) , is also positive definite. From this, we are able to derive simple sufficient conditions to ensure that any static equilibrium in \mathcal{Q} is guaranteed to be stable and unique within \mathcal{Q} . In particular, this was applied to a regular ladder network with cutoff voltages set at V^* to derive sufficient conditions for stability in \mathcal{Q} of the form:

$$V^{*2} > f(n)PR \quad (3.55)$$

where V^* is the cutoff voltage of the loads and $f(n)$ is a monotonically increasing function in n .

The final step to ensure system stability is to ensure that dynamic equilibria do not occur. We first presented a brief overview on the formation of dynamic equilibria. Next, under the condition that cutoff voltages are non-decreasing with distance from the load,

we demonstrated how systematic steady-state analysis may be used to derive sufficient conditions to ensure that dynamic equilibria are prevented from occurring. In particular, we applied steady-state analysis to regular ladder networks with cutoff voltages set at $\frac{V}{2}$ to derive sufficient conditions to avoid dynamic equilibria:

$$V^2 > g(n)PR \quad (3.56)$$

where $g(n)$ is a monotonically increasing function of n that is dependent on the cutoff voltage. The results for $n \geq 3$ are only sufficient conditions. In contrast, the result for $n = 2$ is a necessary and sufficient condition.

Finally, we put both pieces of the puzzle together for regular RCP-ladder networks and conclude that if conditions given in (3.55) and (3.56) are simultaneously satisfied by a ladder network with one known static equilibrium, that equilibrium is guaranteed to be the globally stable and unique equilibrium and the system is stable. Empirically, it was observed that the condition (3.56) tends to supersede condition (3.55) and that the coefficients for both conditions are close to within an factor of 2 for networks of order less than 15.

Chapter 4

Computing Equilibria for a Network

From earlier discussions that any arbitrary RCP-tree network can be modeled as a gradient system, we know that the state of any system will eventually settle down at an equilibrium point within the region \mathcal{W} , where $0 < v_i < V$ for $i = 1, \dots, n$. Hence, it is imperative in the study of system stability to be able to compute the equilibria for a given system. We present in this chapter a survey of the methods that can be employed to obtain both the static and dynamic equilibria of an RCP-tree network. We also introduce an aggregated-model approximation that allows us to approximate the steady-state behavior of a higher-order system with a first-order network.

4.1 Static Equilibria

4.1.1 Direct Numerical Solution

From the properties of gradient systems as presented in Section 2.2, we know that we can obtain the operational equilibria of the system by finding solutions to the system of equations

$$\frac{dE_n}{d\mathbf{v}}(\mathbf{v}) = 0 \tag{4.1}$$

where \mathbf{v} is assumed to lie in \mathcal{P} , the region of \mathfrak{R}^n such that $V_k^* \leq v_k < V$ for $k = 1, \dots, n$. Each equation in the system will be quadratic in v_i , $i = 1, \dots, n$. By recursively performing substitutions, we eventually end up with a $2n$ th-order polynomial equation in v_i . A numerical package like Maple V [5] can then be employed to solve for the roots numerically. In general, it will be true that most of the roots thus obtained will be complex and can hence be ignored. We then substitute the real roots obtained to produce a set of new equations of order $2n - 2$ on another variable $v_j, j \neq i$.

Recursive numerical root finding and substitution will eventually produce several sets of solutions. Substitution of these sets of solutions into the original system described by (4.1) will allow us to eliminate the inadmissible solutions generated by the squaring operation. Also, we can use the fact that any equilibrium must satisfy the condition that nodal voltages are monotonically decreasing with distance from the source, i.e. $V \geq v_1 \geq v_2 \geq \dots \geq v_n$, to prune away intermediate results. We can also use the fact that $\mathbf{v} \in \mathcal{P}$, to eliminate the solutions incompatible with the cutoff voltages. This procedure is demonstrated with examples in Appendix C.

It should be clear at this point that the static equilibria for the system outside \mathcal{P} can be obtained in a similar fashion. In general, to obtain all the static equilibria of an n th-order system involves computations for 2^n regions. However, if the cutoff voltages of the loads are equal, all the static equilibria must occur in \mathcal{P} (see Section 3.3.1) and we can avoid this extra work.

For a second-order system, it is also possible to find the equilibria graphically by plotting the curves defined by (4.1); the resulting equilibria may then be characterized graphically with a field plot. This method is good because it also provides us with some insight into the dynamic evolution of the system as well. Appendix C contains examples of such plots obtained with Maple V. For higher-order systems, the most practical method of characterizing the equilibria obtained is to evaluate the Hessian of the energy function at the equilibrium and test it for positive and negative definiteness.

4.1.2 Small-Resistance Approximation

Under normal operating conditions, a typical network will generally have a stable operational equilibrium. Under certain conditions, it is possible to obtain a reasonably good approximation of the stable equilibrium. More specifically, if the resistances in the network are small relative to the source voltage and the power ratings of the constant-power loads, a “Small-Resistance Approximation” may be made. The following example will illustrate this point.

Second-Order System

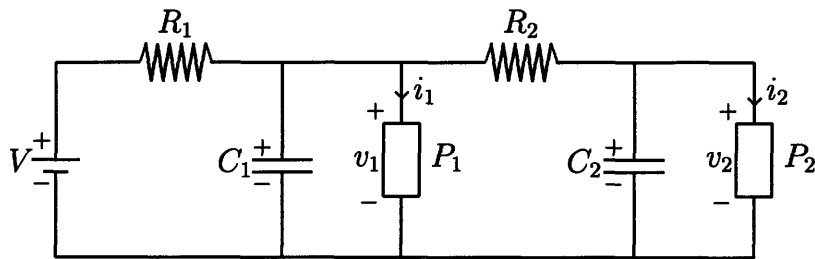


Figure 4-1: Second-order system.

For the second-order system shown in Figure 4-1, if the resistance R_2 is small relative to the supply voltage V , the voltage drop across R_2 will be small. Hence, $v_1 \simeq v_2$. With this assumption,

$$\frac{P_1}{i_1} \simeq \frac{P_2}{i_2} \quad (4.2)$$

Hence,

$$i_2 \simeq \frac{P_2}{P_1} i_1 \quad (4.3)$$

Since the current $i_1 + i_2$ flows through R_1 ,

$$v_1 = V - (i_1 + i_2)R_1 \quad (4.4)$$

$$P_1 = i_1 v_1 \quad (4.5)$$

$$= i_1(V - (i_1 + i_2)R_1) \quad (4.6)$$

$$\simeq i_1(V - (1 + \frac{P_2}{P_1})i_1R_1) \quad (4.7)$$

We can rewrite (4.7) as

$$(1 + \frac{P_2}{P_1})R_1i_1^2 - Vi_1 + P_1 = 0 \quad (4.8)$$

Applying the quadratic formula, we obtain

$$i_1 = \frac{V - \sqrt{V^2 - 4(P_1 + P_2)R_1}}{2(1 + \frac{P_2}{P_1})R_1} \quad (4.9)$$

which we call a *first-guess equation*. Now that we have an approximation for i_1 , we consider the next node to obtain

$$v_2 = v_1 - i_2R_2 \quad (4.10)$$

$$= V - (i_1 + i_2)R_1 - i_2R_2 \quad (4.11)$$

$$= V - i_1R_1 - (R_1 + R_2)i_2 \quad (4.12)$$

$$P_2 = i_2v_2 \quad (4.13)$$

$$= i_2(V - i_1R_1 - (R_1 + R_2)i_2) \quad (4.14)$$

Now we rewrite (4.14) as

$$(R_1 + R_2)i_2^2 - (V - i_1R_1)i_2 + P_2 = 0 \quad (4.15)$$

Finally, we have

$$i_2 = \frac{(V - i_1R_1) - \sqrt{(V - i_1R_1)^2 - 4(R_1 + R_2)P_2}}{2(R_1 + R_2)} \quad (4.16)$$

Once we find i_1 and i_2 , we have effectively solved for v_1 and v_2 since $P_1 = i_1v_1$ and $P_2 = i_2v_2$. Applying the above results to a case where all resistances and loads are equal:

$V = 90\text{V}$, $R_1 = R_2 = 2\Omega$ and $P_1 = P_2 = 100\text{W}$, we obtain

$$v_1 = 85.311\text{V}, v_2 = 82.826\text{V}$$

We can compare these results with the results obtained by solving for the equilibrium numerically in Section C.1, which are

$$v_1 = 85.23889858\text{V}, v_2 = 82.82414376\text{V}$$

Actually, we can do even better than this. We can substitute the numerical result obtained with (4.16) back into (4.6) to obtain an even better approximation for i_1 . We rewrite (4.6) as

$$R_1 i_1^2 - (V - i_2 R_1) i_2 + P_1 = 0 \quad (4.17)$$

Finally, we have

$$i_1 = \frac{(V - i_2 R_1) - \sqrt{(V - i_2 R_1)^2 - 4R_1 P_1}}{2R_1} \quad (4.18)$$

With this further iteration, we obtain

$$v_1 = 85.239\text{V}, v_2 = 82.826\text{V}$$

In fact, it should be apparent now that we have an initial guess and an iterative algorithm for computing i_1 and i_2 and hence indirectly v_1 and v_2 . A further iteration for i_2 with Equation (4.16) yields

$$v_1 = 85.2390\text{V}, v_2 = 82.8241\text{V}$$

We refer to (4.16) and (4.18) as *iterative equations*. Notice that we have arrived at an accuracy of 5 significant figures within two iterations.

Third-Order System

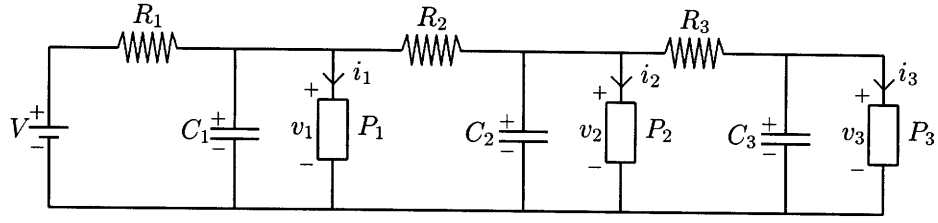


Figure 4-2: Third-order system.

Now we repeat the procedure with the third-order ladder shown in Figure 4-2. Given that $v_1 \simeq v_2 \simeq v_3$ because the resistances R_2 and R_3 are small, we obtain the following first-guess equations:

$$i_1 = \frac{V - \sqrt{V^2 - 4(P_1 + P_2 + P_3)R_1}}{2(1 + \frac{P_2}{P_1} + \frac{P_3}{P_1})R_1} \quad (4.19)$$

$$i_2 = \frac{V - i_1R_1 - \sqrt{(V - i_1R_1)^2 - 4(P_1 + P_2)(R_1 + R_2)}}{2(1 + \frac{P_2}{P_1})(R_1 + R_2)} \quad (4.20)$$

The following are the iterative equations for i_1 , i_2 and i_3

$$i_1 = \frac{V'_1 - \sqrt{V_1'^2 - 4P_1R_1}}{2R_1} \quad (4.21)$$

$$i_2 = \frac{V'_2 - \sqrt{V_2'^2 - 4P_2(R_1 + R_2)}}{2(R_1 + R_2)} \quad (4.22)$$

$$i_3 = \frac{V'_3 - \sqrt{V_3'^2 - 4P_3(R_1 + R_2 + R_3)}}{2(R_1 + R_2 + R_3)} \quad (4.23)$$

where

$$V'_1 = V - (i_2 + i_3)R_1 \quad (4.24)$$

$$V'_2 = V - (i_1 + i_3)R_1 - i_3R_2 \quad (4.25)$$

$$V'_3 = V - (i_1 + i_2)R_1 - i_2R_2 \quad (4.26)$$

The details for the derivations of these equations are found in Appendix D.

Applying the above results to a case where all resistances and loads are equal: $V =$

90V, $R_1 = R_2 = R_3 = 2\Omega$ and $P_1 = P_2 = P_3 = 100\text{W}$, we obtain the following solution after two iterations:

$$v_1 = 82.28900156\text{V}, v_2 = 76.99294897\text{V}, v_3 = 74.29875511\text{V}$$

We compare these results with that obtained in Section C.2:

$$v_1 = 82.27967469\text{V}, v_2 = 76.99008334\text{V}, v_3 = 74.29822913\text{V}$$

In general, to derive the first-guess and the iterative equations, we first divide the set of currents drawn by the loads into two sets: one set with known values and one set with unknown values. Next, we consider one current loop at a time and model it as a first-order network. The “known” set has a *Source Voltage Reducing Effect* while the “unknown” set has a *Resistor Multiplying Effect* on the result. Once we obtain the equivalent first order network, we have effectively derived the required equation. An example to illustrate this process is given in Appendix D.

Robustness and Convergence

In order to examine the robustness of the above algorithm, we repeat the above process with a range of different values for R_1 and R_2 , especially for rather large values of R_2 . Table 4.1 lists the results for various values of R_1 and R_2 , as well as results when P_1 , P_2 and V are varied. The approximations listed are obtained after two iterations.

Table 4.2 shows the convergence for the algorithm on a third-order system where all resistances and loads are equal: $V = 90\text{V}$, $R_1 = R_2 = R_3 = 2\Omega$ and $P_1 = P_2 = P_3 = 100\text{W}$. The results from direct numerical solution obtained in Section C.2 are

$$v_1 = 82.27967469\text{V}, v_2 = 76.99008334\text{V}, v_3 = 74.29822913\text{V}$$

Table 4.1: Table of Approximation Results for a Second-Order System

R_1	R_2	P_1	P_2	V	Exact v_1	Exact v_2	Approx. v_1	Approx. v_2
1	1	100	100	90	87.7044	86.5490	87.7044	86.5490
1	2	100	100	90	87.6879	85.3444	87.7200	85.3449
1	4	100	100	90	87.6517	82.8221	87.7200	82.8230
1	8	100	100	90	87.5626	77.1999	87.7200	77.2023
1	10	100	100	90	87.5057	73.9904	87.7200	73.9939
1	12	100	100	90	87.4356	70.3870	87.7200	70.3920
1	14	100	100	90	87.3444	66.1947	87.7200	66.2021
1	16	100	100	90	87.2133	60.9715	87.7200	60.9837
1	18	100	100	90	86.9634	53.0032	87.7200	53.0338
2	2	50	100	90	86.4650	84.0865	86.4650	84.0865
2	2	100	100	90	85.2390	82.8241	85.2389	82.8241
2	2	200	100	90	82.6668	80.1720	82.6667	80.1720
2	2	300	100	90	79.9046	77.3176	79.9043	77.3175
2	2	500	100	90	73.5848	70.7571	73.5834	70.7568
2	2	650	100	90	67.7072	64.6085	67.7028	64.6072
2	2	800	100	90	60.0000	56.2182	59.5686	55.9970
2	2	100	50	90	86.5166	85.3449	86.5166	85.3449
2	2	100	100	90	85.2390	82.8241	85.2389	82.8241
2	2	100	200	90	82.3928	77.2114	82.3920	77.2114
2	2	100	300	90	78.9528	70.4282	78.9473	70.4280
2	2	100	400	90	77.0156	61.3035	74.2190	61.1327
2	2	100	100	75	69.0769	66.0485	69.0766	66.0485
2	2	100	100	90	85.2390	82.8241	85.2389	82.8241
2	2	100	100	110	106.1989	104.2809	106.1988	104.2809
2	2	100	100	130	126.8260	125.2289	126.8260	125.2289
2	2	100	100	150	147.2712	145.9004	147.2712	145.9004

Table 4.2: Demonstration of Convergence

	v_1	v_2	v_3	Error in v_1	Error in v_2	Error in v_3
1	82.74917217	77.22351918	74.33132085	0.46949748	0.23343584	0.03309172
2	82.28900156	76.99294897	74.29875511	0.00932687	0.00286563	0.00052598
3	82.27979473	76.99012810	74.29823648	0.00012004	0.00004476	0.00000735
4	82.27967626	76.99008376	74.29822919	0.00000157	0.00000042	0.00000006
5	82.27967422	76.99008352	74.29822913	-0.00000047	0.00000018	0
6	82.27967490	76.99008311	74.29822913	0.00000021	-0.00000023	0
7	82.27967490	76.99008311	74.29822913	0.00000021	-0.00000023	0

It is interesting to note that the algorithm converges to a solution which differs from the solution obtained with direct numerical solution in the last two decimal places. It is likely that the error is due limited floating point precision. The error convergence is reproduced in graphical form in Figure 4-3. From the figure, it is apparent that the rate at which the error converges is approximately 2 orders of magnitude per iterative cycle.

It should be noted here that we do not have a proof that this algorithm always converges when a real solution exists. Empirically, it was found that when a real solution does not exist, one of more of the expressions under the square root signs in some of the first-guess or iterative equations will turn out to be negative.

Finally, the derivation of the results above also yields a necessary condition for operational equilibria to exist. As an example, consider the second-order example shown in Figure 4-1. Given that a stable operational equilibria does indeed exist for the system, it is obvious that the first-guess for i_1 , as given in (4.9), is a lower bound on the actual operational current. Hence, i_1 must be real and so the expression under the square root sign in (4.9) must be non-negative. So,

$$V^2 > 4(P_1 + P_2)R_1 \quad (4.27)$$

In general, we can conclude that an operational equilibrium can exist for an n th-order

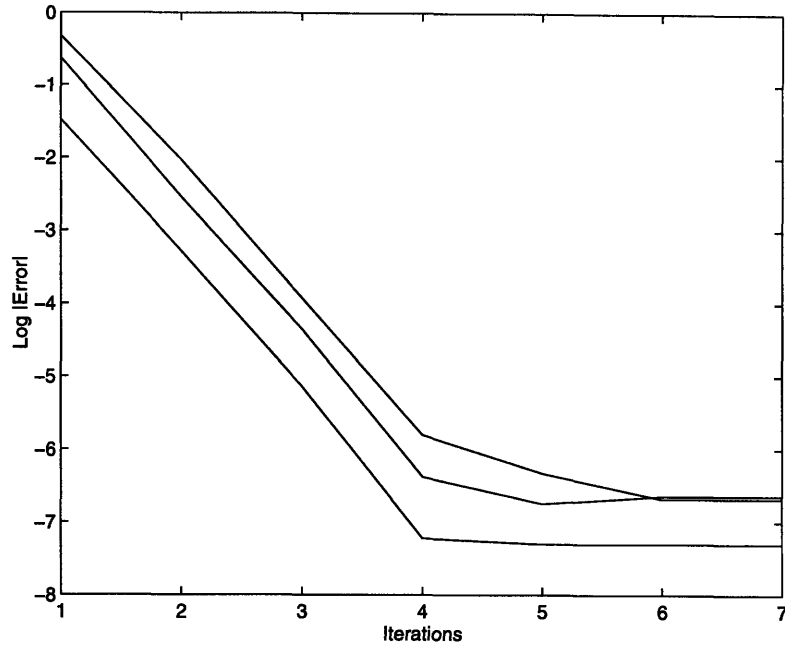


Figure 4-3: Error convergence.

ladder network only if

$$V^2 > 4\left(\sum_{i=1}^n P_n\right)R_1 \quad (4.28)$$

4.1.3 Approximation Using Aggregated Models

Thévenin and Norton models are extremely useful for analyzing resistive DC circuits. This section proposes two aggregated models for modeling simple second-order RCP configurations. The studied series and parallel configurations are shown in Figures 4-4 and 4-5 respectively. Essentially, we would like to find a first-order network as shown in Figure 4-6 which approximates these configurations in terms of steady-state behavior and loosely in terms of dynamic behavior.

Assumptions

Unlike the Thévenin and Norton models, the nonlinearity in these circuits make it impossible for two RCP networks of differing order from being exactly equivalent, but under the following assumptions, we can obtain rather good approximations:

- The voltage drops across resistors R_1 and R_2 are small compared to the voltage source. This condition ensures that the power dissipation in the aggregated model is close to the power dissipation in modeled configuration. This is the most important assumption in the derivation of the results for the models.
- The cutoff voltage for both constant-power loads are equal, or at least very close, i.e. $V_1^* \simeq V_2^*$. This condition ensures that both loads will turn on at approximately the same time.
- Time constants (R_1C_1 and R_2C_2 in the parallel case; R_1C_1 and $(R_1 + R_2)C_2$ in the series case) are of similar magnitude. This condition supplements the above condition to ensure that both loads will turn on at approximately the same time. With widely differing time constants, one load would turn on before the other.
- The voltage source is a low frequency source.

If the above conditions are satisfied, the following aggregated models are reasonably good first-order approximations for the total steady-state current drawn from the source, the total power dissipation and transient rise times. A detailed evaluation of these models with some worked examples is given in Appendix E.

Series Model

The assumptions above imply that $V \simeq v_1 \simeq v_2$. Hence, the currents through P_1 and P_2 respectively are $\frac{P_1}{V}$ and $\frac{P_2}{V}$. It is intuitively reasonable to assume that P' in the aggregated system is the sum of P_1 and P_2 . Similarly, we assume a small voltage drop across the resistor in the aggregated system so $i' = \frac{P'}{V}$. Now, we try to match the power dissipation through the resistances:

$$(i_1 + i_2)^2 R_1 + i_2^2 R_2 = i'^2 R' \quad (4.29)$$

$$\left(\frac{P_1}{V} + \frac{P_2}{V}\right)^2 R_1 + \left(\frac{P_2}{V}\right)^2 R_2 = \frac{P_1 + P_2^2}{V} R' \quad (4.30)$$

$$R' = R_1 + \frac{R_2 P_2^2}{(P_1 + P_2)^2} \quad (4.31)$$

Hence, the approximation of the second-order series configuration in Figure 4-4 by the first-order configuration shown in Figure 4-6 yields the following parameters:

$$R' = R_1 + \frac{R_2 P_2^2}{(P_1 + P_2)^2} \quad (4.32)$$

$$C' = C_1 + C_2 \quad (4.33)$$

$$P' = P_1 + P_2 \quad (4.34)$$

Since the cutoff voltages of the two original loads are equal, the resultant cutoff voltage of the aggregated model is taken to be the same as that for the two original cutoff voltages.

Parallel Model

By matching power dissipation in the resistors of the second-order system to that in the first-order aggregated model, we obtain the approximation of the second-order parallel configuration as shown in Figure 4-5:

$$R' = \frac{R_1 P_1^2 + R_2 P_2^2}{(P_1 + P_2)^2} \quad (4.35)$$

$$C' = C_1 + C_2 \quad (4.36)$$

$$P' = P_1 + P_2 \quad (4.37)$$

As above, the resultant cutoff voltage of the aggregated model is taken to be the same as that for the original loads.

Application

By repeated application of the series and parallel models, it is possible to reduce any arbitrary higher-order RCP-tree network into a first-order network, which is relatively easy to

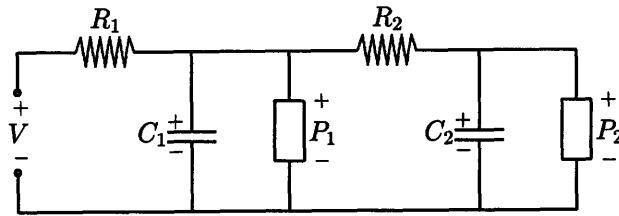


Figure 4-4: Second-order series configuration.

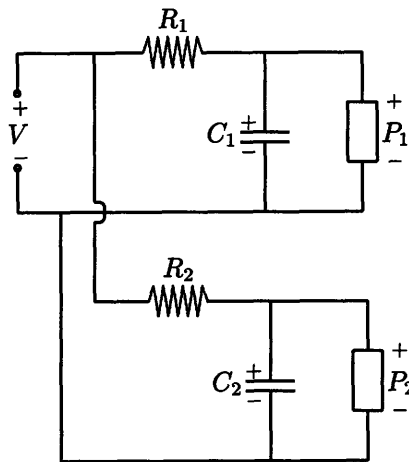


Figure 4-5: Second-order parallel configuration.

solve. With this first-order approximation, the resultant simple system is solved to produce an approximation for the total current drained from the source. This value is then used to compute the resistive drop across the resistor closest to the load in the original network to estimate the voltage of the node nearest the source. Next, we then repeat the above process by considering the original network with the source removed and the first load replaced by a voltage source of value equal to the obtained estimate. Eventually, we will obtain approximations to all the nodal voltages for the original network. Simple examples of this procedure performed on second-order and third-order networks are given in Appendix E.

Iterative equations, as described in Section 4.1.2, may be employed to further reduce the error. Overall, this technique is useful to obtain a quick back-of-the-envelope estimate for the total current drained from the source, as well as the first-order rise times for the

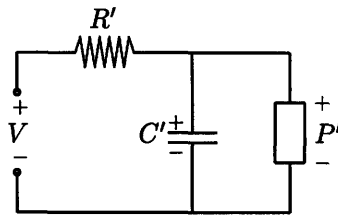


Figure 4-6: Aggregated model.

system during network design.

4.1.4 Iteration and Circuit Simulation

We can also compute equilibria using computer software like a spreadsheet that support iterations (such as Microsoft® Excel) or a general purpose circuit simulator (such as PSPICE®). For a spreadsheet, the solution can be found simply by defining the nodal voltages and currents in cells and then letting the system converge to a solution; for a circuit simulator, we simply define the circuit with its initial conditions and let the software perform the simulation.

There are two main drawbacks for these methods: firstly, given an arbitrary system, we cannot tell if the program will converge to a solution; even if convergence occurs, we cannot systematically guaranteed that all possible equilibria are found. Empirically, it was found that a spreadsheet will always tend to converge on an operational equilibrium when it exists. On the other hand, the solution that a circuit simulator will converge to is dependent on the chosen initial conditions. The other problem is that we will not be able to find unstable equilibria since it is not likely that simple iterative methods will converge on them. In fact, this problem is common to both the methods described in the previous two subsections as well. It seems likely that direct numerical solution is the only feasible way to find such equilibria.

Finally, it must be commented that in the event that we are only interested in solving for one operational equilibrium and we need to do this for several systems with the same

layout but different parameter values, a spreadsheet may actually be the most convenient and efficient way for doing so, if it converges to the required solution. Most of the other methods require much more book-keeping.

4.2 Dynamic Equilibria

The set of analytic equations which define a dynamic equilibrium is exactly that defined in (4.1) with some equations replaced by constant-voltage constraints. Overall, the task of computing dynamic equilibria is no different from that for static ones once these constraints are recognized.

To obtain all possible equilibria, we would essentially have to solve (4.1) once for each of the 2^n possible permutations of constraints imposed by different subsets of the loads operating in the metastable region. Fortunately, in practical situations, we usually deal with networks where all the loads have the same cutoff voltage. It can be shown easily that the direction of current flow in equilibrium is fixed, so if the cutoff voltages are monotonically non-decreasing with distance from the source, any load that is downstream of a load in cutoff must also be in cutoff (see Section 3.4.2). This reduces the number of cases that we have to examine to a polynomial number.

Once we know the constraints, we can either solve for the equilibria numerically in a manner similar to that described in Section 4.1.1, or use software like a spreadsheet or circuit simulator, as described in Section 4.1.4. For a spreadsheet, this simply involves setting certain the voltages at constrained nodes equal to the cutoff voltage of the load at the node; for a circuit simulator, it simply involves replacing the each constrained load with a voltage source.

After we have obtained the solutions to the constrained system mentioned above, we identify dynamic equilibria by checking the currents entering the voltage-constrained nodes for each solution obtained. The dynamic equilibria are the solutions where the currents

drawn by the loads do not exceed the maximum current capacity of the loads at the corresponding nodes. If none of the solutions satisfy this last condition, then dynamic equilibria do not exist for the system.

Chapter 5

Network Design

In this chapter, we attempt to reconcile the theoretical results from the previous chapters with the actual process of designing a network. We discuss some important issues in network design and then proceed to evaluate our theoretical results in the context of a broadband power network. In particular, we examine a proposed series model in detail and evaluate our conditions for guaranteed stability. Also, we discuss the effectiveness of the aggregated-model approximation as a means for estimating total operational current and power dissipation. Finally, we evaluate the merit of choosing $\frac{V}{2}$ as the cutoff voltage.

5.1 Background

The fundamental goal in the design of a broadband power network is to guarantee that the network is functional when powered up, i.e. when the source turns on, all the constant-power loads get turned on after a finite-length transition period. More specifically, we want to ensure that there exists a stable and desirable operational equilibrium. Furthermore, we want to guarantee that the network will reach this equilibrium point from zero initial conditions. There is also a fundamental constraint on the total current drawn by the network, since a practical power source can only supply a finite amount of current.

Given that the above conditions are satisfied, other conditions are sometimes imposed. For example,

- minimization of power dissipation by parasitic resistance in the conducting cables,
- minimization of cable length,
- minimization of total costs (cable costs + energy costs), and
- minimization of total current drawn from the source.

Ultimately, these are only secondary issues, so this chapter focuses on the main design concern of ensuring system stability and evaluates a network design in this light. We will assume for the purposes of this thesis that the current-limiting constraint on the source can always be satisfied.

One last practical consideration is that constant-power loads are mass-produced with identical power ratings and cutoff voltages. Resistances may vary according to the cable length and type. As mentioned previously, ladder networks are of particular interest since bus-type architectures are commonly implemented.

In essence, network design is the process of making compromises among a variety of different factors that are often conflicting. It is clear from the results presented in previous chapters that by increasing the supply voltage and the cutoff voltages, we can give stronger guarantees on the stability of the resultant system. Unfortunately, the voltage of the power source is often limited by safety regulations that prohibit the voltage from exceeding a certain fixed limit. Also, since voltage falls monotonically along the network, the size of a network is limited by the cutoff voltage. In practical terms, having a high cutoff voltage provides better stability properties, but limits the range of the network, while having a low cutoff voltage increases the maximum range, but possibly at the expense of system stability. Similarly, it is clear that it is possible to increase the range of a network by reducing the resistance in the cables. However, this involves the use of thicker cables, which will increase the total cost of laying the network.

5.2 Benchmark Model for a Practical Broadband Power Network

A benchmark model of a broadband power network as proposed by the engineers at Lucent Technologies is shown in Figure 5-1. In this model, a string of identical Optical Network Units (ONUs) arranged in series are powered by a single power node. The distances between ONUs are identical and equal to d ; the distance between the power node and the first ONU is $\frac{d}{2}$.

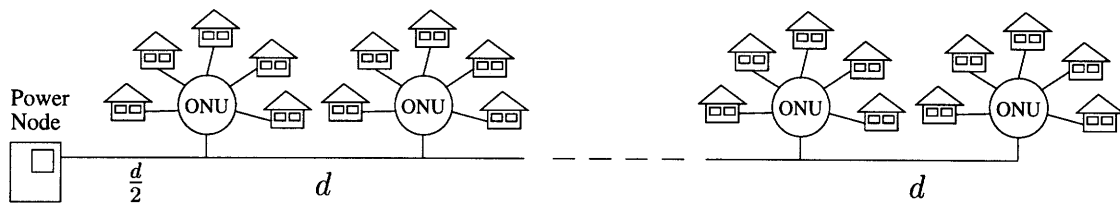


Figure 5-1: Schematic for practical series broadband network layout.

We assume that the cable carrying the power from the power node to the ONUs is of the same type throughout the network and of uniform resistance per unit length. Hence, a circuit model for the network is shown in Figure 5-2. The cables between the ONUs are modeled as resistors and the ONUs themselves are modeled as constant-power loads.

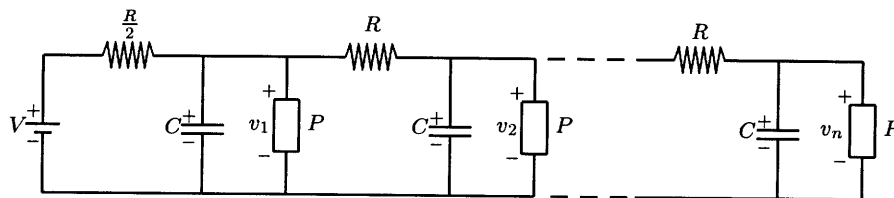


Figure 5-2: Practical model for broadband network.

5.3 Stability Conditions

In Chapter 3, by analyzing the static and dynamic equilibria of a system, we discussed methods that can be used to derive sufficient conditions for stability. In this section, we apply these results for the RCP-ladder network modeled by the circuit shown in Figure 5-2.

5.3.1 Static Equilibria

If we apply the results of Section 3.3 to the network in Figure 5-2, we can obtain conditions on the cutoff voltage that guarantee the uniqueness and stability of the operational equilibrium, in much the same way as that for regular networks.

As before, a sufficient condition for an n th-order network with the configuration shown in Figure 5-2 to have only one stable static equilibrium in \mathcal{P} , the region of \Re^n such that $V^* \leq v_k < V$ for $k = 1, \dots, n$ is of the form:

$$V^{*2} > f(n)PR \quad (5.1)$$

where V^* is the cutoff voltages of the loads. The coefficients, $f(n)$, are shown in Table 5.1.

5.3.2 Dynamic Equilibria

In a similar manner, we repeat the analysis in Section 3.4.2, assuming a cutoff voltage of $\frac{V}{2}$, where V is the source voltage, to obtain the following sufficient condition to ensure that dynamic equilibria do not occur:

$$V^2 > g(n)PR \quad (5.2)$$

With some algebra, we obtain

$$g(n) = h'(n) + 2 + \sqrt{h'(n)^2 + 16h'(n) + 48}, \text{ for } n \geq 3 \quad (5.3)$$

Table 5.1: Cutoff Voltage Coefficients for Broadband Power Network Model (Static Equilibria)

Order, n	$f(n)$
1	0.5000000
2	1.7071069
3	3.7320508
4	6.5685356
5	10.2158646
6	14.6738702
7	19.9424954
8	26.0217174
9	32.9115239
10	40.6119094
11	49.1228718
12	58.4444074
13	68.5765134
14	79.6444671
15	91.2724465

where $h'(n) = n^2 - 6$. Values of $g(n)$ for $n = 1, \dots, 15$ are given in Table 5.2.

Also given in Table 5.2 are the corresponding values of the coefficient sufficient for ensuring that there can exist only one stable operational equilibrium (see equation (5.1)). It should be noted here that the sufficient condition on V to ensure that dynamic equilibria do not occur is more stringent than that which is sufficient to guarantee the uniqueness and stability of the operational equilibrium.

5.4 Application of Results

5.4.1 Guaranteeing Stability

We can summarize the results from Section 5.3 in the following way: if an RCP-ladder network of the form shown in Figure 5-2 with the cutoff voltages of its loads set at $\frac{V}{2}$ is

Table 5.2: Cutoff Voltage Coefficients for Broadband Power Network Model (Dynamic Equilibria)

Order, n	$g(n)$	$4f(n)$
1	2.000000	2.000000
2	7.291503	6.828428
3	17.246951	14.928203
4	31.549929	26.274142
5	49.702060	40.863458
6	71.788887	58.695481
7	97.842895	79.769982
8	127.878676	104.086870
9	161.903558	131.646096
10	199.921539	162.447638
11	241.934942	196.491487
12	287.945195	233.777630
13	337.953210	274.306054
14	391.959592	318.577868
15	449.964755	365.089786

known to have an operational equilibrium, and the condition

$$V^2 > \max(g(n), 4f(n))PR \quad (5.4)$$

is satisfied, the given operational equilibrium is the unique and globally stable equilibrium of the system. The system will eventually end up at this equilibrium in steady state starting from any initial conditions.

Next, we consider the network shown in Figure 5-2 with the following parameter values: $V = 90\text{V}$, $V^* = 45\text{V}$, $d = 240'$ and $P = 100\text{W}$. The resistance per unit length of the cable is $1.9 \text{ m}\Omega/\text{foot}$, so $R = 0.456\Omega$. With these parameter values, we obtain

$$\frac{V^2}{PR} = 177.63 \quad (5.5)$$

Comparing this value with the coefficients in Table 5.2, we find that we can guarantee that any network of order 9 or lower will be stable, provided that an operational equilibrium

Table 5.3: Steady-State Voltages and Currents for 9th-order System

Node, k	v_k	i_k	$i_{t,k}$
1	87.10	1.15	12.72
2	81.82	1.22	11.58
3	77.10	1.30	10.35
4	72.97	1.37	9.06
5	69.47	1.44	7.69
6	66.62	1.50	6.25
7	64.45	1.55	4.75
8	63.00	1.59	3.19
9	62.27	1.61	1.61

exists.

It is found that operational equilibria exist for systems with these parameters up to the 10th order. This computation was performed with a spreadsheet as described in Section 4.1.4. The nodal voltages and currents for a 9th-order system and a 10th-order system are found in Tables 5.3 and 5.4 respectively, where v_k is the voltage of the k th node and i_k is the total current flowing through the k th resistor. From these results, it comes as no surprise that the sufficient conditions we derived cannot guarantee stability for the 10th-order system, since the voltage of the last node dips to a mere 49.02V, which is just 3.02V higher than the cutoff voltage. On the other hand, the last node for the 9th-order system is some 17.3V higher than the cutoff voltage.

One possible design decision is to replace the cable with a thicker one so that the resistance is lower. In the above example, the results from Table 5.2 suggest that if we want to guarantee stability for a 10th-order network, we should pick

$$R < 0.405\Omega \tag{5.6}$$

Effectively, this implies that if we replace the present cable with a new type that has a resistance per unit length less than 1.69 m Ω /foot, we can again guarantee stability.

Table 5.4: Steady-State Voltages and Currents for 10th-order System

Node, k	v_k	i_k	$i_{t,k}$
1	86.21	1.16	16.62
2	79.16	1.26	15.46
3	72.69	1.38	14.20
4	66.84	1.50	12.82
5	61.68	1.62	11.32
6	57.25	1.75	9.70
7	53.63	1.86	7.96
8	50.85	1.97	6.09
9	48.97	2.04	4.12
10	48.02	2.08	2.08

5.4.2 Estimating Operational Current Load and Power Dissipation

It was mentioned in Section 4.1.3 that aggregated models may be used to provide back-of-the-envelope calculations for the total current drawn from the power source by the network in equilibrium. We will evaluate the effectiveness of the approximate model for the network shown in Figure 5-2.

We find that we can approximate an n th-order network with the first order network shown in Figure 5-3 by successive application of the series aggregate model. With some algebra, we obtain the following parameters:

$$R_n = \frac{2n^2 + 1}{6n} R \quad (5.7)$$

$$P_n = nP \quad (5.8)$$

$$C_n = nC \quad (5.9)$$

With this, we conclude that

$$i_{est} = \frac{V - \sqrt{V^2 - \frac{8(2n^2+1)}{6} PR}}{\frac{2n^2+1}{3n} R} \quad (5.10)$$

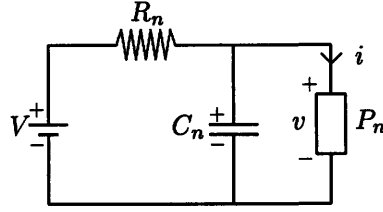


Figure 5-3: First-order aggregated-model approximation.

Table 5.5: Steady-State Currents and Aggregated-Model Estimates

Order, n	$i_{t,n}$	i_{est}	Fractional Error	ni_{max}	Fractional Error
1	1.114256	1.114256	0.000000	2.22222	0.994354
2	2.241349	2.241311	-0.000017	4.44444	0.982933
3	3.395345	3.394975	-0.000109	6.66667	0.963473
4	4.593119	4.591302	-0.000396	8.88889	0.935262
5	5.856816	5.850362	-0.001102	11.11111	0.897125
6	7.218385	7.199149	-0.002665	13.33333	0.847135
7	8.729326	8.676949	-0.006000	15.55556	0.781988
8	10.486231	10.346575	-0.013318	17.77778	0.695345
9	12.723293	12.322140	-0.031529	20.00000	0.571920
10	16.619012	14.858297	-0.105946	22.22222	0.337157

Table 5.5 compares the estimates made with the aggregated model with the actual currents drawn. Here, $i_{t,n}$ is the actual total current drawn by an n th-order network and i_{est} is the estimate of the current drawn by an n th-order network using the aggregated-model approximation; ni_{max} is a naive estimation of the current drawn, obtained by simply multiplying the maximum current drawn by a load (i_{max}) by the total number of loads.

From the results in Table 5.5, it is apparent that although the aggregated-model approximation tends to underestimate the total current drawn, it does give a reasonably good estimate. In fact, it is good to within 3% up to the 9th-order network. If we follow the above design guidelines and limit the network to 9th-order, we have a very simple but good method for estimating the total current. It is also apparent from the table that the naive estimate obtained by simply multiplying the maximum current capacity of the loads with

the total number of loads is very bad.

Since the power dissipated by the network is intrinsically equal to the power drawn from the source, Vi , and V is fixed, the power dissipated is totally dependent on the current drawn. This means that the error in the estimation of power dissipation using the aggregated model is identical to the error in the estimation of the current. Since we have shown above that the estimation of the current drawn is good, we conclude that the estimation of power dissipation is equally good, i.e. the error is to within 3% for a network with up to 9 loads.

5.5 Varying the Cutoff Voltage

It is clear from Table 5.1 that, given the parameter values above, the minimum cutoff voltage that we know will guarantee the uniqueness and stability of the operational equilibrium for a 10th-order system is given by

$$V^* > 43.0337V \quad (5.11)$$

The natural question is then: is it possible to do any better if we can vary the cutoff voltage of the load, instead of fixing it at $\frac{V}{2}$. In order to find the coefficients for a cutoff of αV , we need to solve

$$(V - h'(n)\frac{PR}{2\alpha V})(\frac{2PR}{V} + \frac{V}{2}) > 8(\frac{PR}{V})^2 + \alpha^2 V^2 + (6\alpha + 1)PR \quad (5.12)$$

where $h'(n) = n^2 - 6$ for $n \geq 3$. From here, it is quite straightforward to obtain

$$g_\alpha(n) = \frac{6\alpha - 1 + \frac{h'(n)}{2} + \sqrt{(6\alpha - 1 + \frac{h'(n)}{2})^2 + 4\alpha(1 - \alpha)(8 + \frac{h'(n)}{\alpha})}}{2\alpha(1 - \alpha)} \quad (5.13)$$

With (5.13), we proceed to minimize $g_\alpha(n)$ over α for each value of n . The results are shown in Table 5.6. From this table, it is clear that the coefficient obtained with a cutoff of

Table 5.6: Minimization of Coefficient $g_\alpha(n)$.

Order, n	$g_{0.5}(n)$	$\min_\alpha g_\alpha(n)$	α	αV
3	17.246951	15.980833	0.35808172	32.227
4	31.549929	30.964361	0.43116569	38.805
5	49.702060	49.351048	0.45782074	41.204
6	71.788887	71.552601	0.47126013	42.414
7	97.842895	97.672305	0.47910339	43.119
8	127.878676	127.749479	0.48409902	43.569
9	161.903558	161.802212	0.48748635	43.874
10	199.921539	199.839864	0.48989177	44.090
11	241.934942	241.867692	0.49166262	44.250
12	287.945195	287.890918	0.49300460	44.370
13	337.953210	337.905272	0.49404615	44.464
14	391.959592	391.918350	0.49487085	44.538
15	449.964755	449.928877	0.49553509	44.598

$\frac{V}{2}$ is very close to the optimal solution for $n \geq 5$. Hence, a cutoff of $\frac{V}{2}$ is a good choice.

5.6 Summary

In this chapter, we applied the results from Chapters 2 and 3 on a proposed RCP-ladder network to produce a set of sufficient conditions to guarantee system stability. We then showed how these sufficient conditions may be used as a guide for network design.

We also investigated the use of the series aggregated model for the approximation of the total operational current load on the source as well as the total power dissipated. The estimate obtained was found to be reasonably good.

Finally, we concluded that $\frac{V}{2}$ is a good choice for the cutoff voltage. Although we can sometimes do a little better with a slightly lower cutoff voltage, the improvement in the results obtained is numerically insignificant.

Chapter 6

Conclusion

In this thesis, we demonstrated that an RCP-tree network satisfying a set of layout constraints can be modeled as a modified gradient system with non-differentiable boundaries, but a continuous energy function $E_n(\mathbf{v})$. We showed that even though the gradient is discontinuous across these boundaries, the dynamic behavior of the system on a boundary is governed by the limiting behavior on both sides of the boundary. The net effect is that as long as the state of the system is confined to a discontinuous boundary, its dynamic behavior is determined by a reduced set of state equations, which can in turn be expressed as a lower-order gradient system. Hence, the energy function $E_n(\mathbf{v})$ can be shown to be monotonically decreasing with time as long as the system is not in equilibrium.

We also established that all equilibria in the system must be contained within \mathcal{W} , the region of \mathfrak{R}^n such that $0 \leq v_i \leq V$ for $i = 1, \dots, n$, and cannot occur on the upper or lower boundaries, i.e. where $v_k = 0$ or $v_k = V$ for some node k . We showed that the system must eventually settle down at an equilibrium, and that the bounding box for the state of the system is positive-invariant. As a result, by studying the static and dynamic equilibria of a system in detail, we were able to derive simple sufficient conditions to guarantee that the system ends up at a desired stable equilibrium.

In particular, for a regular RCP-ladder network where all resistances, all capacitances

and all loads are identical, we found sufficient conditions to ensure the uniqueness and stability of an operational equilibrium. This was done by evaluating the Hessian of the associated energy function and ensuring that it is positive definite in the region of interest. In addition, for the same network, we found sufficient conditions that ensure that dynamic equilibria cannot occur. From these two results, we concluded that a sufficient condition to guarantee stability for an n th-order regular RCP-ladder network is

$$V^2 > g(n)PR \quad (6.1)$$

where $g(n)$ is a monotonically increasing function with n that is determined by the chosen cutoff voltage.

We introduced two aggregated models that allow us to approximate quite accurately, with a first-order network, the steady-state behavior of a high-order network. In the same way that Thévenin and Norton models are used to replace complex resistive DC circuits with simpler equivalent circuits, our aggregated models allow us to recursively reduce a higher-order RCP-tree network into a simpler network which has the same approximate steady-state behavior if certain conditions are satisfied.

Finally, we applied the derived sufficient stability conditions to a benchmark model for a broadband power network to demonstrate how these sufficient conditions may be used as a guide for network design. The model we used was proposed by the engineers at Lucent Technologies. The series aggregated model was applied to the network to approximate the operational current load on the source as well as the total power dissipated. The estimate obtained was found to be reasonably good. With a little analysis, it was also found that $\frac{V}{2}$ is a good choice for the cutoff voltage.

In conclusion, we have answered several important questions regarding the design of broadband powering network and we have acquired a deeper understanding of both the dynamic and static behavior of RCP-tree networks. However, even more interesting questions which demonstrate potential for research into this field have been raised in the process.

6.1 Future Work

In our model of the constant-power load, there is an implicit assumption that there is no hysteresis in the cutoff voltage. This assumption is crucial in our analysis of dynamic equilibria. It would be good to know how our results would change for an RCP-tree network in the case where there is hysteresis in the cutoff voltage. Adding hysteresis to the model of the constant-power load would undoubtedly cause the analysis to become more complex. More importantly, it is still unclear how the hysteresis should be modeled.

We have found sufficient conditions that ensure that a given RCP-tree network will end up at a desired equilibrium, independently of its initial conditions. However, it is sometimes possible to exert limited control over the intermediate states of a system. For example, a given RCP-tree network can be powered up in stages. As such, it is conceivable that the conditions sufficient to ensure that the network will end up at the desired equilibrium can be made less stringent. The questions of interest here include the following: what are the implications of a multi-stage powering scheme? Is it possible to quantitatively obtain some sufficient conditions for stability in such a situation? It is clear that such a scheme would impose a cost in terms of additional control and monitoring required, but would the additional cost incurred offset the benefits derived?

At a more practical level, it would be valuable to understand how we can design networks which would minimize one or more of the following factors:

- power dissipation by parasitic resistance in the conducting cables,
- cable length,
- total costs (cable costs + energy costs), and
- total current drawn from the source,

without compromising stability. The nonlinearity of the problem makes optimization using traditional mathematical techniques particularly difficult [1]. It would be interesting to

know if the aggregated approximation models proposed may be applied in some way to these problems.

Several methods for obtaining static and dynamic equilibria were presented in Chapter 4. Of these, the direct numerical method is evidently the most reliable. Unfortunately, it is extremely cumbersome and it would be impractical to use it to compute the equilibria for a large network. Although the iterative methods are easier to program and more convenient, we do not yet understand the convergence properties of such methods. It would be extremely helpful in network design to have a good iterative algorithm that is guaranteed to converge in a finite number of steps, if an equilibrium does exist. It would also be useful to have a simple method for determining the existence of static equilibria in a given system that does not require too much explicit computation.

Finally, another possible research area is the modeling and study of component failure within an RCP-tree network. For example, it would be useful to analyze the effect of a short circuit that occurs at a load in the network while the network is in operation. Reliability is a critical issue for broadband networks, so it is important that isolated component failures within a network can be contained and do not cause the entire network to fail.

Appendix A

Detailed Boundary Analysis for Second-Order System

This appendix contains the detailed analysis for the behavior of a second-order system, as described in Section 2.3, at the cutoff boundaries $v_1 = V_c$ and $v_2 = V_c$. The following arguments can actually be applied to the more general case of different cutoff voltages, but doing so simply makes the analysis more complicated without yielding any more insight. Also, in practical terms, having the same cutoff voltages for all the loads in the system is a reasonable assumption since the loads that we have in mind (the ONUs and NIUs mentioned in Chapter 1) are usually mass-manufactured. We will restrict the region of interest to one where $v_1 \geq v_2$. The reason for doing so is that when $v_1 < v_2$, capacitor C_2 will discharge and the system is obviously not in equilibrium; eventually, the system has to end up in a state where $v_1 \geq v_2$.

A.1 Boundary: $v_1 = V_c$

Considering the currents in the first node when $v_1 = V_c$, we obtain

$$i_1 = \frac{V - V_c}{R_1} - \frac{V_c - v_2}{R_2} \quad (\text{A.1})$$

We observe that once the system reaches the boundary $v_1 = V_c$, it will remain on this boundary as long as $0 \leq i_1 \leq \frac{P_1}{V_c}$. Physically, under this condition P_1 operates in the *metastable* region and capacitor C_1 is prevented from charging or discharging. The inequality $i_1 \leq \frac{P_1}{V_c}$ implies

$$v_2 < \frac{P_1 R_2}{V_c} + \left(1 + \frac{R_2}{R_1}\right)V_c - \frac{R_2}{R_1}V \quad (\text{A.2})$$

To see that the system is constrained to move along $v_1 = V_c$ when $0 \leq i_1 \leq \frac{P_1}{V_c}$, consider $\frac{dv_1}{dt}$ at $v_1 = V_c - \epsilon$ and at $v_1 = V_c + \epsilon$:

$$\left. \frac{dv_1}{dt} \right|_{v_1=V_c-\epsilon} = \frac{1}{C_1 R_1} \left(V - \left(1 + \frac{R_1}{R_2}\right)v_1 + \frac{R_1}{R_2}v_2 \right) \quad (\text{A.3})$$

$$\left. \frac{dv_1}{dt} \right|_{v_1=V_c+\epsilon} = -\frac{1}{C_1 R_{\parallel} v_1} \left(v_1^2 - R_{\parallel} \left(\frac{V}{R_1} + \frac{v_2}{R_2} \right) v_1 + P_1 R_{\parallel} \right) \quad (\text{A.4})$$

$$(\text{A.5})$$

We find that for $v_1 = V_c - \epsilon$, $\frac{dv_1}{dt} > 0$ when

$$v_2 > \left(1 + \frac{R_2}{R_1}\right)V_c - \frac{R_2}{R_1}V = k_2 < k_1 \quad (\text{A.6})$$

where $k_1 = \frac{P_1 R_2}{V_c} + \left(1 + \frac{R_2}{R_1}\right)V_c - \frac{R_2}{R_1}V$. Similarly, for $v_1 = V_c + \epsilon$, $\frac{dv_1}{dt} < 0$ when

$$v_2 < \frac{P_1 R_2}{V_c} + \left(1 + \frac{R_2}{R_1}\right)V_c - \frac{R_2}{R_1}V = k_1 \quad (\text{A.7})$$

Now, we consider the dynamics for v_2 . From (2.37) we have

$$\frac{dv_2}{dt}\bigg|_{v_1=V_c} = \frac{1}{C_2 R_2} (V_c - v_2) \quad (\text{A.8})$$

This implies that $\frac{dv_2}{dt}\big|_{v_1=V_c} > 0$ when $v_2 < V_c$. This gives rise to two possible scenarios, as shown in Figure A-1.

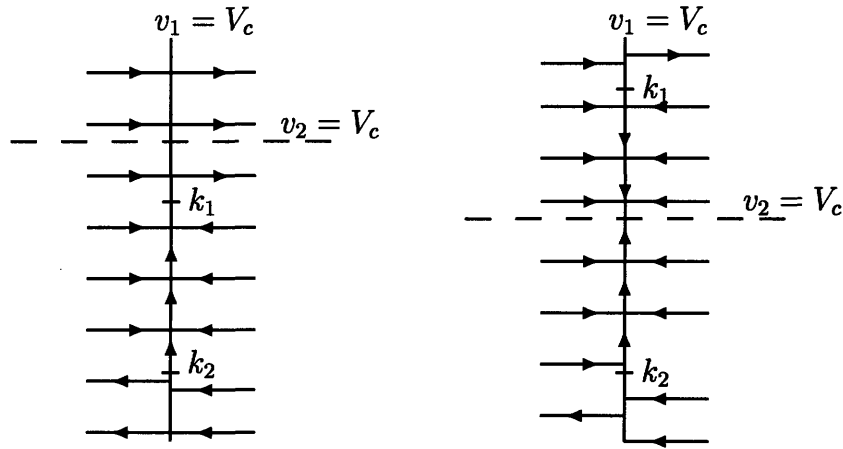


Figure A-1: Diagram of boundary $v_1 = V_c$.

In the scenario where $k_1 > V_c$, there is a distinct possibility for the system to get stuck at $v_1 = v_2 = V_c$. Hence, to ensure that this does not happen, we require $k_1 < V_c$, which implies

$$V > \frac{P_1 R_1}{V_c} + V_c \quad (\text{A.9})$$

A.2 Boundary: $v_2 = V_c$

Next, we consider the boundary $v_2 = V_c$. Considering the currents in the last node, we obtain

$$i_2 = \frac{v_1 - V_c}{R_2} \quad (\text{A.10})$$

Again, if $0 < i_2 < \frac{P_2}{V_c}$, the system is constrained to move along $v_2 = V_c$. This condition is equivalent to

$$V_c < v_1 < \frac{P_2 R_2}{V_c} + V_c \quad (\text{A.11})$$

Now, at $v_2 = V_c - \epsilon$ and at $v_2 = V_c + \epsilon$, we have

$$\left. \frac{dv_2}{dt} \right|_{v_2=V_c-\epsilon} = \frac{1}{C_2 R_2} (v_1 - v_2) \quad \text{and} \quad (\text{A.12})$$

$$\left. \frac{dv_2}{dt} \right|_{v_2=V_c+\epsilon} = -\frac{1}{C_2 R_2 v_2} (v_2^2 - v_1 v_2 + P_2 R_2) \quad (\text{A.13})$$

We find that for $v_2 = V_c - \epsilon$, $\frac{dv_2}{dt} > 0$ when

$$v_1 > V_c \quad (\text{A.14})$$

Similarly, for $v_2 = V_c + \epsilon$, $\frac{dv_2}{dt} < 0$ when

$$v_1 < \frac{P_2 R_2}{V_c} + V_c = k_3 \quad (\text{A.15})$$

Since we are considering the situation when $v_1 \geq v_2$, we consider $\left. \frac{dv_1}{dt} \right|_{v_2=V_c} > 0$, for $v_1 \geq V_c$, which yields

$$\left. \frac{dv_1}{dt} \right|_{v_2=V_c} = -\frac{1}{C_1 R_{\parallel} v_1} (v_1^2 - R_{\parallel} (\frac{V}{R_1} + \frac{V_c}{R_2}) v_1 + P_1 R_{\parallel}) > 0 \quad (\text{A.16})$$

$$(\frac{1}{R_1} + \frac{1}{R_2}) v_1^2 - (\frac{V}{R_1} + \frac{V_c}{R_2}) v_1 + P_1 < 0 \quad (\text{A.17})$$

$$v_1 < \frac{\frac{V}{R_1} + \frac{V_c}{R_2} + \sqrt{(\frac{V}{R_1} + \frac{V_c}{R_2})^2 - 4(\frac{1}{R_1} + \frac{1}{R_2})P_1}}{2(\frac{1}{R_1} + \frac{1}{R_2})} = k_4 \quad (\text{A.18})$$

Again, there are two possible scenarios. From Figure A-2, it is obvious that to ensure that the system does not get stuck at $v_1 = v_2 = V_c$, we require that $k_4 > k_3$, which yields after much algebraic manipulation the stability condition

$$V > V_c + \frac{P_2 R_1 R_2}{V_c R_{\parallel}} + \frac{P_1 R_1}{\frac{P_2 R_2}{V_c} + V_c} \quad (\text{A.19})$$

where $R_{||} = \frac{R_1 R_2}{R_1 + R_2}$. For the case where $V_c = \frac{V}{2}$, $R_1 = R_2 = R$ and $P_1 = P_2 = P$, this condition simplifies to

$$V^4 - 8PRV^2 - 32(PR)^2 > 0 \quad (\text{A.20})$$

which gives

$$V^2 > 4(1 + \sqrt{3})PR \quad (\text{A.21})$$

Comparing this result with the condition in Section 1.5.2 for stability for a simple first-order system, namely $V^2 > 4PR$ when the cutoff voltage is $\frac{V}{2}$, we notice that the second-order condition is more stringent, as expected.

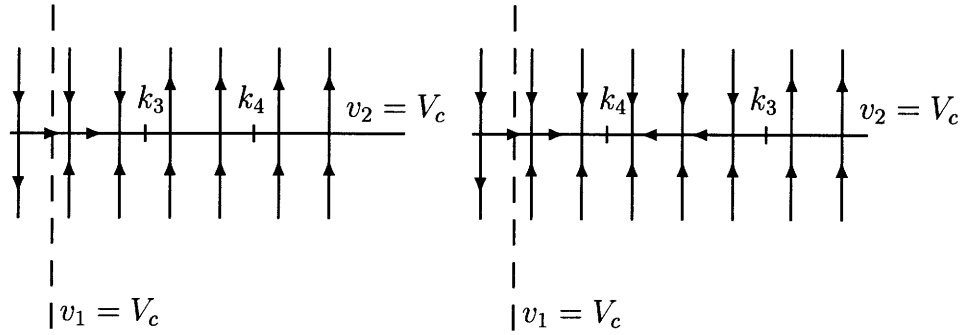


Figure A-2: Diagram of boundary $v_2 = V_c$.

Appendix B

Determinant Calculations

This appendix shows the detailed computations for obtaining the determinants of the Hessian for the energy functions of regular ladder networks as described in Section 3.3.3. The Hessian for the energy function of a regular n th-order ladder network takes the following form:

$$\frac{d^2 E_n(\mathbf{v})}{d\mathbf{v}^2} = \begin{bmatrix} -\frac{K(v_1)}{v_1^2} + \frac{2}{R} & -\frac{1}{R} & 0 & \cdots & 0 \\ -\frac{1}{R} & -\frac{K(v_2)}{v_2^2} + \frac{2}{R} & -\frac{1}{R} & \cdots & 0 \\ 0 & -\frac{1}{R} & -\frac{K(v_3)}{v_3^2} + \frac{2}{R} & \ddots & 0 \\ \vdots & \vdots & \ddots & \ddots & \vdots \\ 0 & 0 & \cdots & -\frac{1}{R} & -\frac{K(v_n)}{v_n^2} + \frac{1}{R} \end{bmatrix} \quad (\text{B.1})$$

where

$$K(v_k) = \begin{cases} P, & v_k \geq V^* > 0 \\ 0, & v_k < V^* \end{cases}$$

Here, R is the resistance of the resistors, C is the capacitance of the capacitors, V is the supply voltage, V^* is the cutoff voltage and P is the power rating of the loads. We are interested in the case where $v_k > V^*$, $k = 1, \dots, n$, so for the remainder of this appendix, there is an implicit assumption that we are dealing with systems where $v_k > V^*$ holds for $k = 1, \dots, n$.

We are interested in the determinants of the Hessian because we want to check for positive definiteness using *Sylvester's Test*. We define \mathcal{P} as the vector subspace of \mathfrak{R}^n such that $V^* \leq v_i \leq V$ for $i = 1, \dots, n$. Basically, we are interested in finding the conditions that will guarantee positive definiteness in \mathcal{P} . We make this observation: if $\frac{d^2 E_n}{d\mathbf{v}^2}(\mathbf{v})$ is positive definite at $v_i = V^*, i = 1, \dots, n$, then $\frac{d^2 E_n}{d\mathbf{v}^2}(\mathbf{v})$ is positive definite in \mathcal{P} . Let

$$D_n = \begin{bmatrix} -\frac{P}{V^{*2}} + \frac{2}{R} & -\frac{1}{R} & 0 & \cdots & 0 \\ -\frac{1}{R} & -\frac{P}{V^{*2}} + \frac{2}{R} & -\frac{1}{R} & \cdots & 0 \\ 0 & -\frac{1}{R} & -\frac{P}{V^{*2}} + \frac{2}{R} & \ddots & 0 \\ \vdots & \vdots & \ddots & \ddots & \vdots \\ 0 & 0 & \cdots & -\frac{1}{R} & -\frac{P}{V^{*2}} + \frac{1}{R} \end{bmatrix} \quad (\text{B.2})$$

Then,

$$\frac{d^2 E_n}{d\mathbf{v}^2}(\mathbf{v}) = D_n + \begin{bmatrix} \frac{P}{V^{*2}} - \frac{P}{v_1^2} & 0 & \cdots & 0 \\ 0 & \frac{P}{V^{*2}} - \frac{P}{v_2^2} & \cdots & 0 \\ \vdots & \vdots & \ddots & \vdots \\ 0 & 0 & \cdots & \frac{P}{V^{*2}} - \frac{P}{v_n^2} \end{bmatrix} \quad (\text{B.3})$$

Clearly, $\frac{P}{V^{*2}} - \frac{P}{v_i^2} \geq 0$ for $i = 1, \dots, n$ and the sum of a positive definite matrix and a positive semidefinite matrix is positive definite.

B.1 Second-Order System

For a second-order system, we have

$$D_2 = \begin{bmatrix} -\frac{P}{V^{*2}} + \frac{2}{R} & -\frac{1}{R} \\ -\frac{1}{R} & -\frac{P}{V^{*2}} + \frac{1}{R} \end{bmatrix} \quad (\text{B.4})$$

Hence,

$$\begin{vmatrix} -\frac{P}{V^{*2}} + \frac{2}{R} & -\frac{1}{R} \\ -\frac{1}{R} & -\frac{P}{V^{*2}} + \frac{1}{R} \end{vmatrix} = \left(-\frac{P}{V^{*2}} + \frac{2}{R}\right)\left(-\frac{P}{V^{*2}} + \frac{1}{R}\right) - \frac{1}{R^2} \quad (\text{B.5})$$

For $\frac{d^2 E_n}{dv^2}(\mathbf{v}) > 0$ to hold, we require

$$-\frac{P}{V^{*2}} + \frac{1}{R} > 0, \quad (\text{B.6})$$

$$\left(-\frac{P}{V^{*2}} + \frac{2}{R}\right)\left(-\frac{P}{V^{*2}} + \frac{1}{R}\right) - \frac{1}{R^2} > 0 \quad (\text{B.7})$$

Let

$$\alpha = -\frac{P}{V^{*2}} + \frac{2}{R} \quad (\text{B.8})$$

From inequality (B.7), we obtain

$$\alpha\left(\alpha - \frac{1}{R}\right) - \frac{1}{R^2} > 0 \quad (\text{B.9})$$

$$(\alpha R)^2 - \alpha R - 1 > 0 \quad (\text{B.10})$$

$$(\alpha R) > \frac{1 + \sqrt{5}}{2} \quad (\text{B.11})$$

$$2 - \frac{PR}{V^{*2}} > \frac{1 + \sqrt{5}}{2} \quad (\text{B.12})$$

$$\frac{P}{V^{*2}} < \frac{3 - \sqrt{5}}{2R} \quad (\text{B.13})$$

Inequality (B.7) yields the more stringent condition:

$$V^{*2} > \frac{2}{3 - \sqrt{5}} PR \quad (\text{B.14})$$

B.2 Third-Order System

For a third-order system, we have

$$D_3 = \begin{bmatrix} -\frac{P}{V^{*2}} + \frac{2}{R} & -\frac{1}{R} & 0 \\ -\frac{1}{R} & -\frac{P}{V^{*2}} + \frac{2}{R} & -\frac{1}{R} \\ 0 & -\frac{1}{R} & -\frac{P}{V^{*2}} + \frac{1}{R} \end{bmatrix} \quad (\text{B.15})$$

Hence,

$$|D_3| = \left(-\frac{P}{V^{*2}} + \frac{1}{R}\right) \begin{vmatrix} -\frac{P}{V^{*2}} + \frac{2}{R} & -\frac{1}{R} \\ -\frac{1}{R} & -\frac{P}{V^{*2}} + \frac{2}{R} \end{vmatrix} + \frac{1}{R} \begin{vmatrix} -\frac{P}{V^{*2}} + \frac{2}{R} & -\frac{1}{R} \\ 0 & -\frac{1}{R} \end{vmatrix} \quad (\text{B.16})$$

$$= \left(\left(-\frac{P}{V^{*2}} + \frac{2}{R}\right)^2 - \frac{1}{R^2}\right)\left(-\frac{P}{V^{*2}} + \frac{1}{R}\right) - \frac{1}{R^2}\left(-\frac{P}{V^{*2}} + \frac{2}{R}\right) \quad (\text{B.17})$$

$$= \left(\alpha^2 - \frac{1}{R^2}\right)\left(\alpha - \frac{1}{R}\right) - \frac{1}{R^2}\alpha > 0 \quad (\text{B.18})$$

We can now solve this inequality

$$(\alpha R)^3 - (\alpha R)^2 - 2(\alpha R) + 1 > 0 \quad (\text{B.19})$$

$$2 - \frac{PR}{V^{*2}} > 1.802 \quad (\text{B.20})$$

$$\frac{PR}{V^{*2}} < 0.198 \quad (\text{B.21})$$

$$V^{*2} > 5.049PR \quad (\text{B.22})$$

B.3 Higher-Order Generalization

Now generalize the above results for an n th-order system. Applying (3.13) and (3.14), we obtain

$$A_n = \begin{vmatrix} -\frac{P}{V^{*2}} + \frac{2}{R} & -\frac{1}{R} & 0 & \cdots & 0 \\ -\frac{1}{R} & -\frac{P}{V^{*2}} + \frac{2}{R} & -\frac{1}{R} & \cdots & 0 \\ \vdots & \vdots & \ddots & \ddots & \vdots \\ 0 & 0 & \cdots & -\frac{1}{R} & -\frac{P}{V^{*2}} + \frac{1}{R} \end{vmatrix} \quad (\text{B.23})$$

and

$$B_{n+1} = \begin{vmatrix} -\frac{P}{V^{*2}} + \frac{2}{R} & -\frac{1}{R} & 0 & \cdots & 0 \\ -\frac{1}{R} & -\frac{P}{V^{*2}} + \frac{2}{R} & -\frac{1}{R} & \cdots & 0 \\ \vdots & \vdots & \ddots & \ddots & \vdots \\ 0 & 0 & \cdots & -\frac{1}{R} & -\frac{P}{V^{*2}} + \frac{2}{R} \end{vmatrix} \quad (\text{B.24})$$

Then,

$$A_0 = B_1 = 1 \quad (\text{B.25})$$

$$A_1 = \alpha - \frac{1}{R} \quad (\text{B.26})$$

$$B_2 = \alpha \quad (\text{B.27})$$

$$A_n = \left(\alpha - \frac{1}{R}\right)B_n - \frac{1}{R^2}B_{n-1}, \quad n \geq 2 \quad (\text{B.28})$$

$$B_{n+1} = \alpha B_n - \frac{1}{R^2}B_{n-1}, \quad n \geq 2 \quad (\text{B.29})$$

Now, we can obtain the sufficient condition for $n = 4$:

$$A_4 > 0 \quad (\text{B.30})$$

$$\left(\alpha - \frac{1}{R}\right)B_4 - \frac{1}{R^2}B_3 > 0 \quad (\text{B.31})$$

$$\alpha\left(\alpha - \frac{1}{R}\right)\left(\alpha^2 - \frac{2}{R^2}\right) - \frac{1}{R^2}\left(\alpha^2 - \frac{1}{R^2}\right) > 0 \quad (\text{B.32})$$

$$(\alpha R)^4 - (\alpha R)^3 - 3(\alpha R)^2 + 2(\alpha R) + 1 > 0 \quad (\text{B.33})$$

$$2 - \frac{PR}{V^{*2}} > 1.879 \quad (\text{B.34})$$

$$\frac{PR}{V^{*2}} < 0.121 \quad (\text{B.35})$$

$$V^{*2} > 8.291PR \quad (\text{B.36})$$

In the same way, the coefficients for higher-order systems can be obtained from solving the inequality for the respective determinant. There is nonlinearity in the process, so a closed form solution is not readily available, but in principle, the coefficient can be computed for a system of any arbitrary order.

B.4 Computing the Inequality Coefficient

The results from the previous sections can be generalized into the following algorithm for generating the inequality coefficient: let $a_0(x) = 1$, $b_0(x) = 1$ and $b_1(x) = x$. We define

$$a_n(x) = (x - 1)b_n(x) - b_{n-1}(x), \text{ for } n \geq 1 \quad (\text{B.37})$$

$$b_n(x) = xb_{n-1}(x) - b_{n-2}(x), \text{ for } n \geq 2 \quad (\text{B.38})$$

Let β_n be the largest real root of $a_n(x)$ such that $1 < \beta_n < 2$. The coefficient of the inequality for an n th-order ladder is $\frac{1}{2-\beta_n}$.

B.5 Approximation for Sufficient Condition Coefficient

From above, it is apparent that the condition for an n th-order system is of the form:

$$V^{*2} > f(n)PR \quad (\text{B.39})$$

The computation of the coefficient, $f(n)$, is rather cumbersome. Table B.1 shows a list of coefficients for $n = 1, \dots, 15$. A plot of $f(n)$ is shown in Figure B-1. From the figure, it is apparent that the resulting function is convex. We try to approximate this curve with a simple quadratic function. After some experimentation,

$$f'(n) = 0.4n^2 + 0.5n - 0.3 \quad (\text{B.40})$$

was found to be a reasonably good approximation. Table B.1 also shows the error in the approximation. The fractional error is also plotted in Figure B-2. We find that the error is within 5% for $n = 3, \dots, 15$, so the following is a reasonably good approximation for a sufficient condition to ensure that a regular ladder system can have only one unique and

Table B.1: Errors for Approximation of $f(n)$

Order, n	$f(n)$	$f'(n)$	Error	Fractional Error
1	1.0000000	0.6	0.4000000	0.400000
2	2.6180339	2.3	0.3180339	0.121478
3	5.0489077	4.8	0.2489077	0.049299
4	8.2908599	8.1	0.1908599	0.023021
5	12.3435379	12.2	0.1435379	0.011629
6	17.2068587	17.1	0.1068587	0.006210
7	22.8807819	22.8	0.0807819	0.003531
8	29.3652984	29.3	0.0652984	0.002224
9	36.6603989	36.6	0.0603989	0.001648
10	44.7660837	44.7	0.0660837	0.001476
11	53.6823401	53.6	0.0823401	0.001534
12	63.4091685	63.3	0.1091685	0.001722
13	73.9465573	73.8	0.1465573	0.001982
14	85.3179715	85.1	0.2179715	0.002555
15	97.4530641	97.2	0.2530641	0.002597

stable operational equilibrium:

$$n = 1 : V^{*2} > PR \quad (\text{B.41})$$

$$n = 2 : V^{*2} > 2.62PR \quad (\text{B.42})$$

$$n \geq 3 : V^{*2} > f'(n)PR \quad (\text{B.43})$$

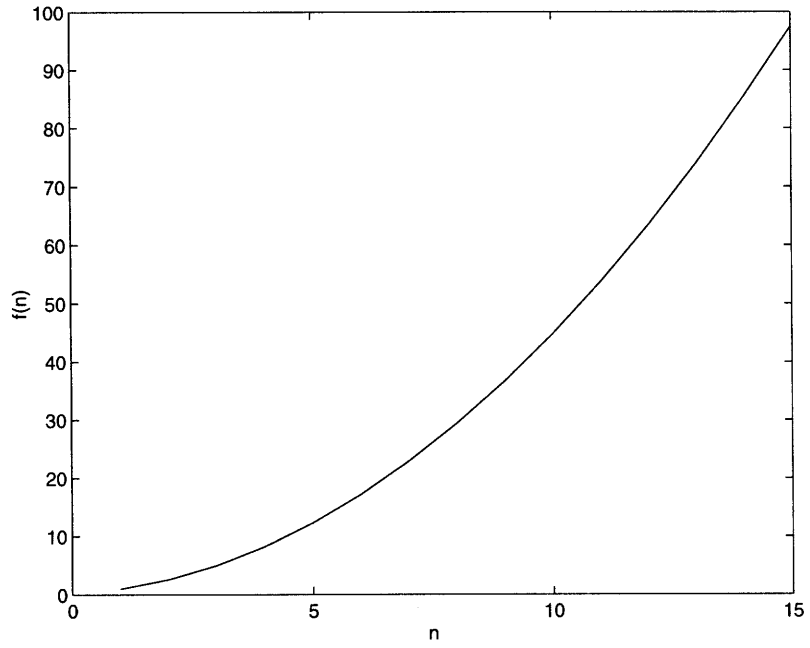


Figure B-1: Plot of $f(n)$ against n .

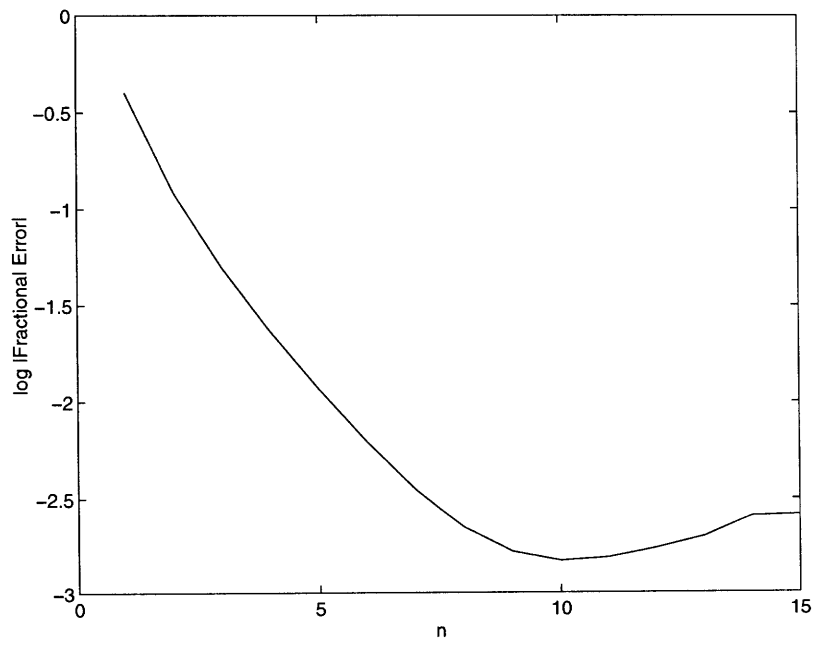


Figure B-2: Error for approximation of $f(n)$.

Appendix C

Numerical Solutions with Maple V

This appendix demonstrates the use of Maple V Release 3 as a tool for obtaining the static equilibria for a second-order system with constant-power loads.

C.1 Second-Order System

First, we consider a network where all the resistances and all the loads are identical: $V = 90\text{V}$, $R_1 = R_2 = 2\Omega$ and $P_1 = P_2 = 100\text{W}$. We assume the cutoff voltages of both loads to be 45V . The circuit diagram is shown in Figure 2-1.

$$\begin{aligned} > \text{En} &:= (1/2) * (1/R1 + 1/R2) * v1^2 + (1/2) * (1/R2) * v2^2 \\ &- (V/R1) * v1 - v1 * v2 / R2 + P1 * \log(v1/V) + P2 * \log(v2/V); \\ \text{En} &:= \frac{1}{2} \left(\frac{1}{R1} + \frac{1}{R2} \right) v1^2 + \frac{1}{2} \frac{v2^2}{R2} - \frac{V v1}{R1} - \frac{v1 v2}{R2} + P1 \ln \left(\frac{v1}{V} \right) \\ &+ P2 \ln \left(\frac{v2}{V} \right) \\ > \text{Eq1} &:= -\text{diff}(\text{En}, v1) = 0; \\ \text{Eq1} &:= - \left(\frac{1}{R1} + \frac{1}{R2} \right) v1 + \frac{V}{R1} + \frac{v2}{R2} - \frac{P1}{v1} = 0 \\ > \text{Eq2} &:= -\text{diff}(\text{En}, v2) = 0; \\ \text{Eq2} &:= - \frac{v2}{R2} + \frac{v1}{R2} - \frac{P2}{v2} = 0 \end{aligned}$$

```

> System := subs({V=90, P1=100, P2=100, R1=2, R2=2}, {Eq1, Eq2})
System :=  $\left\{ -v1 + 45 + \frac{1}{2} v2 - 100 \frac{1}{v1} = 0, -\frac{1}{2} v2 + \frac{1}{2} v1 - 100 \frac{1}{v2} = 0 \right\}$ 

> Soln1 := solve(System, {v1, v2});
Soln1 :=  $\left\{ v2 = -\frac{1}{100} \%1^3 + \frac{27}{20} \%1^2 - \frac{85}{2} \%1 + 90, v1 = \%1 \right\}$ 
          %1 := RootOf(  $_{Z^4 - 135 Z^3 + 4450 Z^2 - 18000 Z + 20000}$  )

> V1 := evalf(allvalues(Soln1[2]));
          V1 := v1 = 85.23889858, v1 = 45.27187414,
          v1 = 2.24461364 + .3801326891 I,
          v1 = 2.24461364 - .3801326891 I

> v1a := rhs( V1[1] );
          v1a := 85.23889858

> v1b := rhs( V1[2] );
          v1b := 45.27187414

> System1 := subs(v1=v1a, System);
System1 :=
 $\left\{ -\frac{1}{2} v2 + 42.61944929 - 100 \frac{1}{v2} = 0, -41.41207188 + \frac{1}{2} v2 = 0 \right\}$ 

> v2a := solve(System1[2], v2);
          v2a := 82.82414376

> Set1 := {v1=v1a, v2=v2a};
          Set1 := {v2 = 82.82414376, v1 = 85.23889858}

> System2 := subs(v1=v1b, System);
System2 :=
 $\left\{ -2.480751106 + \frac{1}{2} v2 = 0, -\frac{1}{2} v2 + 22.63593707 - 100 \frac{1}{v2} = 0 \right\}$ 

> v2b := solve(System2[1], v2);
          v2b := 4.961502212

> Set2 := {v1=v1b, v2=v2b};
          Set2 := {v2 = 4.961502212, v1 = 45.27187414}

```

```

> subs(Set1, System);
      { -0.1 10-8 = 0, 0.2 10-8 = 0 }

> subs(Set2, System);
      { 0 = 0, -0.6 10-7 = 0 }

> with(plots);
  [animate, animate3d, conformal, contourplot, cylinderplot, densityplot,
   display, display3d, fieldplot, fieldplot3d, gradplot, gradplot3d,
   implicitplot, implicitplot3d, loglogplot, logplot, matrixplot,
   odeplot, pointplot, polarplot, polygonplot, polygonplot3d,
   polyhedraplot, replot, setoptions, setoptions3d, spacecurve,
   sparsematrixplot, sphereplot, surfdata, textplot, textplot3d,
   tubeplot]

> implicitplot({System[1], System[2]}, v1=0..90, v2=0..90);

> with(DEtools);
  [DEplot, DEplot1, DEplot2, Dchangevar, PDEplot, dfieldplot,
   phaseportrait]

> dfieldplot([lhs(System[1]), lhs(System[2])], [v1, v2],
  0..90, v1=0..90, v2=0..90);

```

For a system with ideal loads, the two equilibria are (85.2, 82.8) and (45.3, 5.0), which correspond to the higher stable equilibrium and the lower unstable equilibrium respectively, as described in Section 2.1, respectively. However, since we have assumed that we are dealing with non-ideal loads with a cutoff voltage of 45V, the lower static equilibrium point at (45.3, 5.0) is inadmissible.

As mentioned previously in Section 4.1.1, a graphical way to obtain the solutions to the system is to plot each equation for the system and find the intersections, as shown in Figure C-1. The field plot for the system with ideal loads in the case where $C_1 = C_2$ is shown in Figure C-2. We repeat the field plot for the system where loads are assumed

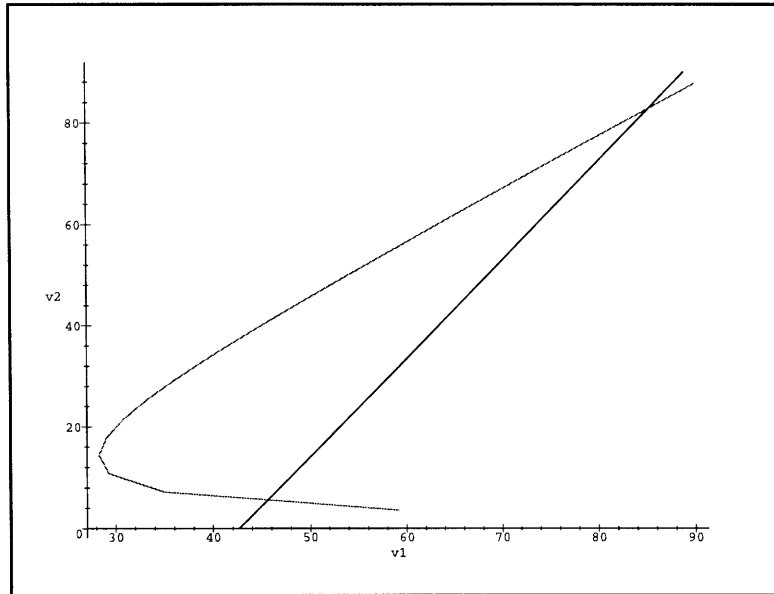


Figure C-1: Graphical method for obtaining solutions to a second-order system.

to be non-ideal with a cutoff voltage of 45V in Figure C-3. We observe in the latter case, the lower unstable equilibrium is eliminated, and the system is left with a single globally unique and stable equilibrium.

C.2 Third-Order Ladder

We repeat the exercise described in Section C.1 with a third-order ladder network where all resistances and loads are equal: $V = 90\text{V}$, $R_1 = R_2 = R_3 = 2\Omega$ and $P_1 = P_2 = P_3 = 100\text{W}$. The circuit diagram is shown in Figure 3-6.

$$\begin{aligned}
 > \quad E_n := & (1/2) * (1/R_1 + 1/R_2) * v_1^2 + (1/2) * (1/R_2 + 1/R_3) * v_2^2 \\
 & + (1/2) * (1/R_3) * v_3^2 - (V/R_1) * v_1 - v_1 * v_2 / R_2 - v_2 * v_3 / R_3 \\
 & + P_1 * \log(v_1/V) + P_2 * \log(v_2/V) + P_3 * \log(v_3/V); \\
 E_n := & \frac{1}{2} \left(\frac{1}{R_1} + \frac{1}{R_2} \right) v_1^2 + \frac{1}{2} \left(\frac{1}{R_2} + \frac{1}{R_3} \right) v_2^2 + \frac{1}{2} \frac{v_3^2}{R_3} - \frac{V v_1}{R_1} - \frac{v_1 v_2}{R_2} \\
 & - \frac{v_2 v_3}{R_3} + P_1 \ln \left(\frac{v_1}{V} \right) + P_2 \ln \left(\frac{v_2}{V} \right) + P_3 \ln \left(\frac{v_3}{V} \right)
 \end{aligned}$$

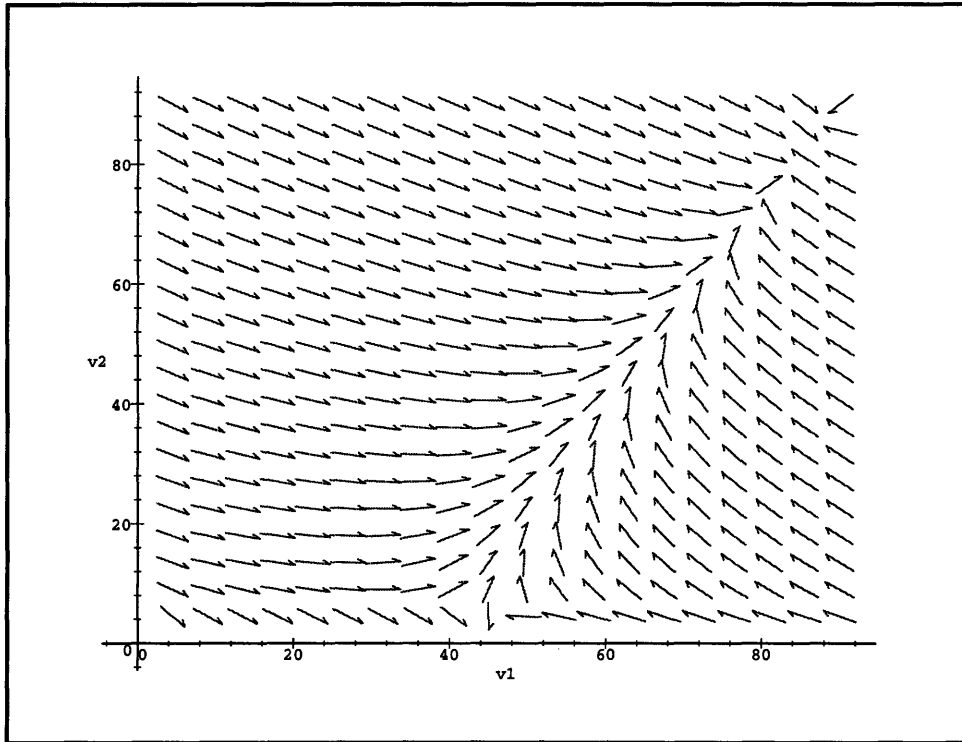


Figure C-2: Example field plot for second-order system (ideal loads).

```

> Eq1 := -diff(En,v1) = 0 ;
      Eq1 := - ( 1/R1 + 1/R2 ) v1 + V/R1 + v2/R2 - P1/v1 = 0
> Eq2 := -diff(En,v2) = 0 ;
      Eq2 := - ( 1/R2 + 1/R3 ) v2 + v1/R2 + v3/R3 - P2/v2 = 0
> Eq3 := -diff(En,v3) = 0 ;
      Eq3 := - v3/R3 + v2/R3 - P3/v3 = 0

> System := subs({V=90, P1=100, P2=100, P3=100, R1=2,
R2=2, R3=2}, {Eq1, Eq2, Eq3});
System := { v1 - 45 - 1/2 v2 + 100/v1 = 0, v2 - 1/2 v1 - 1/2 v3 + 100/v2 = 0,
1/2 v3 - 1/2 v2 + 100/v3 = 0 }

```

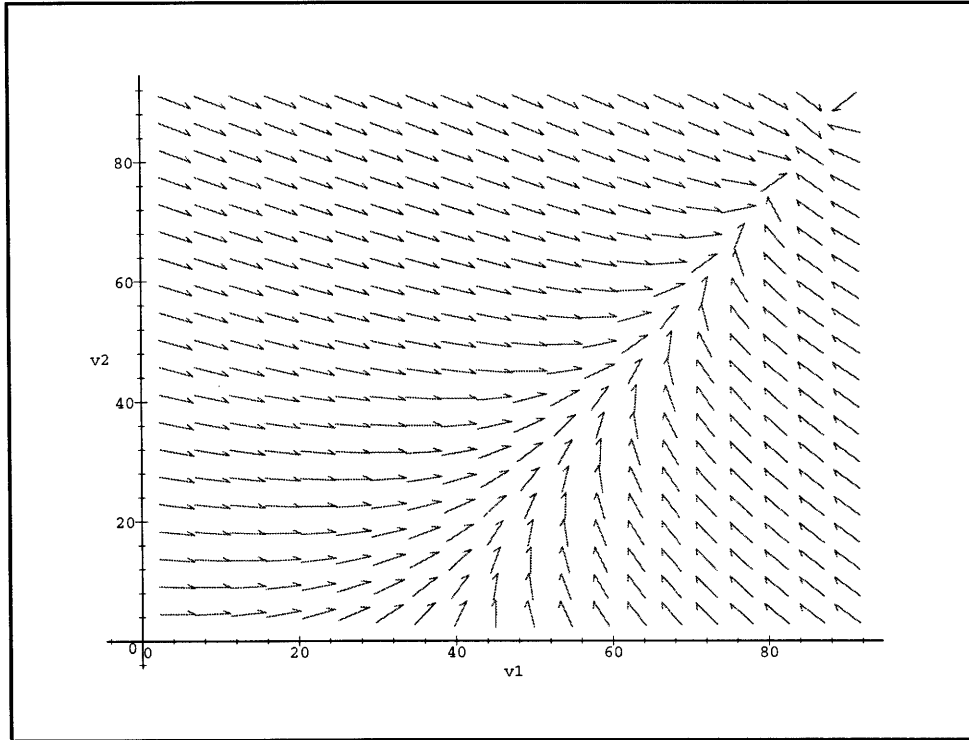


Figure C-3: Example field plot for second-order system (non-ideal loads).

```
> Soln1 := solve(System, {v1, v2, v3});
Soln1 := {v2 = -\frac{1}{48000000} \%1^7 + \frac{3}{1600000} \%1^6 - \frac{11}{240000} \%1^5
+ \frac{3}{1600} \%1^4 - \frac{31}{1200} \%1^3 + \frac{9}{20} \%1^2 - \frac{19}{6} \%1 + 30, v3 = \%1, v1 =
-\frac{28}{3} \%1 + \frac{27}{20} \%1^2 + \frac{3}{320000} \%1^6 + \frac{33}{4000} \%1^4 - \frac{1}{9600000} \%1^7
-\frac{13}{60000} \%1^5 - \frac{5}{48} \%1^3 + 60}
%1 := RootOf(-Z^8 + 2200_Z^6 + 1240000_Z^4 + 200000000_Z^2
+ 96000000000 - 90_Z^7 - 90000_Z^5 - 21600000_Z^3
- 1440000000_Z)

> V1 := evalf(allvalues(Soln1[2]));
V1 := v3 = .1681877825 - 10.84475727 I,
v3 = .1681877825 + 10.84475727 I,
v3 = .9240691622 - 25.89511604 I,
```

$$v3 = .9240691622 + 25.89511604 I,$$

$$v3 = 2.089068762 - 13.06918538 I,$$

$$v3 = 2.089068762 + 13.06918538 I, v3 = 9.339119458,$$

$$v3 = 74.29822913$$

> v3a := rhs(V1[7]);

$$v3a := 9.339119458$$

> v3b := rhs(V1[8]);

$$v3b := 74.29822913$$

> System1 := subs(v3=v3a, System);

$$System1 := \left\{ v2 - \frac{1}{2} v1 - 4.669559729 + 100 \frac{1}{v2} = 0, \right. \\ \left. 15.37720732 - \frac{1}{2} v2 = 0, v1 - 45 - \frac{1}{2} v2 + 100 \frac{1}{v1} = 0 \right\}$$

> Sol1 := solve({System1[1], System1[2]}, {v1, v2});

$$Sol1 := \{ v2 = 30.75441464, v1 = 58.67284124 \}$$

> Set1 := {v3=v3a} union Sol1;

$$Set1 := \{ v3 = 9.339119458, v2 = 30.75441464, v1 = 58.67284124 \}$$

> System2 := subs(v3=v3b, System);

$$System2 := \left\{ v2 - \frac{1}{2} v1 - 37.14911457 + 100 \frac{1}{v2} = 0, \right. \\ \left. 38.49504167 - \frac{1}{2} v2 = 0, v1 - 45 - \frac{1}{2} v2 + 100 \frac{1}{v1} = 0 \right\}$$

> Sol2 := solve({System2[1], System2[2]}, {v1, v2});

$$Sol2 := \{ v2 = 76.99008334, v1 = 82.27967469 \}$$

> Set2 := {v3=v3b} union Sol2;

$$Set2 := \{ v3 = 74.29822913, v2 = 76.99008334, v1 = 82.27967469 \}$$

> subs(Set1, System);

$$\{ 0 = 0, -.7 10^{-8} = 0, -.1 10^{-8} = 0 \}$$

> subs(Set2, System);

$$\{ .3 10^{-8} = 0, -.3 10^{-8} = 0, -.1 10^{-8} = 0 \}$$

Again, when the loads are assumed to be ideal, there are two equilibria : (82.3, 77.0, 74.3)
and (58.7, 30.8, 9.4).

Appendix D

Small-Resistance Approximation

In this appendix, we will provide the details for the derivation of the first-guess and iterative equations for a third-order ladder network. We will also illustrate the generalized method for an arbitrary higher-order network with an example.

D.1 Third-Order System

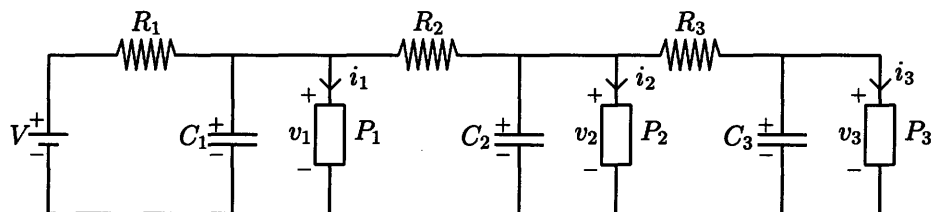


Figure D-1: Third-order system.

We repeat the procedure outlined in Section 4.1.2 with the third-order ladder shown in Figure D-1. Given that $v_1 \simeq v_2 \simeq v_3$ because the resistances R_2 and R_3 are small, we obtain

$$\frac{P_1}{i_1} \simeq \frac{P_2}{i_2} \simeq \frac{P_3}{i_3} \quad (\text{D.1})$$

Hence,

$$i_2 \simeq \frac{P_2}{P_1} i_1 \quad (\text{D.2})$$

$$i_3 \simeq \frac{P_3}{P_1} i_1 \quad (\text{D.3})$$

Under these assumptions, we obtain

$$\left(1 + \frac{P_2}{P_1} + \frac{P_3}{P_1}\right) R_1 i_1^2 - V i_1 + P_1 = 0 \quad (\text{D.4})$$

which yields

$$i_1 = \frac{V - \sqrt{V^2 - 4(P_1 + P_2 + P_3)R_1}}{2\left(1 + \frac{P_2}{P_1} + \frac{P_3}{P_1}\right)R_1} \quad (\text{D.5})$$

Now that we have an approximation for i_1 , we take i_1 as given and consider the next stage:

$$v_2 = V - (i_1 + i_2 + i_3)R_1 - (i_2 + i_3)R_2 \quad (\text{D.6})$$

$$= (V - i_1 R_1) - (i_2 + i_3)(R_1 + R_2) \quad (\text{D.7})$$

$$\simeq (V - i_1 R_1) - \left(1 + \frac{P_3}{P_2}\right)(R_1 + R_2) \quad (\text{D.8})$$

Finally, we obtain

$$\left(1 + \frac{P_3}{P_2}\right)(R_1 + R_2)i_2^2 - (V - i_1 R_1)i_2 + P_2 = 0 \quad (\text{D.9})$$

which yields

$$i_2 = \frac{V - i_1 R_1 - \sqrt{(V - i_1 R_1)^2 - 4(P_1 + P_2)(R_1 + R_2)}}{2\left(1 + \frac{P_3}{P_2}\right)(R_1 + R_2)} \quad (\text{D.10})$$

Finally, the equation for the last node is

$$(R_1 + R_2 + R_3)i_3^2 - (V - (i_1 + i_2)R_1 - i_2 R_2)i_3 + P_3 = 0 \quad (\text{D.11})$$

which yields

$$i_3 = \frac{V_3' - \sqrt{V_3'^2 - 4P_3(R_1 + R_2 + R_3)}}{2(R_1 + R_2 + R_3)} \quad (\text{D.12})$$

where

$$V_3' = V - (i_1 + i_2)R_1 - i_2R_2$$

Repeating the above process, we obtain the iterative formulae for i_1 and i_2 :

$$i_1 = \frac{V_1' - \sqrt{V_1'^2 - 4P_1R_1}}{2R_1} \quad (\text{D.13})$$

$$i_2 = \frac{V_2' - \sqrt{V_2'^2 - 4P_2(R_1 + R_2)}}{2(R_1 + R_2)} \quad (\text{D.14})$$

$$(\text{D.15})$$

where

$$V_1' = V - (i_2 + i_3)R_1$$

$$V_2' = V - (i_1 + i_3)R_1 - i_3R_2$$

D.2 Generalization

If we examine the process of obtaining the first-guess equations and the iterative equations carefully, we will note that the process is really one of considering one current loop at a time, reducing it to an equivalent first-order system, and then solving the simpler system.

First, let us state the results for a simple first-order circuit as shown in Figure D-2. In equilibrium, we have:

$$V - iR = \frac{P}{i} \quad (\text{D.16})$$

$$Ri^2 - Vi + P = 0 \quad (\text{D.17})$$

$$i = \frac{V - \sqrt{V^2 - 4PR}}{2R} \quad (\text{D.18})$$

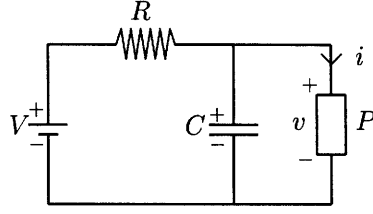


Figure D-2: Circuit diagram for first-order system.

The process of obtaining the first-guess and iterative equations is best demonstrated with the following example. Consider the third-order system with branching shown in Figure D-3. First, consider the current loop including the source and P_1 , as shown on the left in Figure D-4. The first fundamental idea is that $v_1 \simeq v_2 \simeq v_3$, so

$$i_2 \simeq \frac{P_2}{P_1} i_1 \text{ and} \quad (\text{D.19})$$

$$i_3 \simeq \frac{P_3}{P_1} i_1 \quad (\text{D.20})$$

If we consider only this loop, we obtain:

$$V - (i_1 + i_2 + i_3)R_1 = \frac{P_1}{i_1} \quad (\text{D.21})$$

$$V - \left(1 + \frac{P_2}{P_1} + \frac{P_3}{P_1}\right)R_1 i_1 \simeq \frac{P_1}{i_1} \quad (\text{D.22})$$

Hence, it is apparent that the loop is in effect equivalent to the first-order system on the right in Figure D-4, where $R'_2 = \left(1 + \frac{P_2}{P_1} + \frac{P_3}{P_1}\right)R_1$. We apply the result to (D.18) to obtain

$$i_1 = \frac{V - \sqrt{V^2 - 4P_1\left(1 + \frac{P_2}{P_1} + \frac{P_3}{P_1}\right)R_1}}{2\left(1 + \frac{P_2}{P_1} + \frac{P_3}{P_1}\right)R_1} \quad (\text{D.23})$$

$$= \frac{V - \sqrt{V^2 - 4(P_1 + P_2 + P_3)R_1}}{2\left(1 + \frac{P_2}{P_1} + \frac{P_3}{P_1}\right)R_1} \quad (\text{D.24})$$

We will call this the *Resistor Multiplying Effect*.

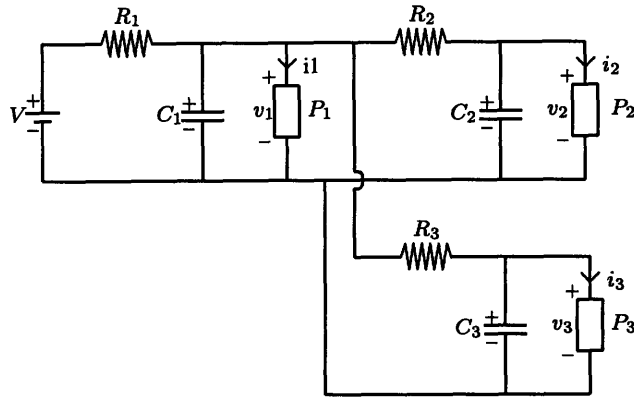


Figure D-3: A third-order example with branching.



Figure D-4: Example loop with equivalent circuit.

Now, we consider the current loop as shown on the left in Figure D-5:

$$V - (i_1 + i_2 + i_3)R_1 - i_2R_2 = \frac{P_2}{i_2} \quad (\text{D.25})$$

$$(V - i_1R_1) - \left(1 + \frac{P_3}{P_2}\right)R_1 + R_2)i_2 \simeq \frac{P_2}{i_2} \quad (\text{D.26})$$

Hence, it is apparent that the loop is in effect equivalent to the first-order system on the right in Figure D-5, where $R'_2 = (1 + \frac{P_3}{P_2})R_1 + R_2$ and $V'_2 = V - i_1R_1$. The contribution of $\frac{P_3}{P_2}$ to R_1 , we recognize as the *Resistor Multiplying Effect*. We notice here that the source voltage is also effectively reduced. We call this the *Source Voltage Reducing Effect*. We apply the result from (D.18) to obtain

$$i_2 = \frac{V'_2 - \sqrt{V'^2_2 - 4P_2R'_2}}{2R'_2} \quad (\text{D.27})$$

where

$$R'_2 = \left(1 + \frac{P_3}{P_2}\right)R_1 + R_2 \quad (\text{D.28})$$

$$V'_2 = V - i_1 R_1 \quad (\text{D.29})$$

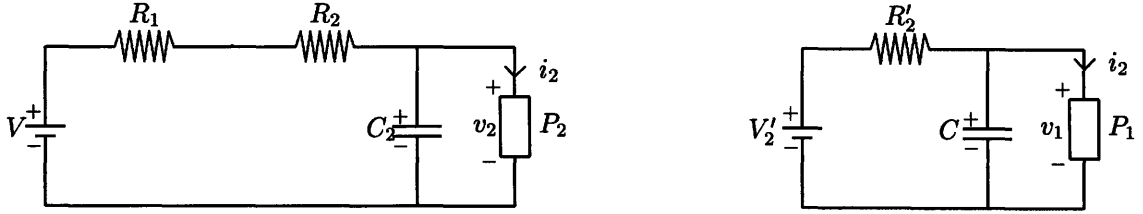


Figure D-5: Example loop II with equivalent circuit.

Similarly, by symmetry, for i_3 we have

$$i_3 = \frac{V'_3 - \sqrt{V'_3{}^2 - 4P_2R'_3}}{2R'_3} \quad (\text{D.30})$$

where

$$R'_3 = \left(1 + \frac{P_2}{P_3}\right)R_1 + R_3 \quad (\text{D.31})$$

$$V'_3 = V - i_1 R_1 \quad (\text{D.32})$$

Lastly, by the *Source Voltage Reducing Effect*, we derive that the effective source voltage seen by i_1 given that both i_2 and i_3 are known is $V - (i_2 + i_3)R_1$ to obtain

$$i_1 = \frac{V'_1 - \sqrt{V'_1{}^2 - 4P_2R_1}}{2R_1} \quad (\text{D.33})$$

where

$$V'_3 = V - (i_2 + i_3)R_1 \quad (\text{D.34})$$

In summary, in order to derive the first-guess and the iterative equations, we first divide

the set of currents drawn by the loads into two sets: one set with known values and one set with unknown values. Next, we consider one current loop at a time and reduce the result to an equivalent first-order system. The “known” set has a *Source Voltage Reducing Effect* while the “unknown” set causes a *Resistor Multiplying Effect*. Once this is clear, we can apply the result from (D.18) directly to obtain the required solution.

Appendix E

Evaluation of Aggregated Models

In this appendix, we evaluate the use of the following aggregated models by applying these models to some specific networks and comparing their input/output characteristics as well as the total power dissipation. First-order transients are also compared.

E.1 The Models

E.1.1 Series Model

The approximation of the second-order series configuration shown in Figure 4-4 by a first-order configuration as shown in Figure 4-6 yields the following parameters:

$$R' = R_1 + \frac{R_2 P_2^2}{(P_1 + P_2)^2} \quad (\text{E.1})$$

$$C' = C_1 + C_2 \quad (\text{E.2})$$

$$P' = P_1 + P_2 \quad (\text{E.3})$$

E.1.2 Parallel Model

The approximation of the second-order parallel configuration shown in Figure 4-5 by a first-order configuration as shown in Figure 4-6 yields the following parameters:

$$R' = \frac{R_1 P_1^2 + R_2 P_2^2}{(P_1 + P_2)^2} \quad (\text{E.4})$$

$$C' = C_1 + C_2 \quad (\text{E.5})$$

$$P' = P_1 + P_2 \quad (\text{E.6})$$

E.2 Evaluation of the Series Model

In this section, we evaluate the effectiveness of the series model for approximating second-order and third-order networks.

E.2.1 Approximation in Second-order System

Consider the second-order series network and its associated aggregated model shown in Figure E-1. The cutoff voltage for all the constant-power loads is 45V.

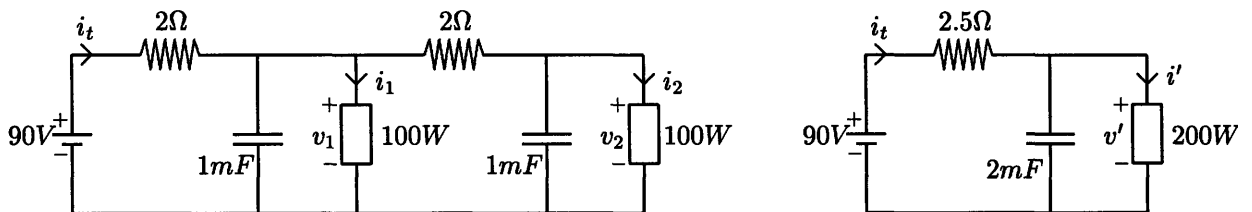


Figure E-1: Second-order series configuration with aggregated model.

Table E.1 shows the results for the series configuration and the aggregated model. Figures E-2 and E-3 show the plots of total current drawn from the source for the second-order configuration and its aggregated model respectively. It is apparent from these results that the approximation are reasonably good. To first-order, the transient currents look almost identical and the final steady-state results are correct to 3 significant figures.

Table E.1: Table of Results for Series Configuration (Second-Order)

Parameter	Series	Aggregated	Fractional Error
i_1	1.173	-	-
i_2	1.207	-	-
i_t	2.381	2.380	0.0004
v_1	85.239	-	-
v_2	82.824	-	-
v'	-	84.051	-
Power, P	214.250	214.155	0.0004

We can use the result for i_t from the aggregated model to obtain an approximation for v_1 in the original model:

$$v_1 \simeq V - 2i_t = 85.24\text{V}$$

Next, we consider v_1 to be fixed at 85.24V and consider the remainder of the network as a first-order system. From (1.3), we obtain

$$\begin{aligned} v_2 &= \frac{v_1 + \sqrt{v_1^2 - 4PR}}{2} \\ &= 82.8\text{V} \end{aligned}$$

These approximations compare well with the actual values of the second-order system shown in Table E.1.

E.2.2 Approximation in Third-order System

We repeat the above analysis with the third-order system shown in Figure E-4. The first-order and second-order systems resulting from applying the series model successively are shown in Figure E-5.

Table E.2 shows the results for the series configuration and the aggregated models. Figures E-6 and E-7 show the plots of the voltage at the first node for the third-order series

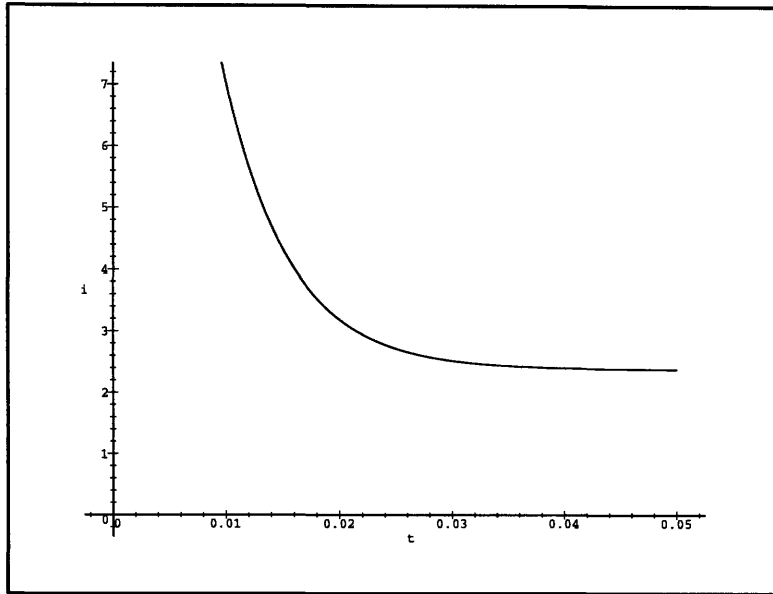


Figure E-2: Plot of current vs time for second-order series configuration.

configuration and its second-order aggregated model respectively. It is apparent from these results that the approximation are reasonably good. To first-order, the transient behavior of the voltage at the first nodes look almost identical and the final steady-state results are quite close — less than 0.05 % for the second-order approximation and about 0.5 % for the first-order approximation.

As before, we can use the first-order aggregated model to estimate the voltage of the first node:

$$v_1 \simeq V - 2i_t = 82.31\text{V}$$

Next, we approximate v'_2 as

$$\begin{aligned} v'_2 &= \frac{v_1 + \sqrt{v_1^2 - 4PR}}{2} \\ &= 75.71\text{V} \end{aligned}$$

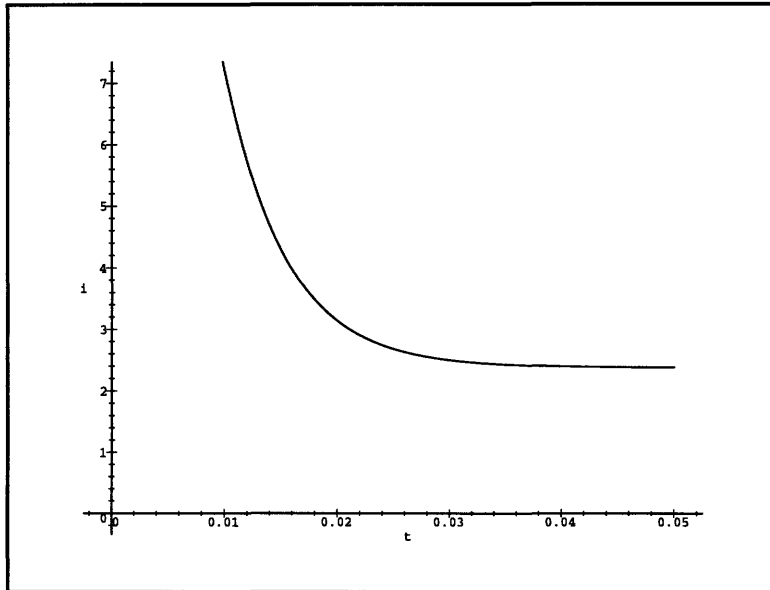


Figure E-3: Plot of current vs time for series aggregated model (second-order).

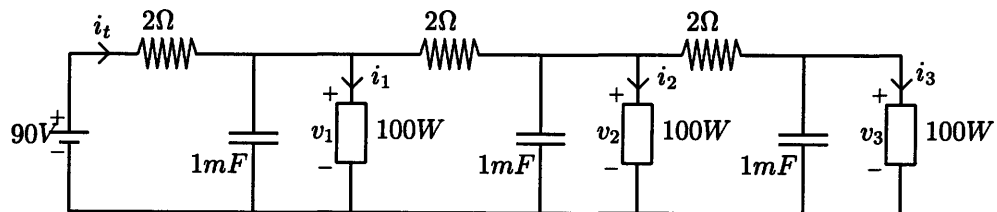


Figure E-4: Example third-order series configuration.

We approximate v_2 with

$$\begin{aligned} v_2 &\simeq v_1 - 2 \frac{v_1 - v_2'}{2.5} \\ &= 77.03\text{V} \end{aligned}$$

Finally,

$$\begin{aligned} v_3 &= \frac{v_2 + \sqrt{v_2^2 - 4PR}}{2} \\ &= 74.34\text{V} \end{aligned}$$

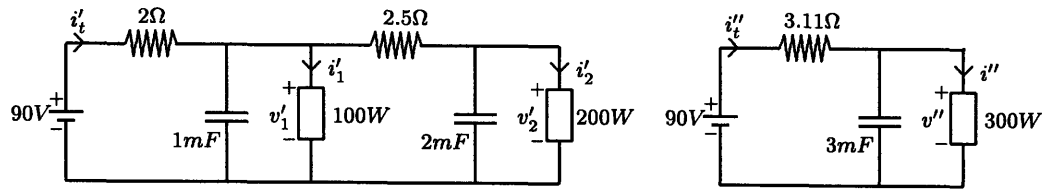


Figure E-5: Aggregated models for third-order series configuration.

Table E.2: Table of Results for Series Configuration (Third-Order)

Parameter	Series	Aggregated (2nd)	Fractional Error	Aggregated (1st)	Fractional Error
i_1	1.215	-	-	-	-
i_2	1.299	-	-	-	-
i_2	1.346	-	-	-	-
i'_1	-	1.215	-	-	-
i'_2	-	2.643	-	-	-
i_t, i'_t, i''_t	3.860	3.858	-0.00052	3.844	-0.0041
v_1, v'_1	82.280	82.284	4.8×10^{-5}	-	-
v_2	76.990	-	-	-	-
v_3	74.298	-	-	-	-
v'_2	-	75.677	-	-	-
v''	-	-	-	78.04	-
Power, P	347.415	347.232	-0.00052	345.975	-0.0041

In summary, approximation with the aggregated model yields:

$$v_1 = 82.31\text{V}, v_1 = 77.03\text{V}, v_1 = 74.34\text{V}$$

which compares favorably with the actual nodal voltages. The errors are within 0.1%.

E.3 Evaluation of the Parallel Model

In this section, we evaluate the effectiveness of the parallel model for approximating second-order and third-order networks.

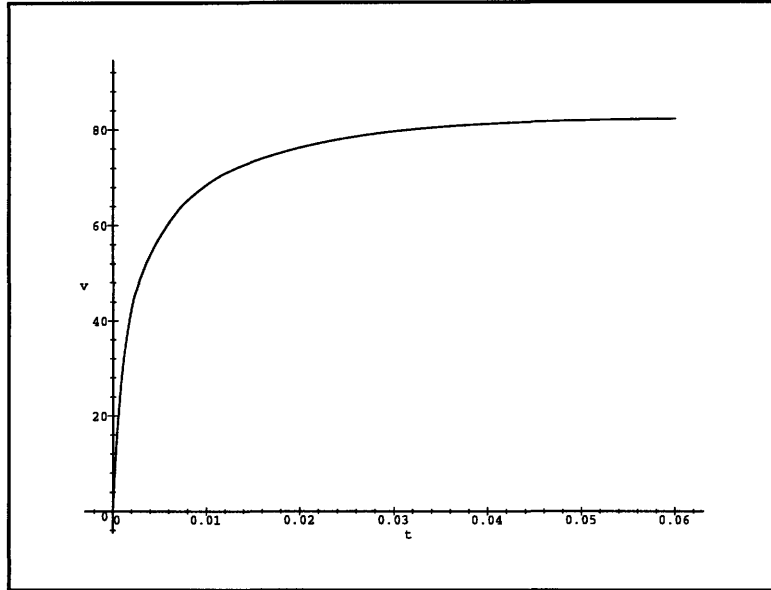


Figure E-6: Plot of v_1 vs t for third-order series configuration.

E.3.1 Approximation in Second-order System

We consider the second-order parallel network and its associated aggregated model shown in Figure E-8. The results for the parallel configuration and the aggregated model are shown Table E.3. It is apparent from these results that the approximation is reasonably good.

Table E.3: Table of Results for Parallel Configuration (Second-Order)

Parameter	Parallel	Aggregated	Fractional Error
i_1	1.375	-	-
i_2	0.917	-	-
i_t, i'	2.292	2.292	0
v_1	87.249	-	-
v_2	87.249	-	-
v'	-	87.249	-
Power, P	206.305	206.306	4.8×10^{-6}

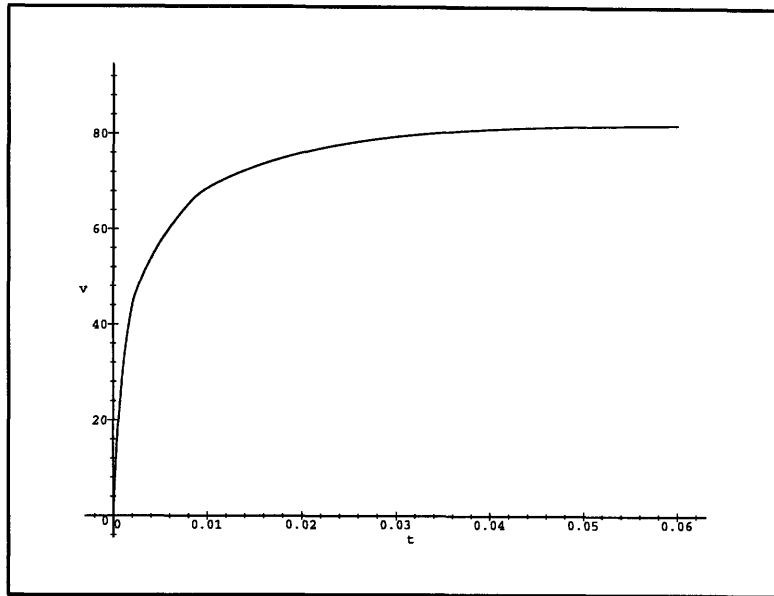


Figure E-7: Plot of v'_1 vs t for series approximation (third-order).

E.3.2 Approximation in Third-order System

We repeat the above analysis with the third-order system shown in Figure E-9. The first-order and second-order systems resulting from applying the series model successively are shown in Figure E-9.

Table E.4 shows the results for the parallel configuration and the aggregated model. Figures E-11 and E-12 show the plots of the voltage of the first node for the third-order configuration and its aggregated model respectively. It is apparent from these results that the approximation are good. To first-order, the transient responses in the voltages are very similar and the final steady-state results are extremely close.

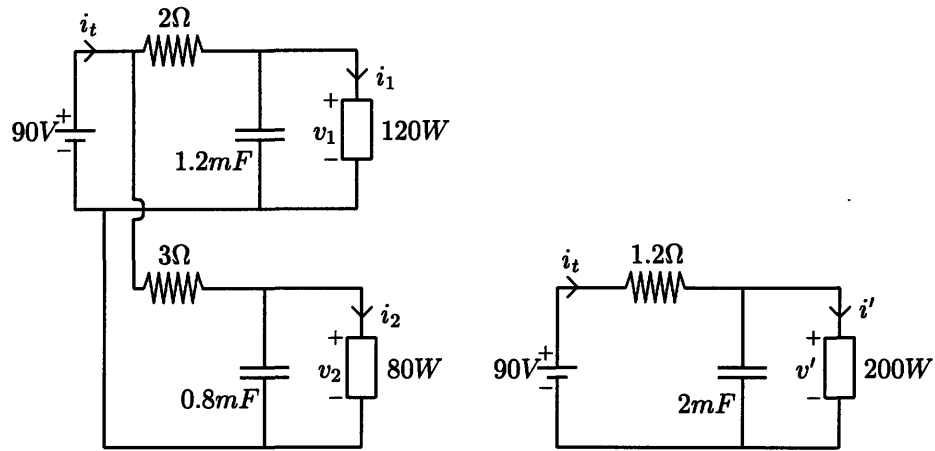


Figure E-8: Second-order parallel configuration with aggregated model

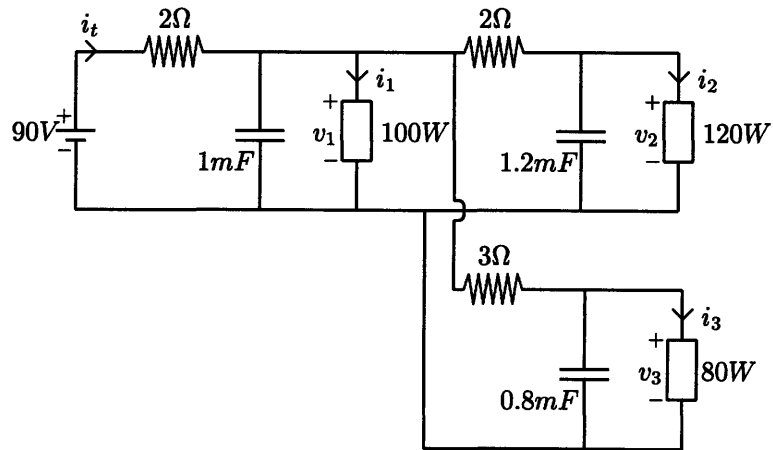


Figure E-9: Example third-order parallel configuration.

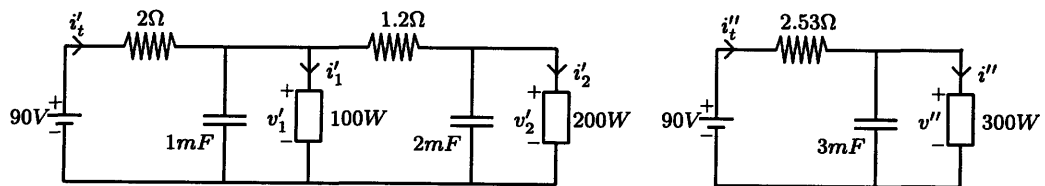


Figure E-10: Aggregated model for third-order parallel configuration.

Table E.4: Table of Results for Parallel Configuration (Third-Order)

Parameter	Parallel	Aggregated (2nd)	Fractional Error	Aggregated (1st)	Fractional Error
i_1	1.211	-	-	-	-
i_2	1.509	-	-	-	-
i_3	1.006	-	-	-	-
i'_1	-	1.211	-	-	-
i'_2	-	2.515	-	-	-
i_t, i'_t, i''_t	3.726	3.726	0	3.724	0.00054
v_1, v'_1	82.548	82.548	0	-	-
v_2	79.530	-	-	-	-
v_3	79.530	-	-	-	-
v'_2	-	79.530	-	-	-
v''	-	-	-	80.567	-
Power, P	335.359	335.358	-3.0×10^{-6}	335.125	-0.00070

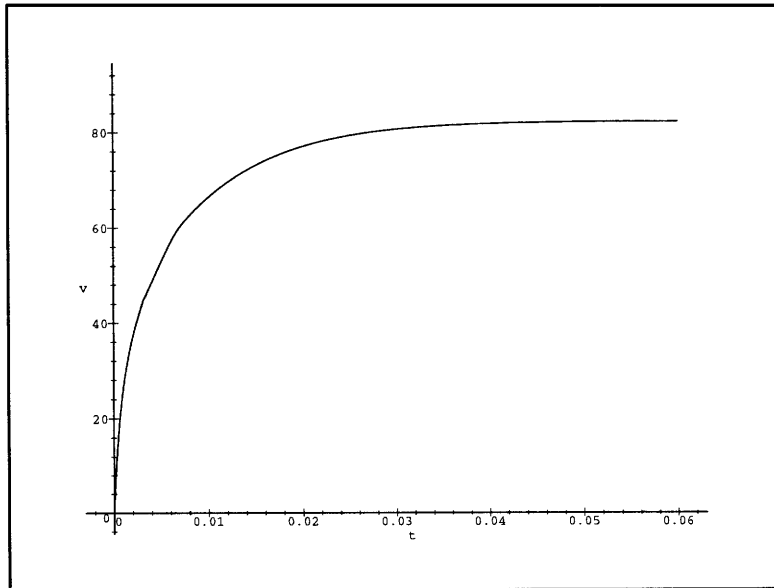


Figure E-11: Plot of v_1 vs t for third-order parallel configuration.

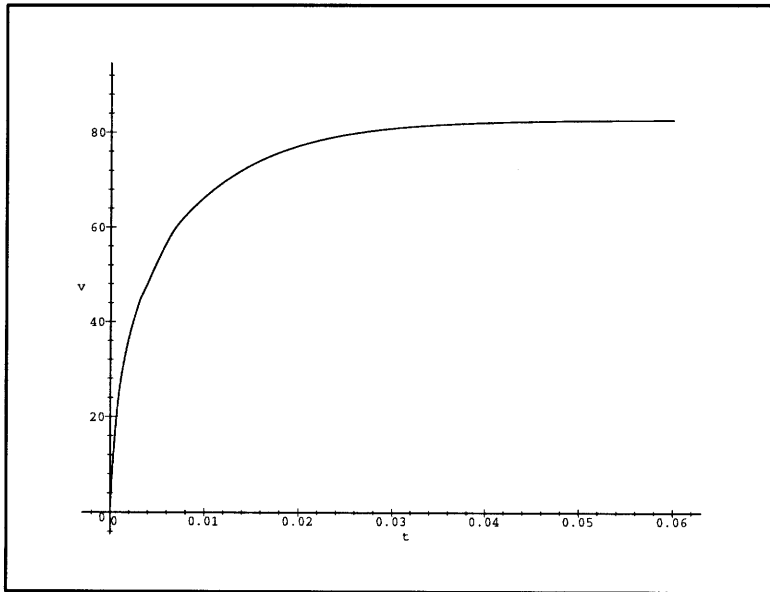


Figure E-12: Plot of v'_1 vs t for parallel approximation (third-order).

Bibliography

- [1] Thottuvelil, Joseph V., and Kakalec, Robert J., "Analysis and Design of Broadband Power Systems". *IEEE International Telecommunications and Energy Conference (INTELEC)*. Boston: 1996.
- [2] Hirsch, Morris, and Smale, Stephen. *Differential Equations, Dynamical Systems and Linear Algebra*. New York: Academic Press, Inc., 1974.
- [3] Perko, Lawrence. *Differential Equations and Dynamical Systems*. New York: Springer-Verlag New York, Inc., 1991.
- [4] Slotine, Jean-Jacques E., and Li, Weiping. *Applied Nonlinear Control*. New Jersey: Prentice Hall, 1991.
- [5] Heal, K. M., Hansen, M. L and Rickard, K.M.. *Maple V Learning Guide*. New York: Waterloo Maple, Inc., 1996.
- [6] Adams, Steven G.. *Maple Talk*. New Jersey: Prentice Hall, 1997.
- [7] Heal, Robertson, John S.. *Engineering Mathematics with Maple*. New York: McGraw-Hill, Inc., 1996.
- [8] Heck, André. *Introduction to Maple*. New York: Springer-Verlag New York, Inc., 1993.